Pedro Henrique Juliano Nardelli

Analysis of the Spatial Throughput in Interference Networks

Análise da Vazão Espacial em Redes de Interferência

Campinas
2013

Universidade Estadual de Campinas
Faculdade de Engenharia Elétrica e de Computação

Pedro Henrique Juliano Nardelli

Analysis of the Spatial Throughput in Interference Networks

Análise da Vazão Espacial em Redes de Interferência

Doctorate thesis presented to the Postgraduate Programme of Electrical Engineering of the School of Electrical Engineering of the State University of Campinas to obtain the Ph.D. degree in Electrical Engineering, in the field of Telecommunications and Telematics.

Tese de Doutorado apresentada ao Programa de Pós-Graduação em Engenharia Elétrica da Faculdade de Engenharia Elétrica e de Computação da Universidade Estadual de Campinas para obtenção do título de Doutor em Engenharia Elétrica, na área de Telecomunicações e Telemática.

Supervisor/*Orientador*: Prof. Dr. Paulo Cardieri

Este exemplar corresponde à versão final da tese defendida pelo aluno Pedro Henrique Juliano Nardelli, e orientada pelo Prof. Dr. Paulo Cardieri

---

Campinas
2013

Ficha catalográfica
Universidade Estadual de Campinas
Biblioteca da Área de Engenharia e Arquitetura
Rose Meire da Silva - CRB 8/5974

N166a

Nardelli, Pedro Henrique Juliano, 1984-
Analysis of the spatial throughput in interference networks / Pedro Henrique Juliano Nardelli. – Campinas, SP : [s.n.], 2013.

Orientador: Paulo Cardieri.
Tese (doutorado) – Universidade Estadual de Campinas, Faculdade de Engenharia Elétrica e de Computação.

1. Sistema de comunicação sem fio. I. Cardieri, Paulo,1964-. II. Universidade Estadual de Campinas. Faculdade de Engenharia Elétrica e de Computação. III. Título.

Informações para Biblioteca Digital

Título em outro idioma: Análise da vazão espacial em redes de interferência
Palavras-chave em inglês:
Wireless communication systems
Área de concentração: Telecomunicações e Telemática
Titulação: Doutor em Engenharia Elétrica
Banca examinadora:
Paulo Cardieri [Orientador]
Matti Sakari Latva-aho
Daniel Benevides da Costa
Kimmo Kansanen
Richard Demo Souza
Data de defesa: 29-08-2013
Programa de Pós-Graduação: Engenharia Elétrica

COMISSÃO JULGADORA - TESE DE DOUTORADO

Candidato: Pedro Henrique Juliano Nardelli

Data da Defesa: 29 de agosto de 2013

Título da Tese: "Analysis of the Spatial Throughput in Interference Networks"

Prof. Dr. Paulo Cardieri (Presidente): _____

Prof. Dr. Matti Sakari Latva-aho: _____

Prof. Dr. Daniel Benevides da Costa: _____

Prof. Dr. Kimmo Kansanen: _____

Prof. Dr. Richard Demo Souza: _____

Abstract

In this thesis we study the spatial throughput of interference-limited wireless networks from different perspectives, considering that the spatial distribution of nodes follows a 2-dimensional homogeneous Poisson point process and transmitters employ Gaussian point-to-point codes. To carry out this analysis, we model the interrelations between network elements using concepts from stochastic geometry, communication theory and information theory. We derive closed-form equations to compute/approximate the performance metric that is chosen to evaluate the system for each given specific scenario. Our first contribution is an investigation about whether it is preferable to have a large number of short single-hop links or a small number of long hops in multi-hop wireless networks, using a newly proposed metric denominated *aggregate multi-hop information efficiency*. For single-hop systems, we revisit the transmission capacity framework to study medium access protocols that use asynchronous transmissions and allow for packet retransmissions, showing when a carrier sensing capability is more suitable than synchronous transmissions, and vice-versa. We also cast the effective link throughput and the network spatial throughput optimization problems to find the combination of medium access probability, coding rate and maximum number of retransmissions that maximize each metric under packet loss and queue stability constraints, evincing when they do (and do not) have the same solution. Furthermore we analyze the expected maximum achievable sum rates over a given area - or spatial capacity - based on the capacity regions of Gaussian point-to-point codes for two decoding rules, namely (i) treating interference as noise (IAN) and (ii) jointly detecting the strongest interfering signals treating the others as noise (OPT), proving the advantages of the second. We additionally demonstrate that, when the same decoding rule and network density are considered, the spatial-capacity-achieving scheme always outperforms the spatial throughput obtained with the best predetermined fixed rate strategy. With those results in hand, we discuss general guidelines on the construction of ad hoc adaptive algorithms that would improve the information flow throughout the interference network, respecting the nodes' internal and external constraints.

Keyword: Wireless communication system

Resumo

Nesta tese, nós estudamos a vazão espacial de redes sem fio limitadas por interferência em diferentes perspectivas, considerando que a distribuição espacial dos nós segue um processo pontual de Poisson homogêneo e em duas dimensões, e os transmissores empregam códigos gaussianos ponto-a-ponto. Para conduzir essa análise, nós modelamos as inter-relações entre os elementos da rede usando conceitos de geometria estocástica, teoria da comunicação e teoria da informação. Nós derivamos equações em fórmula fechada para computar/aproximar a métrica de desempenho que é escolhida para avaliar o sistema para um dado cenário específico. Nossa primeira contribuição é uma investigação sobre se é preferível ter um grande número de saltos curtos ou um pequeno número de saltos longos em uma rede sem fio de múltiplos saltos, usando uma métrica proposta que é denominada eficiência da informação em múltiplos saltos agregada. Para sistemas de saltos simples, nós revisitamos a abordagem da capacidade de transmissão para estudar protocolos de acesso ao meio que usam transmissões assíncronas e permitem retransmissões de pacote, mostrando quando a habilidade de sentir a portadora é mais vantajosa que transmissões síncronas, e vice-versa. Nós também formulamos o problema de otimização da vazão efetiva de um enlace e a vazão espacial da rede para encontrar a combinação da probabilidade de acesso ao meio, taxa de código e número máximo de retransmissões que maximiza cada métrica sobre restrições de perda de pacotes e estabilidade de fila, evidenciando quando elas tem (ou não) a mesma solução. Além disso, nós analisamos o valor esperado da soma das taxas máximas atingíveis sobre uma dada área - ou capacidade espacial - baseados nas regiões de capacidade dos códigos gaussianos ponto-a-ponto para duas regras de decodificação: (i) tratar interferência como ruído (IAN) e (ii) detectar conjuntamente os sinais interferentes mais fortes tratando os outros como ruído (OPT), provando as vantagens da segunda. Nós adicionalmente demonstramos que, quando as mesmas regras de decodificação e densidade da rede são consideradas, o esquema que atinge a capacidade espacial sempre tem um melhor desempenho que a estratégia da melhor taxa pré-determinada (abordagem mais usual). Com esses resultados em mão, nós discutimos linhas gerais para a construção de algoritmos ad hoc adaptativos que melhorariam os fluxos de informação pela rede de interferência, respeitando as restrições internas e externas dos nós.

Palavra-chave: Sistema de comunicação sem fio

Contents

To my family: Regina, Eliseu, Celina, Carolina and Dada

Society does not consist of individuals, but expresses the sum of interrelations, the relations within which these individuals stand.

Karl Marx, Grundrisse (1857)

Acknowledgments

First of all I would like to thank my professors Matti Latva-aho and Paulo Cardieri for their friendly and flexible supervision, giving me fully support whenever needed. In addition, I want to thank professor Markku Juntti for the valuable advices regarding the paper work for the credit transference. I also want to thank professors Michel Yacoub, Jose Cândido, Gustavo Fraidenraich, Renato Lopes and Pedro Peres for the time that we spent together at Unicamp. I would like to thank Mariam Kaynia, prof. Marios Kountouris and prof. William A. Kretzschmar Jr. for our collaborative work. A special thanks goes to Jeff Wildman who, besides being a research collaborator, has also helped me in the final proof-reading of this thesis. Besides, I want to express my gratitude to Giuseppe Abreu for first inviting me to come to Oulu.

In addition, I would like to thank all friends and colleagues that I have made in my years in CWC and WissTek, specifically Álvaro, Antti, Behnaam, Brettinho & Laura, Carliche & family, prof. Carlos Pomalaza-Raez, Chatu, Davide & family, Franfresco K, Giuseppe Destino & family, Jari, Jani, Joukko, Heloísa, Hirley, Kalle, Kaveh, Keeth, Maice, Marian, Mehdi, Manosha, Markus, Namal, Nuwan, Pekka, Petri, Portelinha, Rubens, Satya, Simon, Sumudu, Qiang, Stefano, Ugo, Visa amongst others. I also want to thank prof. Daniel Benevides da Costa for indicating me to the available position in CWC when I was finishing my master studies back in 2008.

Besides, I want to thank my friends Abel, Boy, Carol & Primo, David & Saila, Fernanda & family, Free & Ju, Frangão, Guerrero & Karina, Guilherme & family, Marcin & Mira, Mauricio & family, Mucin & Ana, Pira, Piu, Rafaela & Dorival, Renan & family, Ricardo, Righettão, Samango, Xandy & Tati, Toni, Thalita, Zolezzi, my Marimbondos mates (Julião, Dida, Lilão, Shaq, Morde, Lambe, Bixona, Bingola, Bixo, Perninha, Samir, Xupa, Palmito, B2, Predador, Conan etc), people from CABS and Pôneis 02. I would like to thank all my Brazilian jiu-jitsu bros from Oulun Jujutsu, Equipe Franco Penteado, Jiu-jitsu Unicamp and Oulun Kamppailuklubi. OSS.

Furthermore, I would like to thank my parents Regina and Eliseu, my grandmother Celina, Dada and my girlfriend Carolina for their full-time support. I also want to thank my grandfather Alfeu (in memoriam), my aunt Eliete, my uncles Pedro and Roberto, my cousins Lilian, Kátia, César, Nath & Léo, L. Henrique, L. Felipe, tia Mô, Carolina's family and Vanda. Besides, I would like to thank my little friends Honka, Txuca, Luigi and the whole prole.

I also would like to thank the whole administrative stuff from CWC and Unicamp, more specifically Anu, Edson, Elina, Eija, Hanna, Jari, Kirsi, Mazé, Noêmia, Seija, Varpu and Timo. I want to express my gratitude to Infotech Graduate School, Finnish Funding Agency for Technology, and Innovation (Tekes), Nokia Siemens Networks, Elektrobit, HPY:n Tutkimussäätiö Foundation, Finnish Foundation for Technology Promotion, Nokia Foundation, Tauno Tonningin Säätiö, and Riitta and Jorma J. Takanen Foundation for the financial support of this work.

List of figures

List of tables

List of acronyms

2-D	2-dimensional
AIE	aggregate information efficiency
AMIE	aggregate multi-hop information efficiency
ARQ	automatic repeat query
act	active
app	apparent
CDMA	code-division multiple access
CSMA	carrier sensing multiple access
CR	coding rate
DSSS	direct sequence spread spectrum
dom	dominant
EFP	expected forward progress
eff	effective
FH	frequency hopping
G-ptp	Gaussian point-to-point
IAN	interference as noise decoder
IE	information efficiency
ind	individual
JD	joint detection
MAC	multiple access control
MIMO	multiple-input-multiple-output

max	maximal
min	minimal
mh	multi-hop
OSI	open system interconnection
OPT	optimal decoder
QAM	quadrature amplitude modulation
PPP	Poisson point process
RA-TpC	random access transport capacity
RS	Reed-Solomon
RX	receiver
SIC	successive interference cancellation
SIR	signal-to-interference ratio
SINR	signal-to-interference-plus-noise ratio
SS	spread spectrum
sens	sensing
sh	single-hop
TmC	transmission capacity
TpC	transport capacity
TX	transmitter
up	upper bound

List of symbols

A	area of a given region
$\mathcal{A}$	a set of transmitters
α	path loss exponent
B	bandwidth
β	signal-to-interference-plus-noise ratio threshold
$\mathcal{C}$	spatial capacity
$\mathcal{CN}(\cdot,\cdot)$	complex symmetric Gaussian random variable
D	subspace of a topological space
d	distance
$\delta(\cdot)$	Dirac delta function
$d_{\max}$	transmission and reception range
$\mathrm{E}[\,\cdot\,]$	expected value operator
$\mathcal{E}$	outage event
$\mathrm{erf}(\cdot)$	standard error function
$\mathrm{erfi}(\cdot)$	imaginary error function
ϵ	packet loss or outage constraint
Φ	point process (normally a 2-dimensional Poisson point process)
$f(\cdot)$	general notation of a function
g	complex channel gain
ϕ	auxiliary angle
$\Gamma(\cdot)$	Euler Gamma function

$\mathcal{H}$	capacity region
h	channel gain (power)
i	auxiliary variable
j	auxiliary variable
K	auxiliary variable
k	auxiliary variable
κ	constant
$\Lambda(\cdot)$	measure of a topological space
λ	intensity (density) of a Poisson point process
λ_{a}	density of active links
λ_{s}	density of successful links
M	message
$\mathcal{M}$	aggregate multi-hop information efficiency
m	maximum number of retransmissions (or message in Chapter 2)
μ	arrival rate
$N(\cdot)$	number of elements of a set/space
$\mathbb{N}$	natural numbers
$\mathcal{N}$	neighborhood set
n	auxiliary variable (natural number)
Pr[·]	probability that a given event occurs
P	power
P_{b}	back-off probability
P_{min}	receivers' sensitivity
P_{o}	outage probability
P_{pkt}	packet error probability
p	probability that a node is active

p_n	error probability of the G-ptp code
Q	power constraint
Q_k	queue state of node k
R	link rate
$\mathbf{R}$	rate tuple
$\mathbb{R}$	real numbers
$\mathcal{R}$	effective link throughput
r	auxiliary variable
ρ	offered load of a queuing system
S	topological space
$\mathcal{S}$	network spatial throughput
s	sensing range
σ^2	variance of transmit power using G-ptp
T	period of time
$\mathcal{T}$	transmission capacity
$\mathcal{T}^*$	optimal transmission capacity
t	auxiliary variable
t_0	arbitrary point in time
θ	expected value of the service process
$\mathcal{W}_0(\cdot)$	principal branch of the Lambert W function
ν	auxiliary angle
X	auxiliary variable
x	auxiliary variable
Y	auxiliary variable
y	auxiliary variable
Z	auxiliary variable
z	auxiliary variable

Publications related to the thesis

[J7] J. Wildman, P. H. J. Nardelli, S. Weber and M. Latva-aho: "Understanding how directive antennas affect the spatial throughput in interference networks" in preparation, Jul. 2013.

[J6] P. H. J. Nardelli, P. Cardieri, William A. Kretzschmar Jr. and M. Latva-aho: "Interference networks: A complex system view," in preparation to *IEEE Communications Magazine* (available in ArXiv), May 2013.

[J5] P. H. J. Nardelli, P. Cardieri and M. Latva-aho: "Spatial throughput of Poisson wireless networks under different decoding rules," submitted to *IEEE Transactions on Mobile Computing*, Apr. 2013.

[J4] P. H. J. Nardelli, M. Kountouris, P. Cardieri and M. Latva-aho: "Throughput optimization in wireless networks under stability and packet loss constraints," accepted to *IEEE Transactions on Mobile Computing*, Apr. 2013.

[J3] P. H. J. Nardelli, M. Kaynia, P. Cardieri and M. Latva-aho: "Optimal transmission capacity of ad hoc networks with packet retransmissions," *IEEE Transactions on Wireless Communications*, Aug. 2012.

[J2] P. H. J. Nardelli, P. Cardieri and M. Latva-aho: "Efficiency of wireless networks under different hopping strategies," *IEEE Transactions on Wireless Communications*, Jan. 2012.

[J1] P. H. J. Nardelli, P. Cardieri and M. Latva-aho: "Maximising transmission capacity of ad hoc networks via transmission system design," *IET Electronics Letters*, Mar. 2011.

[B1] P. Cardieri and P. H. J. Nardelli: "A survey on characterization of capacity of ad hoc wireless networks," in *Mobile Ad-Hoc Networks: Applications,* Publisher: InTech, Jan. 2011.

[T1] P. Cardieri and P. H. J. Nardelli: "Measuring capacity in wireless ad hoc networks," in *9th International Information and Telecommunication Technologies Symposium* (I2TS), Rio de Janeiro, Brazil, Dec. 2010.

[C9] P. H. J. Nardelli, P. Cardieri and M. Latva-aho: "Spatial capacity of ad hoc wireless networks with Poisson distributed nodes," in *IEEE Wireless Communications and Networking Conference* (WCNC), Paris, France, Apr. 2012.

[C8] P. H. J. Nardelli, M. Kountouris, P. Cardieri and M. Latva-aho: "Stable transmission capacity in Poisson wireless networks with delay guarantees," in *IEEE Wireless Communications and Networking Conference* (WCNC), Paris, France, Apr. 2012.

[C7] M. Kaynia, P. H. J. Nardelli and M. Latva-aho: "Evaluating the information efficiency of multi-hop networks with carrier sensing capability," in *IEEE International Communications Conference* (ICC), Kyoto, Japan, Jun. 2011.

[C6] P. H. J. Nardelli, M. Kaynia and M. Latva-aho: "Efficiency of the ALOHA protocol in multihop networks," in *IEEE International Workshop on Signal Processing Advances in Wireless Communications* (SPAWC), Marrakesh, Marocco, Jun. 2010.

[C5] M. Kaynia, P. H. J. Nardelli, P. Cardieri and M. Latva-aho: “"On the optimal design of MAC protocols in multi-hop ad hoc networks,” in *Sixth Workshop on Spatial Stochastic Models for Wireless Networks* (SpaSWiN), Avignon, France, Jun. 2010.

[C4] P. H. J. Nardelli and G. T. F. de Abreu: “On hopping strategies for autonomous wireless networks,” in *IEEE Global Communications Conference* (Globecom), Hawaii, USA, Nov. 2009.

[C3] P. H. J. Nardelli, G. T. F. de Abreu and P. Cardieri: “Multi-hop aggregate information efficiency in wireless networks,” in *IEEE International Communications Conference* (ICC), Dresden, Germany, Jun. 2009.

[C2] P. H. J. Nardelli and G. T. F. de Abreu: “Analysis of hopping strategies in multi-hop wireless networks,” in *IEEE Workshop on Positioning, Navigation and Communication* (WPNC), Hannover, Germany, Mar. 2009.

[C1] G. Rahmatollahi, M. D. P. Guirao, P. H. J. Nardelli and G. T. F. de Abreu,: “Aggregate information efficiency in IR-UWB ad hoc wireless sensor networks,” in *IEEE Workshop on Positioning, Navigation and Communication* (WPNC), Hannover, Germany, Mar. 2009.

Chapter 1

Introduction

In the end of the 70's, wireless ad hoc networks attracted a vivid attention from from the telecommunications community due to their cheap and flexible implementation [1]. During that time, however, the deployment of practical systems applying such a concept was limited by the available technology, which also constrained further research developments [2]. In the middle 90's, the increasing processing power of hardware and the widespread use of personal computers as well as other mobile devices provided the technological basis needed for real-life ad hoc networks, stimulating once again studies on this subject. Thereafter, important issues regarding the design of such networks have been addressed, including medium access control algorithms, routing protocols, energy consumption, amongst others [3].

We can also identify many features of the ad hoc concept in the upcoming generations of cellular systems, where fully centralized systems are unable to provide the efficiency required by high data rate applications. The main idea behind such systems is to build a multi-layer network where macro-base-stations coexist with a great number of smaller cells, which in turn operate in a more distributed fashion (e.g. the concept of femto-cell networks [4] or more general heterogeneous networks [5]).

Despite their practical appeal and unquestionable technological evolution, the fundamental limits of ad hoc wireless networks still remain elusive and constitute an active research area [6, 7]. One of the main research challenges is the characterization of the co-channel interference since the behavior and the operating parameters of each transmit node may affect other concurrent transmissions.

Situating in this context, this thesis targets those issues by statistically assessing the aggregate network throughput under different conditions. Specifically we attempt to answer *when* and *how* the network operator should employ specific communication strategies such as packet retransmissions, closest neighbor routing or carrier sensing multiple access (CSMA) protocol. To do so, we study wireless networks whose nodes are statistically described with a Poisson point processes (PPP), then apply recently developed methods of stochastic geometry [8, 9, 10, 11, 12, 13].

But before we go deeper into our results, we will first present a historical perspective of the capacity/throughput analysis for ad hoc networks, followed by an informal statement of the interference network problem, the focus of this thesis, and discuss some possible ways to cope with it.

1.1 Literature review

In this section we introduce the most important results concerning the capacity/throughput of ad hoc, interference-limited wireless networks. Particularly we classify these contributions according to the analytical approach used: statistical-based, deterministic or information-theoretic. The *expected forward progress* metric - introduced in Section 1.1.1 - can be cited as an example of a statistical approach. Another example of a statistical-based metric is the *transmission capacity*, which is presented in Section 1.1.2. We also describe in Section 1.1.3 another branch of the statistical analysis based on spatial densities. A deterministic way to evaluate the throughput of wireless networks is introduced in Section 1.1.4, while the most relevant information-theoretic contributions to the interference channel (where ad hoc networks are a special case) are reviewed in Section 1.1.5. Aside from these results, we also discuss other relevant works in Section 1.1.6, where we overview the literature of timing channels, scheduling policies, stability issues and delay analysis in the context of wireless networks.

1.1.1 Expected forward progress and subsequent metrics

In the late 70's, Kleinrock and Silvester published one of the first key results about the statistical performance evaluation of wireless networks [14], where they investigated the relationship between throughput and transmission range in multi-hop systems operating under ALOHA protocol. In [15], Takagi and Kleinrock further developed that framework by considering CSMA protocols. Specifically both works were based on a metric referred to as *expected forward progress* (EFP), measured in [m] and defined in such a way to capture the trade-off between the one-hop normalized throughput and the average one-hop length. Mathematically the EFP is defined as

$$\text{EFP} = d^{*}\ (1 - P_{\text{o}}), \tag{1.1}$$

where d^{*}, measured in [m], is the distance that a packet travels towards its final destination and P_{o} is the single-hop link outage (packet error) probability such that $1 - P_{\text{o}}$ measures the normalized link throughput.

Nelson and Kleinrock generalized in [16] these previous contributions considering scenarios where the transmission range and the capture range (distance that defines whether a node can cause collision) are different. Another extension was proposed in [17], where Hou and Li introduced the concept of *hopping strategy* – a policy used by the transmitters to determine which node in a pool of potential receivers should be selected to relay their packets based on their EFP. In 1987, Kleinrock and Silvester published a reference tutorial [18] containing all these and other important results found until then.

The aforementioned results, despite their great importance, are based on a simple physical layer modeling, where packet collisions are unrelated to relevant aspects of the transmission system design as, for example, the spread spectrum (SS) scheme, the modulation technique and/or the error-correcting code that are used by the communication links. Knowing this limitation, Sousa and Silvester incorporated in the previous studies a more realistic characterization of outage events (packet collisions) [19], evaluated then the optimal transmission range for networks whose links employ a direct sequence spread spectrum (DSSS) technique. Their main contribution was to associate the outage events with the required signal-to-interference-plus-noise ratio (SINR) threshold defined by the SS scheme considered. Following this line, the EPF analysis can be extended to more realistic

channel characterizations as in [20], where Zorzi and Pupolin studied the network performance in the presence of fast-fading and shadowing.

In any case, the advantages of setting modulations with high cardinality or powerful error-correcting codes had not been captured by those contributions since the EPF is built upon the normalized throughput. To extend the EPF idea to understand the trade-offs involving modulation-coding schemes, Subbarao and Hughes introduced the concept of *information efficiency* (IE), measured in [(bits·m)/s/Hz] and defined as the product of the EFP and the link rate (spectral efficiency) [21], yielding

$$\text{IE} = \text{EFP}\ R = d^*\ (1 - P_\text{o})\ R, \tag{1.2}$$

where R, measured in [bits/s/Hz], is the link rate determined by the modulation cardinality and the coding rate of the error-correcting code.

In other words, to go from the EFP formulation to the IE, the normalized throughput metric $(1 - P_\text{o})$ was refined by considering that every link is transmitting with rate (spectral efficiency) R defined by the modulation-coding scheme. The authors then applied this idea to assess networks whose communication links employ M-ary quadrature amplitude modulation (M-QAM) with Reed-Solomon (RS) correcting codes. Following this approach, several other studies have been carried out to evaluate the performance of different strategies as, for example, frequency hopping (FH) [22], direct sequence mobile networks [23], direct sequence code-division multiple access (CDMA) with channel-adaptive routing [24] and coded multiple-input-multiple-output (MIMO) FH-CDMA [25].

It should be noted that, from the perspective of the whole network, the IE of a link does not tell much about how efficiently the radio channel is being spatially reused. Bearing this aspect in mind, the authors extended in [26] the IE concept by considering the network *aggregate information efficiency* (AIE), measured in [(bits·m)/s/Hz/m^2] and defined as the sum of the IE of all active links divided by the area under analysis. This metric reflects the spatial density of the active links throughout the network area[1] and it is mathematically defined as follows:

$$\text{AIE} = \frac{1}{A} \sum_{i \in \mathcal{A}} \text{IE}_i = \lambda\ d^*\ (1 - P_\text{o})\ R, \tag{1.3}$$

where $\mathcal{A}$ is the set of concurrent transmissions and λ [active links/m^2] refers to the spatial density of active links over the network area. The last equality holds in the symmetric case so that all links have the same statistical characterization.

Using this approach, the authors studied transmission systems using M-QAM and RS correcting codes together with automatic repeat query (ARQ) retransmission scheme, providing insights on the best design setting for single-hop ad hoc networks. In [27], the same framework has been applied to assess the effects of outage events on the AIE. Following this line, a generalization of the AIE idea is proposed in Chapter 3 to compare the performance of different hopping strategies in multi-hop scenarios. The AIE metric is also related to the *transmission capacity* and other spatial density metrics, which are our focus in the next two sections.

1.1.2 Transmission capacity

The *transmission capacity* (TmC), measured in [bits/s/Hz/m^2], was firstly introduced in 2005 to evaluate how efficiently the information bits are transmitted in the time, frequency and spatial domains

[1] we will come back to this later in Section 1.1.3

[28]. Particularly in this first work, the authors defined the TmC as the highest spatial throughput - sum of the throughputs of all successful links normalized by the network area - achieved when the network is in its *optimal contention density*, while an outage constraint, i.e. a maximum outage (packet error) probability, is required. Mathematically, the TmC is defined for the symmetric case as

$$\text{TmC} = \lambda^* \, (1 - \epsilon) \, R, \tag{1.4}$$

where λ^* is the optimal contention density in [active links/m^2] and ϵ is the outage constraint. To find λ^*, the probability P_{o} that an outage event occurs during the packet reception should be analyzed as a function of both the density of active links λ and the SINR threshold required for a successful detection. In [28], the authors have considered that the link rate R and the SINR threshold assume constant values and therefore they cannot be optimized.

Using this definition, lower and upper bounds of the TmC have been derived for single-hop networks whose links employ FH-CDMA and direct sequence CDMA techniques, and nodes are spatially distributed following a 2-dimensional (2-D) homogeneous Poisson point process (PPP). Interestingly the authors made use of stochastic geometry concepts for modeling the spatial distribution of nodes over different network realizations, which will be discussed later in Chapter 2.

After this first contribution, the TmC approach has been extensively applied to evaluate well-known communication strategies as, for instance, interference cancellation [29], threshold transmissions [30], channel inversion [30], bandwidth partitioning [31], fractional power control [32], MIMO systems [33] and directional antennas [33]. In [34], Weber et al. presented a monograph containing these and other results.

Besides, other extensions of the TmC framework have been proposed to incorporate other aspects of ad hoc networks such as multi-hop transmissions and more general spatial distributions. In [35] Andrews et al. proposed the *random access transport capacity* (RA-TpC) to capture the particularities of networks where communication over multiple hops is allowed, and obtained the the optimal number of hops for the scenario under analysis. In [36] Vaze further extended the RA-TpC framework by considering a bounded number of packet retransmissions and correlation between the spatial events. Ganti et al. adapted the TmC approach to incorporate general classes of fading and spatial distributions in the high signal-to-interference ratio (SIR) regime [37]. Multicast transmissions in multi-hop scenarios are analyzed in [38], while spectrum-sharing schemes where primary and secondary users coexist are the focus of [39].

In this thesis, the TmC approach is also further developed to incorporate packet retransmissions, contention-based MAC protocols and queue stability. Such results are presented in Chapters 4 and 5.

1.1.3 Spatial density metrics

In 2003 Bacelli et al. presented at the Allerton conference a work, whose journal version was afterwards published in [40], that provided the basis for a different framework to analyze upon they built a different framework to analyze distributed wireless networks. In the development of their approach, the authors also introduced metrics with the same nature of the ones previously described. Here we will devote our attention to the history of such a branch, making the necessary parallels accordingly.

As mentioned before, the authors in [40] introduced a sophisticated treatment of what they called *density of successful transmissions*, defined as the mean number of transmissions per unit area and

measured in [1/m^2]. Based on this definition and considering the slotted-ALOHA access mechanism, they quantified the trade-off between spatial reuse (density of active links) and the successful transmissions (probability that the communication in the active links are successful) based on properties of Poisson point processes and stochastic geometry. Interestingly, they derived an elegant closed-form equation to the success probability as a function of the density of nodes λ, finding then the optimal density of active links λ^*, proceeding similarly to the transmission capacity optimization.

In this same paper, they also slightly modified their scenario to assess the trade-off involving hop length, density of active links and success probability. Employing a metric named *density of progress*, they proposed an approximation to better understand the optimal progress in multi-hop scenarios. In this case, the proposed metric quantifies how the packets are progressing per units of area, measuring it in [(packets·m)/m^2].

Breaking the packets using Shannon capacity formula (as when going from EFP to IE), the density of progress can be converted to the *density of transport* [41], evaluating the performance in [(bits·m)/s/Hz/m^2]. From this perspective, the authors derived the optimal transmission distance d^* for given density λ and slotted-ALOHA access probability p. As one can notice, this metric resembles the AIE presented in equation (1.3) and they indeed have the same physical meaning. In our point of view, such different nomenclatures have arisen from the path that the authors took to develop their analyses, emphasizing the aspects they found more valuable.

Following the same line of thought, the authors also described in [41] the *density of throughput* as the sum rate (also obtained by breaking the packets using Shannon formula) per unit of area, measured thus in [bits/s/Hz/m^2]. As before, the density of throughput has the same physical meaning as the spatial throughput described in the previous section.

For a didactic exposition of these spatial density metrics, one can refer to [41, Sec. III]; the monographs [10, 11] provide a complete presentation of such a research line. All results presented in the following chapters of this thesis are also built on it.

1.1.4 Deterministic approach

Gupta and Kumar introduced in [42] a deterministic way to characterize throughput capacity of ad hoc networks, where they evaluated the relation between the achievable transmission rates and the source-destination distances by using the *transport capacity* (TpC), measured in [bits·m]. They applied such a methodology to quantify how many bit-meters can be sustained by the network when the number of nodes grows to infinity, showing the scaling laws or asymptotic capacity of the network for distinct scenarios based on geometric arguments.

Following this approach, many authors have investigated the TpC for a great variety of scenarios. For example, Liang and Kumar [43] discussed cooperative strategies that are able to improve the TpC scaling laws, while Xue et al. studied the network capacity in fading environments [44]. The effects of path-loss on the asymptotic behavior of the network is analyzed in [45]. In 2006, Xue and Kumar published a reference tutorial [46] presenting these and other contributions that use the TpC framework.

In [47], Grossglauser and Tse introduced an innovative scheme to improve the TpC when mobility is allowed. They showed that, in a scenario with mobile nodes operating under a two-hop relaying transmission strategy, the per-node throughput capacity remains constant as the number of nodes in the network increases, at the cost of unbounded packet delay. This important result motivated

other researchers to further investigate the trade-off between throughput capacity and delay in mobile wireless networks [48, 49, 50].

The asymptotic behavior of the network has been further studied under other different perspectives such as in [51, 52, 53]. We also highlight here two other works [54, 55] that use an unconventional perspective to derive some fundamental properties of wireless networks relying on established methods of electrodynamic and electromagnetic theories. Even though these lines of work are still active, the deterministic approach to quantify the capacity of wireless networks is out of the scope of this thesis.

1.1.5 Information-theoretic results

The interference channel problem was first described using the information-theoretic approach by Shannon in 1961 [56]. Nevertheless, it was only after fourteen years of this exposition that a relevant work regarding the interference channel was published, when Carleial presented a scenario where the communication links under strong interference can achieve rates as high as in the case without interference [57]. Based on that, Carleial further generalized the interference channel problem in [58], obtaining many insights on its capacity region. After this milestone, other contributions have been presented over the years, for example: [59, 60, 61, 62, 63, 64, 65, 66].

Despite all efforts, the capacity region of the interference channel is still unknown and a fruitful research topic [67], where some promising ideas have been recently proposed. For instance, the *interference alignment* strategy was introduced by Cadambe and Jafar [68] to determine the degrees of freedom of the K-user interference channel, showing how every link can get "half of the cake". In 2011, Berry and Tse dealt with the interference channel combining information theory and game theory [69]. We can refer to a recent book by El Gamal and Kim as a comprehensive survey of the most important results and challenges on the field [70].

The contribution to the interference channel studies that is the most relevant for the study carried out in this thesis was proposed by Baccelli et al. in [71]. There the authors derived the capacity region of the interference channel when many pairs using Gaussian point-to-point (G-ptp) codes, showing the decoding rule used to achieve it.

We will review the coding-decoding scheme that achieves this capacity region in Chapter 2, while in Chapter 6 we will investigate the effects of the capacity-achieving strategy on the network spatial throughput. In Chapter 7 we will also discuss the feasibility of employing such a scheme.

1.1.6 Other related works

In the seminal paper [72], Ephremides and Hajek stated many issues regarding the "unconsummated union" between information theory and communication networks. The authors provided a detailed description of the main problems that involve the information-theoretic approach to analyze communication networks using the open system interconnection (OSI) layer division framework. For instance, they cited protocol overhead, multiple access schemes and routing as higher layers' aspects that play an important role in the network performance that have been already the target of information-theorists. In fact, they successfully indicated in 1998 which direction the research in wireless networks would go and, nowadays, the most part of their comments are still valid.

One particular aspect from communications networks that is worth mentioning is the bursty behavior of data sources that generate information according to a given (stochastic) process. Gallager first introduced in [73] the idea of *timing channel*, where the author analyzed the communication between a source-destination pair considering packet arrivals that follow a Poisson process. In 1996, Anantharam and Verdú derived important bounds of the Shannon capacity when bits that arrive in the system are queued before being served [74] . In addition to such works, we can cite, amongst others, [75, 76, 77, 78] as examples that have provided insights on the theory of timing channels.

An interesting detail is that those works applied several analytical tools firstly developed for control theory. Ephremides and Verdú stated already in 1989 the importance of control and optimization theory in the analysis of communication networks [79]. From this perspective, Tassioulas published a series of papers [80, 81, 82] devoted to study stability issues of queuing systems while the network throughput is optimized. The idea behind these contributions is to find the best way to dynamically allocate the network resources to the nodes/links during the access and routing procedures, stimulating the development of admission control and scheduling policies. One important practical result that came from these studies is the *back-pressure algorithm* [80] used to perform resource allocation in multi-hop networks. Following this line of research, a wide range of works addressing stability, resource allocation and scheduling have been proposed in the literature of wireless networks, as summarized in [83, 84].

In the context of this thesis, we can cite the recent works by Haenggi and its group that attempt to include aspects of queuing theory into the stochastic-geometric analysis of wireless networks. Specifically in [85], Stamatiou and Haenggi gave the first step towards the combination of the PPP framework and queuing theory in order to study single-hop ad hoc networks, evaluating their stability and average delay. This work was also extended to other scenarios [86]. In a recently accepted publication [87], Haenggi further developed the framework presented in [85] by assessing the *local delay* for several configurations of Poisson networks. Other contributions regarding delay aspects in Poisson networks can be found in [88, 89, 90, 91, 92]

In Chapter 5 we apply some of those concepts to cast throughput optimization problems where queue stability is guaranteed for all communication links in the network.

1.2 Informal statement: chatting in a party problem

We introduce the problem of people talking at a party as an illustration of the interference network that we will work in this thesis. Our goal with this informal statement is to provide some intuition and show how we, *humans*, attempt to cope with it, imagining some possible decisions and their effects on the network. Whenever we believe appropriate, we indicate which communication engineering strategy is associated to our informal statement.

Let us consider a couple going to a party.. When they arrive, there are only few people around talking to each other. In this situation, our reference couple can successfully have a chat; the others are talking in an acceptable intensity (transmit power is limited); they are most probably far from each other (randomly distributed over the area) and the background music (noise) is the main limiting factor of the conversation (noise-limited scenario). After an hour, however, more people have arrived and thus more people are chatting, increasing the interference level throughout the party place. Moreover, persons are getting closer and closer to our reference couple, which consequently starts facing

problems to communicate. The others start suffering the same problem as well. What should each person do to improve his/her own performance that is affected by external factors? If everyone does the same, is the network still functional or, in other words, are people able to chat in the party?

A straightforward decision when the interference from people in concurrent conversations is disturbing the couple under analysis is to speak louder (power control). This is in fact an optimal solution for a single couple; yet, everyone speaking louder harms the performance of the network and at the end of the day it is completely useless. This is easy to visualize in parties and restaurants when everyone is screaming when talking. So, even if it is optimal for one pair for a given fixed condition of the network, this is not a good decision for the network as whole because other people will also take the same decision of speaking louder. What else can be done then?

Another possible solution is to provide feedback regarding the success of what has been said (ARQ protocol); if the message was not clearly understood by the listener, he would inform the other who will repeat whatever he said before. This would work, but allowing for many repetitions would be inefficient since a successful communication might require many trials. Even worse, if the speaker has a lot to say (arrival process) and stays repeating the same thing for long periods, he would probably forget something (buffer overflow, unstable queues).

A different strategy that could be used by our reference speaker is to say things slowly (lower coding rates). This increases the chances of a successful understanding by her listener while it does not affect the others' chatting. A drawback of this is that when many people are talking at the same time, the speaker should talk very slow, which in turn negatively affect their communication efficiency.

We just listed some possible strategies that help people chat in a party when the number of concurrent conversations increases. As we can see, none of them alone can provide a successful answer for network variations, which also depends on personal limitations on forgetting things before saying or losing information after some communication attempts. Nevertheless, if we think how humans react in a real situation, they use combinations of the possible strategies and they are normally able to talk. Which strategies are employed and how to apply them are abilities learned and acquired from previous experiences.

From Chapter 3 to 6 we mathematically analyze some of the communication strategies informally described before, but considering a wireless network setting. We then discuss in Chapter 7 some implications of those results, indicating guidelines on how distributed (ad hoc) adaptive algorithms should be designed based on the network situation *perceived* by each node. In other words, we identify under which circumstances the strategies should be used and how to properly set the parameters so that the information flow is efficient throughout the whole network.

1.3 Contributions and outline of the thesis

The work presented in this thesis is fully concentrated on the statistical evaluation of the spatial throughput of wireless networks with Poisson distributed nodes. In the following, we outline this thesis, providing the main contributions contained in each chapter.

- **Chapter 2:** We present the mathematical background of this thesis. First we review the capacity region of Gaussian point-to-point codes for interference networks. We then revisit some of the main properties of stochastic geometry and point process theory that are applied in wireless

network modeling with focus on Poisson point processes (PPPs). Finally we investigate how the coding-decoding scheme and the PPPs determine together the system performance.

- **Chapter 3:** We introduce the *aggregate multi-hop information efficiency* metric to quantify the spatial throughput in networks that allows for multi-hop transmissions, evincing when the closest-neighbor hopping strategy is preferable to the furthest-neighbor, and vice-versa.

- **Chapter 4:** We redefine the TmC metric to incorporate packet retransmissions and asynchronous MAC protocols. Based on that, we find the number of retransmissions that optimize the TmC for unslotted ALOHA, slotted ALOHA, CSMA with sensing at the transmitter and CSMA with sensing at the receiver. We also compare the optimal solutions for each of those MAC protocols, showing the conditions when one is preferable to the others.

- **Chapter 5:** We study the throughput optimization problem under packet loss and queue stability constraints. We analytically derive the combination of medium access probability (slotted ALOHA), coding rate, and maximum number of retransmissions that maximizes the spatial throughput, considering that packets arrive at the transmitters following a geometrical distribution. We also discuss when the per-link throughput optimization does or does not provide the optimal solution in terms of the network spatial throughput.

- **Chapter 6:** We analyze the expected maximum spatial throughput based on the capacity regions of Gaussian point-to-point codes under two decoding rules, namely (i) treating interference as noise, and (ii) jointly detecting the strongest interfering signals, treating the others as noise. We also compare these results to the ones obtained for a scenario where transmitters code their messages at predetermined fixed rates that are tuned to optimize the average spatial throughput (this is the approach used in the previous chapters), regardless of particular realizations of the network. We analytically show that, when the same decoding rule and network density are considered, the spatial-capacity-achieving scheme always outperforms the spatial throughput obtained with the best predetermined fixed rate strategy.

- **Chapter 7:** We discuss the results presented in the other chapters and state several claims about the optimal design setting as a function of the network condition. Based on these claims, we indicate how an adaptive ad hoc algorithm should be designed so as to improve the system performance.

- **Chapter 8:** We conclude the thesis and provide some possible future directions based on this work.

It is important to note that the core of our mathematical results are found from Chapter 3 to Chapter 6. In each of them, we model the network and use the performance metric in such a way that the effects of the communication mechanisms under analysis are properly captured. Hence, even though the essence of the network modeling is the same, each chapter is based on different assumptions, which are justified therein. As mentioned before, we discuss the implications of those results in a more general setting in Chapter 7.

1.4 Author's publications related to the thesis

This thesis is based on two published international journal papers [93, 94], one accepted journal [95] (conference version [96]) and one submitted journal [97] (conference version [98]), in which the author had the main responsibility in the analytical derivations and the writing procedure.

Besides, the author published another journal [99] and other seven related conference papers [100, 101, 102, 103, 104, 105, 106] that are not covered by this thesis. The author also partially contributed in the preparation of a survey concerning the different ways to measure capacity in ad hoc networks [107], which served as the basis of a tutorial presentation [108].

At the time that this thesis was finished, the author was working on two other related publications: one magazine paper targeting a complexity science view of the interference network problem, and one journal paper (in collaboration with Jeffrey Wildman and Prof. Steven Weber) attempting to characterize and optimize the spatial throughput when directive antennas are employed.

Chapter 2

Definitions and mathematical background

2.1 Coding-decoding scheme

This section reviews the capacity region of Gaussian point-to-point (G-ptp) codes for an arbitrary number of communication pairs, which was firstly stated by Baccelli et al. in [71, Sec. II] and is the basis of the coding-decoding scheme used in this thesis.

For convenience let us assume a network with area A, measured in [m^2], where $K+1$ transmitter-receiver pairs (also called source-destination pairs) coexist[1]. Each source node $i \in [0,\ K]$ wants to transmit an independent message $M_i \in \left[1,\ 2^{nR_i}\right]$ to its respective destination i at rate R_i measured in [bits/s/Hz], where n is the codeword length. Let X_j be the complex signal transmitted by source $j \in [0,\ K]$ and let $Z_i \sim \mathcal{CN}(0,1)$ be the complex circularly symmetric Gaussian random variable that represents the noise effect at receiver i. The detected signal Y_i at receiver i is then:

$$Y_i = \sum_{j=0}^{K} g_{ij} X_j + Z_i, \tag{2.1}$$

where g_{ij} are the complex channel gains between transmitter j (TX$_j$) and receiver i (RX$_i$). We assume that every transmitted signal is subject to the same power constraint of Q, measured in [W/Hz], so the received signal between TX$_j$ and RX$_i$ is given by $P_{ij} = |g_{ij}|^2 Q$.

Each transmitter node uses a G-ptp code with a set of randomly and independently generated codewords $x_i^n(m_i) = (x_{i1}, ..., x_{in})(m_i)$ following i.i.d. $\mathcal{CN}(0, \sigma^2)$ sequences such that $0 < \sigma^2 \leq Q$, where $m_i \in \left[1,\ 2^{nR_i}\right],\ i \in [0,\ K]$. RX$_i$ receives a signal y_i^n over the interference channel given by (2.1) and then estimates the transmitted message as $\hat{m}_i(y_i^n) \in \left[1,\ 2^{nR_i}\right]$. An error event during decoding happens when the transmitted message differs from the estimated one. Therefore the error probability of the G-ptp code is:

$$p_n = \frac{1}{1+K} \sum_{i=0}^{K} \Pr[\hat{M}_i \neq M_i], \tag{2.2}$$

where $\Pr[\cdot]$ represents the probability that a given event occurs.

Next we use (2.2) to define the achievable rates and the capacity region for G-ptp codes.

[1] It is important to keep in mind that when $A = \mathbb{R}^2$, then $K \to \infty$.

Definition 2.1 (achievable rates and capacity region)**.** *Let $\overline{p}_n$ be the average of the error probability p_n over G-ptp codes where n is the codeword length. Then, a rate tuple $\mathbf{R} = (R_0, ..., R_K)$ is said to be achievable if $\overline{p}_n \to 0$ when $n \to \infty$. In addition, the capacity region using G-ptp codes is the closure of the set of achievable tuple rates $\mathbf{R}$.*

This definition is important in our context because the spatial-capacity-achieving setting always requires achievable rates, as we will discuss later. But before that, we apply Definition 2.1 to establish the the capacity region of G-ptp codes.

Theorem 2.1 (capacity region from [71])**.** *Let $\mathcal{A}$ be the set of all $K+1$ transmitters in the network. Let $\mathcal{A}_i$ denote a subset of $\mathcal{A}$ that contains TX$_i$ with $i \in [0,\ K]$ and $\bar{\mathcal{A}}_i$ its complement. RX$_i$ then observes a multiple access channel whose capacity region $\mathcal{H}_i$ is computed as*

$$\mathcal{H}_i = \left\{ \mathbf{R} :\ \sum_{k \in \mathcal{A}_i} R_k \leq \log_2 \left(1 + \frac{\sum\limits_{k \in \mathcal{A}_i} P_{ik}}{1 + \sum\limits_{j \in \bar{\mathcal{A}}_i} P_{ij}} \right) \forall\ \ \mathcal{A}_i \subseteq \mathcal{A} \right\}. \tag{2.3}$$

The capacity region $\mathcal{H}$ of the Gaussian interference channel with G-ptp codes is the intersection of the capacity regions $\mathcal{H}_i$ of all TX$_i$-RX$_i$ links with $i \in [0,\ K]$, i.e.

$$\mathcal{H} = \bigcap_{i=0}^{K} \mathcal{H}_i. \tag{2.4}$$

Proof. The proof of this theorem is found in[2], [71, Sec. II]. □

The capacity region stated above requires a decoder that treats some of the interferers as noise, while others have their messages jointly decoded with the desired one. This result is the basis of the optimal (OPT) decoder for G-ptp codes strategy. Next we present a corollary that states the achievable rates for OPT.

Corollary 2.1 (achievable rates for OPT decoder)**.** *Assuming that the noise is Gaussian and the TXs employ G-ptp codes, then the rate R_k associated with a given link TX$_k$-RX$_k$ is said to be achievable when the OPT decoder is employed if, and only if, the following inequality holds:*

$$R_k \leq \log_2 \left(1 + \frac{\sum\limits_{i \in \mathcal{A}_k^*} P_{ki}}{1 + \sum\limits_{j \in \bar{\mathcal{A}}_k^*} P_{kj}} \right) - \sum_{i \in \mathcal{A}_k^* \setminus \{k\}} R_i, \tag{2.5}$$

where $\mathcal{A}_k^*$ represents the subset of transmitters whose messages are decoded by receiver k and $\mathcal{A}_k^* \cup \bar{\mathcal{A}}_k^* = \mathcal{A}$ is the set of all active transmitters throughout the network.

Proof. To obtain (2.5), we proceed with a simple manipulation of equation (2.3) in order to isolate the rate R_k related to TX$_k$-RX$_k$ link, considering the subsets $\mathcal{A}_k^*$ that lead to achievable rates. □

[2]This theorem is a generalization of the Ahlswede's theorem [109] proposed for the two sender-two receiver case. More information about MAC and interference channels analyses can be found in [70, Chs. 4, 6]

Another possibility of decoder is simply treat all interfering signals as noise, denoting this strategy as interference-as-noise (IAN) decoding rule. This strategy is the one used in most chapters of this thesis as well as in the available literature in the field[3]. Based on Theorem 2.1 we can state the achievable rates under the IAN rule as follows.

Corollary 2.2 (achievable rates for IAN decoders)**.** *Assuming the noise is Gaussian and considering that TXs employ G-ptp codes, the rate R_k associated with a given link TX_k-RX_k is achievable when IAN decoders are used if, and only if, the following inequality holds:*

$$R_k \leq \log_2 \left(1 + \frac{P_{kk}}{1 + \sum\limits_{j \in \mathcal{A} \setminus \{k\}} P_{kj}} \right), \tag{2.6}$$

where $\mathcal{A}$ represents the set of active transmitters.

Proof. This is a special case of (2.3) assuming that RX_k only decodes the message of TX_k while the other TXs are treated as noise. □

We are now able to say whether a rate is achievable when IAN or OPT decoding rules are employed, given the SINR experienced by the receiver under analysis. In the next section, we introduce some basic properties of PPPs and how to apply them to statistically characterize the SINR distribution and outage events in wireless networks based on G-ptp codes described here.

2.2 Poisson point processes

Wireless ad hoc networks are generally composed of a random number of devices, whose positions are also random. This characteristic suggests that stochastic geometry can be a powerful tool for modeling and analyzing such networks [8, 9, 10, 11, 12, 13, 110]. In particular spatial point process theory provides the background necessary to characterize random patterns of points distributed in high dimensional spaces [111]. Specifically we consider here that the spatial distribution of nodes over the network area follows a Poisson point process (PPP).

In this section, we revisit the main properties of PPPs and apply them to study how the nodes affect each other based on the coding-decoding scheme and the channel modeling assumed (i.e. what is the power level of a signal emitted by a given node at any other node in the network?).

2.2.1 Basic properties

We introduce here the formal definition of PPPs and some of their fundamental properties. The mathematical formalism used here follows the notes presented in [111].

Definition 2.2 (general Poisson process)**.** *Let S be a space and Λ a measure on S. A given point process is defined as a Poisson point process on S if the following properties hold.*

- *For every compact set $D \subset S$, the count $N(D)$ has a Poisson distribution with mean $\Lambda(D)$.*

[3] A detailed discussion about when it is worth using IAN or OPT is presented in Chapters 6 and 7.

- *If $D_1, ..., D_n$ are disjoint compact sets, then $N(D_1), ..., N(D_n)$ are independent.*

Directly from this general definition, we can state the specific case used in this thesis, namely 2-dimensional (2-D) PPP.

Definition 2.3 (2-D PPP)**.** *A 2-D PPP is obtained when $S = \mathbb{R}^2$ and $\Lambda(D) = \int_D \lambda(x, y)\, dxdy$, where $\lambda(x, y) > 0$ is the intensity function of the spatial process and $(x, y) \in \mathbb{R}^2$.*

More specifically, we can define the case where a 2-D PPP is homogeneously distributed throughout the Euclidean space as follows.

Definition 2.4 (2-D homogeneous PPP)**.** *A 2-D PPP is called homogeneous when $\Lambda(D) = \lambda A(D)$, where the intensity of the process $\lambda > 0$ is constant throughout $\mathbb{R}^2$ and $A(D)$ denotes the area over D.*

We now use the definition presented above to state some interesting properties of 2-D homogeneous PPP, whose proofs can be found in [110], [111, Ch.1].

Property 2.1 (probability distribution [111])**.** *Let us consider a 2-D homogeneous PPP in $D \in \mathbb{R}^2$ with density λ. Let n denote the number of points contained in D. Then,*

$$\Pr[n \text{ in } D] = \frac{(\lambda A(D))^n}{n!}\, e^{-\lambda A(D)}. \tag{2.7}$$

Property 2.2 (Euclidean distance to nth neighbor [110])**.** *Let us consider a 2-D homogeneous PPP in $\mathbb{R}^2$ with density λ. Let x_n be the distance from a given point to its nth neighbor and $f(x_n)$ its probability density function (pdf). Then,*

$$f(x_n) = \frac{2\,(\lambda\pi x_n^2)^n}{x_n(n-1)!}\, e^{-\lambda\pi x_n^2}. \tag{2.8}$$

Property 2.3 (Euclidean distance to the furthest neighbor in a sector within a given maximum distance [110])**.** *Let us consider a 2-D homogeneous PPP in $\mathbb{R}^2$ with density λ. Let ϕ denote the angle that defines the sector of interest and d_{max} be the maximum distance considered. If x represents the distance between a given reference point and its furthest neighbor in the sector ϕ within the maximum distance d_{max}, then the pdf of x, referred as to $f(x)$, is*

$$f(x) = \frac{\lambda\phi x\; e^{-\lambda\phi x^2/2}}{e^{\lambda\phi d_{\text{max}}^2/2} - 1}. \tag{2.9}$$

Property 2.4 (superposition transformation [111])**.** *Let Φ_1 and Φ_2 be two independent homogeneous PPP with intensities λ_1 and λ_2, respectively. Then, a superposition between this two processes, denoted $\Phi_1 \cup \Phi_2$, is still a homogeneous PPP and it has intensity $\lambda_1 + \lambda_2$.*

Property 2.5 (independent thinning transformation [111])**.** *Let Φ_0 be a homogeneous PPP with intensity λ_0. Considering that each point of Φ_0 has an independent probability p to be active (or probability $1 - p$ to be deleted), we can then establish a new point process Φ_{a} with intensity λ_{a} to characterize the active elements of Φ_0. This transformation from Φ_0 to Φ_{a} is called independent thinning such that Φ_{a} is still a homogeneous PPP and it has intensity $\lambda_{\text{a}} = p\lambda_0$.*

Here we present two theorems of point process theory that will be fundamental in the derivations presented in this thesis. Their proofs are found in [8, Ap. A].

Theorem 2.2 (Campbell formula [8])**.** *Let Φ be a 2-D homogeneous PPP in $\mathbb{R}^2$ with intensity λ. If the set $\mathcal{A}$ denotes the points of a realization of Φ, then*

$$\mathrm{E}\left[\sum_{i\in\mathcal{A}} f(i)\right] = \lambda \int_{\mathbb{R}^2} f(x)\, dx, \tag{2.10}$$

where $f(\cdot)$ represents a measurable function $f(x) : \mathbb{R}^2 \to [0, \infty)$.

This theorem tells us that it is possible to compute the expected value (over different network realizations) of the sum of a function of the points of the process as the integral of the same function in $\mathbb{R}^2$.

Theorem 2.3 (Mecke-Slivnyak [8])**.** *Let the reduced Palm distribution be the distribution of a point process conditioning on the existence of a point located at x, but not counting it. Then, for a homogeneous PPP, the reduced Palm distribution is equal to the distribution of the PPP .*

In other words, Theorem 2.3 allows us to include a point in a homogeneous PPP without affecting the distribution of the other points.

2.2.2 Applying PPPs to model wireless networks

We now focus on the application of the concepts previously stated to model wireless ad hoc networks. Let us consider an infinite network (i.e. $\mathbb{R}^2$) composed by a random set $\mathcal{A}$ of nodes that are actively transmitting information to their respective receivers at some time during a specific observation period related to a packet transmission using G-ptp codes[4]. We then associate such a period to a realization of a 2-D homogeneous PPP denoted by Φ, whose density (intensity) is λ [nodes/m^2]. We also assume the *high mobility random walk model* [10] so each observation period can be analyzed an independent realization of Φ (refer to the application of the displacement theorem in [10, Ex. 1.3.10] for more details).

As the channel model, we consider a composition between a deterministic distance-dependent path-loss with exponent $\alpha > 2$ and a channel gain (either random or fixed) [113] so the detected power P_{ij} at RX$_i$ due to TX$_j$ is $P_{ij} = |g_{ij}|^2 Q = h_{ij} d_{ij}^{-\alpha} Q$, where d_{ij} and h_{ij} denote the distance and the channel gain[5] between these nodes, and Q is the power constraint.

Assuming that all nodes transmit using omni-directional antennas over the same frequency channel with bandwidth (narrow-band), we can compute the signal-to-interference-plus-noise ratio (SINR) experienced by RX$_k$ when TX$_k$ is its associated transmitter and IAN is the decoding rule employed[6]

[4]This observation period is considered to be large enough to sustain rates arbitrarily close to the channel capacity, which implies that the code length goes to infinity. The effect of finite-length codes on the error probability in spatial wireless networks is studied in [112].

[5]This is in fact a simplified model that may lead to meaningless results for $x_{ij} < 1$. As pointed in [114], modified versions of this model just increase the complexity of the analysis without providing significant differences.

[6]We can define the SINR when OPT is used in a similar way. For simplicity, we prefer to present in this section only results regarding the IAN rule. The mathematical treatment of OPT is provided in Chapter 6.

as

$$\text{SINR}_{kk} = \frac{h_{kk} d_{kk}^{-\alpha}}{1 + \sum\limits_{i \in \mathcal{A} \setminus \{k\}} h_{ki} d_{ki}^{-\alpha}}, \tag{2.11}$$

where $\mathcal{A}$ is the set of active transmitters (interferers) that disturb the reference link.

Clearly, the SINR is a random variable which depends on random distances, (random) channel gains and the Gaussian noise. The computation of the SINR probability distribution, though, is usually a very hard task, many times impossible, and closed-form equations can be found only for few specific cases (e.g. [9, 115, 116, 117, 118, 119, 120, 121]).

Knowing this, we have decided to use in this thesis two of the simplest SINR modeling found in the literature, namely *path loss only using the closest interferer approximation* and *i.i.d. Rayleigh fading channels*. For simplicity, we further assume an interference-limited system so the effects of the Gaussian noise can be neglected[7]. In this case, our goal is to associate the signal-to-interference ratio (SIR) to outage events that will determine the link performance. But before that, we need to define an outage event as follows.

Definition 2.5 (outage event)**.** *A given link TX_k-RX_k is said to be in outage if the coding rate R_k is not achievable during any period of the message transmission. In other words, an outage event occurs whenever $SIR_{kk} < \beta_k$, where β_k is the SIR threshold of RX_k determined by the channel capacity.*

We can now relate the outage event to both the coding-decoding scheme that yields β and the nodes' positions in a given network realization. The following two propositions state the outage probability for the two cases mentioned before, assuming the high mobility random walk modeling, the IAN decoding rule and the bipolar model[8] introduced by Baccelli et al.[10].

Definition 2.6 (dominant interferer)**.** *A transmitter is said to be a dominant interferer of a given receiver RX_k if, and only if, such a transmitter is able to cause alone an outage event in the TX_k-RX_k transmission.*

Proposition 2.1 (outage probability for dominant interferer approximation [34])**.** *Let Φ be a 2-D homogeneous PPP in $\mathbb{R}^2$ with intensity $\lambda > 0$ [transmitters/m^2] that characterizes the transmitter positions in a wireless network following the bipolar model. Assuming that the channel gains h_{ij} between transmitter TX_j and receiver RX_i are fixed (i.e. $h_{ij} = h$ and the channel modeling reduces to the distance-dependent path loss), we can approximate the outage probability, denoted by P_{o}, of a typical link TX_0-RX_0 using the dominant interferer approximation as*

$$P_{\text{o}} = \Pr\left[\text{SIR}_{00} = \frac{d^{-\alpha}}{\sum\limits_{i \in \mathcal{A}} d_{0i}^{-\alpha}} < \beta\right] \approx 1 - e^{-\lambda \pi d^2 \beta^{2/\alpha}}, \tag{2.12}$$

where d is the transmitter-receiver distance, d_{0i} is distance between the reference receiver and its ith interfering node, $\mathcal{A}$ is the set of active transmitters, and $\alpha > 2$ is the path loss exponent.

[7] We can cite [30] as an example when the thermal noise is considered.

[8] In this model, the transmitters are generated by the point process and each of them is associated with one receiver, located at a fixed distance d from it in a random orientation, to establish a communication link. By this definition the receivers are not part of the generating point process.

Proposition 2.2 (outage probability for Rayleigh fading [10])**.** *Let Φ be a 2-D homogeneous PPP in $\mathbb{R}^2$ with intensity $\lambda > 0$ [transmitters/m^2] that characterizes the transmitter positions in a wireless network following the bipolar model. Assuming that the channel gains h_{ij} between transmitter TX_j and receiver RX_i are independent exponentially distributed random variables with unity mean (i.e. independent Rayleigh fading channel), we can compute the outage probability, denoted by P_{o}, of a typical link TX_0-RX_0 as*

$$P_{\mathrm{o}} = \Pr\left[\mathrm{SIR}_{00} = \frac{h_{00}d^{-\alpha}}{\sum\limits_{j\in\mathcal{A}} h_{0i}d_{0i}^{-\alpha}} < \beta\right] = 1 - e^{-\lambda\kappa d^2\beta^{2/\alpha}} \tag{2.13}$$

where $\kappa = \pi\Gamma(1+2/\alpha)\Gamma(1-2/\alpha)$ with $\Gamma(\cdot)$ being the Euler Gamma function, d is the transmitter-receiver distance, d_{0i} is distance between the reference receiver and its ith interfering node, $\mathcal{A}$ is the set of active transmitters, and $\alpha > 2$ is the path loss exponent.

The proof of these propositions can be found in the references [34, 10], respectively. To give an idea on how they are derived, both cases apply the Mecke-Slivnyak Theorem (Theorem 2.3) to include a typical link in the PPP and Campbell Theorem (Theorem 2.2) to compute the expected value of the aggregate interference at the typical receiver over different spatial realizations of the network to then compute outage probability. In the first case, the proof is based on the existence of a dominant interferer by associating the SIR threshold β to a circle within which no other transmitter may reside, or outage occurs. In the second case, the proof is based on computing the aggregate interference statistics using Laplace transforms.

Despite the mathematical details behind the proofs, these propositions show elegant closed-form equations to evaluate the probability that a typical link of the network is in outage. In the following chapters, we use some variations of those propositions[9] to compute the outage probability in the scenario under analysis. It is worth noting that the only difference between (2.12) and (2.13) is the factor κ in the exponential term, which only depends on the path-loss exponent. Hence the behavior of the curves are similar when the same α is assumed and the use of one model over the other will depend on the convenience of the scenario under study. In any case, we argue that the lessons learned from the results obtained using one model can be extended to the other one.

[9] We present proofs of our new propositions whenever they are necessary.

Chapter 3

Analysis of hopping strategies

In this chapter we investigate whether it is preferable to have a large number of short single-hop links or a small number of long single-hops in a multi-hop wireless network. We derive analytical expressions to compute the proposed metric *aggregate multi-hop information efficiency* (AMIE) under different hopping strategies, and analyze the trade-off involving robustness of single-hop links, co-channel interference and hopping strategy. Our results show that, the best hopping strategy is closely related to the relation involving the reliability of single-hop links and the interference caused by multiple transmissions of the same packet in a multi-hop link. For instance, as we will see later, if the spectral efficiency of single-hop links is high, meaning that we have less robust links, the highest AMIE is achieved when short single-hops are used, even though this may lead to a larger number of hops and, consequently, higher interference levels. Conversely, when links with low spectral efficiency are used, the best hopping strategy is to transmit to the furthest neighbor. It should be noted that our analysis does not focus on the optimum number of hops, which is not a design parameter in our framework, but rather a consequence of the hopping strategy adopted.

3.1 Aggregate multi-hop information efficiency

The *aggregate multi-hop information efficiency* (AMIE) is proposed here as an extension for multi-hop scenarios of the metrics *transmission capacity* and *information efficiency* (cf. Chapter 2). Let d_{mh} and R_{mh} be the separation distance between source and destination nodes measured in [m], and the spectral efficiency of multi-hop links measured in [bits/s/Hz], respectively. Also, let λ_{s}, measured in [links/m^2] denote the density of successful transmissions over multiple hops. Then, the AMIE metric is defined as follows.

Definition 3.1 (AMIE)**.** *The aggregate multi-hop information efficiency of a wireless network, denoted by $\mathcal{M}$, is defined as*

$$\mathcal{M} = \lambda_{\text{s}}\, d_{\text{mh}}\, R_{\text{mh}}, \tag{3.1}$$

with $\mathcal{M}$ measured in [(bits·m)/s/Hz/m^2].

It is important to point out that AMIE and the transport capacity (cf. Section 1.1.4) have a similar purpose, namely to quantify the effects of the progress of information bits on the efficiency of the

network. Nevertheless, while the latter metric was built to be a deterministic physical limit of the network when its density grows to infinity (asymptotic analysis), the former is a statistical quantification of the network efficiency under specific strategies and more realistic scenarios. Since our objective is to provide guidelines on how a network designer should choose the appropriate hopping strategy to statistically guarantee higher efficiencies, the transport capacity is therefore not the best choice of metric to evaluate the scenario studied here. In this case, the AMIE metric has the same purpose of the spatial density of transport (cf. Section 1.1.3), assessing the network in a statistical manner.

If the average transmitter-receiver separation distance in single-hop links is d_{sh}, then the average number of hops k between source and destination can be bounded as $k \geq d_{\text{mh}}/d_{\text{sh}}$. Equality in this expression is only valid when the route connecting those nodes is a straight line. We consider here such routing and thus the transmission of a packet requires on average $k = d_{\text{mh}}/d_{\text{sh}}$ channel usages. If we further assume that all single-hop links have the same spectral efficiency R_{sh}, the overall spectral efficiency R_{mh} of a multi-hop link is $R_{\text{mh}} = R_{\text{sh}}/k$, and the product $d_{\text{mh}}\ R_{\text{mh}}$ can be written as

$$d_{\text{mh}}\ R_{\text{mh}} = d_{\text{sh}}\ R_{\text{sh}}. \tag{3.2}$$

The multi-hop spectral efficiency R_{mh} is used here to allow us to compare the spectral efficiency of multi-hop links with different number of hops, assuming that only one single-hop (transmitter-receiver pair) of a given multi-hop link can be active during packet transmission (regenerative forwarding).

Now, let λ_{a} and P_{o} denote the density of active single-hop links and the single-hop outage probability (i.e., probability that a packet is not successfully transmitted over a single-hop link), respectively. Assuming independence between hops[1] and that packets detected in error are not retransmitted, the density of successful multi-hop links λ_{s} can be evaluated as

$$\lambda_{\text{s}} = \lambda_{\text{a}}\ (1 - P_{\text{o}})^k. \tag{3.3}$$

Inserting (3.2) and (3.3) into (3.1), we can rewrite the AMIE as a function of single-hop link parameters and the average number of hops as

$$\mathcal{M} = d_{\text{sh}}\ \lambda_{\text{a}}\ (1 - P_{\text{o}})^k\ R_{\text{sh}}. \tag{3.4}$$

It is important to remind that this equation is only valid for the case when routes connecting sources to destinations are straight lines, implying that $k = d_{\text{mh}}/d_{\text{sh}}$. If actual routes deviate from these perfect routes, then $k \geq d_{\text{mh}}/d_{\text{sh}}$, and, consequently, equation (3.4) can be viewed as an upper bound on the AMIE.

In the next section, we will present the network modeling used in our analysis and derive expressions for the parameters needed to evaluate equation (3.4).

3.2 Network modeling

Let us consider an infinite network composed by nodes with packets to be transmitted (potential transmitters) and nodes capable of receiving those packets (potential receivers) so they can interact

[1] This assumption will be justified later in Section 3.2.

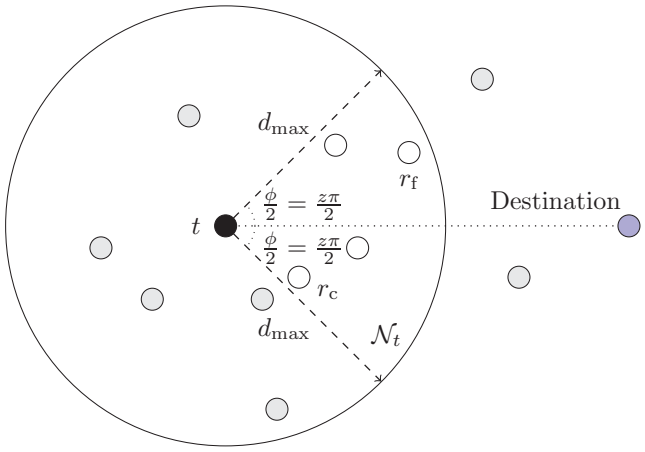

Fig. 3.1: Illustrative example of the neighborhood set $\mathcal{N}_t$ of a transmitter t, defined by the angle $\phi = z\pi$ and the transmission range $d_{\max}$. The white-colored circles represent potential receivers, and belong to $\mathcal{N}_t$. The potential receivers r_{f} and r_{c} are the furthest and the closest neighbors, respectively.

in time slot basis to form communication links. These two sets are modeled as two different 2-D homogeneous PPPs with densities λ_{t} and λ_{r}. We also assume the high mobility random walk model (cf. [10]) such that each time slot can be viewed as an independent realization of both point processes, which guarantees the independence between hops.

Using the distance-dependent path loss as our channel modeling such that the detected power P_{ij} at a given RX_i is $P_{ij} = hd_{ij}^{-\alpha}$, where d_{ij} is the distance between RX_i and TX_j that emitted the signal, and h is a fixed channel gain determined by the transmit power (we do not consider fading channels in this chapter). We assume that all nodes use the same transmit power that is equal to 1 without loss of generality, and all receivers operate with the same sensitivity level $P_{\min}$, which defines a necessary condition for decoding. From this, we can obtain the *transmission range* of a transmitter, denoted by $d_{\max}$ and measured in [m], as

$$d_{\max} = \left(\frac{1}{P_{\min}}\right)^{\frac{1}{\alpha}}. \tag{3.5}$$

By symmetry, the *reception range* of a receiver - the maximum separation distance between the transmitter and receiver such that packets can be correctly received - is also equal to $d_{\max}$. Note that transmission and reception ranges are defined from receiver sensitivity perspective only, assuming that interference is not present. In other words, the transmitter-receiver distance being smaller than $d_{\max}$ is necessary for successful communication, but it is not sufficient since outage events may still happen. Based on the definition of transmission and reception ranges, we can now define the neighborhood sets of a node.

Definition 3.2 (neighborhood sets)**.** *The neighborhood set $\mathcal{N}_t$ of a transmitter t is defined as the set of potential receivers located within the circular sector centered at t, with radius equals to the transmission range $d_{\max}$ of t and angle $\phi = z\pi$, with $0 < z < 1$ (refer to Fig. 3.1). On the other hand, the neighborhood set $\mathcal{N}_r$ of a receiver r is the set of potential transmitters located within the circular region centered at r, with radius equals to its reception range $d_{\max}$.*

Note that the angle that defines the neighborhood of a transmitter must be smaller than π in order to guarantee that packets are forwarded toward their destinations [17], as illustrated in Fig. 3.1.

Next, we describe a simple medium access scheme that operates based on the relative distances between transmitters and their neighbors.

3.2.1 Medium access procedure and hopping strategies

We assume that packets are transmitted on a time slot basis and that transmitters select their corresponding receiver among the nodes in their neighborhood sets based on their respective distances. Three selection criteria, or *hopping strategies*, will be considered: closest neighbor, furthest neighbor and random selection. In the event that two or more transmitters select the same node as their associate receiver, one of those transmitters is randomly chosen to effectively pair up with that node, while the others will be turned off during that time slot.

If neighborhood set $\mathcal{N}_t$ of transmitter t is empty during a given time slot, t will be inactive during that time slot and, consequently, it will be disconnected from the network. In the next time slots, new realizations of the point processes that define the spatial distribution of potential transmitters and receivers are considered and, thus, nodes disconnected during a given time slot may be connected in subsequent ones.

Here it is important to mention that the hopping strategy assessed in this chapter is fixed, opposing to the opportunistic strategies introduced in [11, Ch. 17], [41]. In that case, the transmitters select, at each time slot, their respective receivers that maximize the packet effective progress. As one can expect, this adaptive strategy will outperform any of the fixed rule policies that are the focus of this chapter. Nevertheless, the benefits of the opportunistic strategy are obtained at the expense of more complex computations when maximizing the packet progress in each time slot.

3.2.2 Network parameters

In this section, we derive the expressions needed for evaluating the parameters used to calculate the AMIE, considering the three hopping strategies previously mentioned.

Proposition 3.1 (single-hop distance)**.** *Let r^* denote the receiver selected by a given transmitter t. The average TX-RX separation distance d_{sh} between t and r^* for the furthest neighbor, the closest neighbor and the random selection hopping strategies are given by*

$$d_{\text{sh,f}} = \frac{1}{2\sqrt{\lambda_{\text{r}} z}} \frac{2d\sqrt{\lambda_{\text{r}} z}\; e^{\lambda_{\text{r}} z \pi d_{\text{max}}^2} + \operatorname{erfi}(\sqrt{\lambda_{\text{r}} z \pi}\, d_{\text{max}})}{1 - e^{\lambda_{\text{r}} z \pi d_{\text{max}}^2}}, \tag{3.6}$$

$$d_{\text{sh,c}} = \frac{1}{2} \frac{2d_{\text{max}}\sqrt{\lambda_{\text{r}} z} - e^{\lambda_{\text{r}} z \pi d_{\text{max}}^2} \operatorname{erf}(\sqrt{\lambda_{\text{r}} z \pi}\, d_{\text{max}})}{1 - e^{\lambda_{\text{r}} z \pi d_{\text{max}}^2}}, \tag{3.7}$$

$$d_{\text{sh,r}} = \frac{2}{3}\, d_{\text{max}}, \tag{3.8}$$

where $\operatorname{erf}(x) = \frac{2}{\sqrt{\pi}} \int_0^x e^{-y^2}\, dy$ *and* $\operatorname{erfi}(x) = -\sqrt{-1}\; \operatorname{erf}(x\sqrt{-1})$ *are the standard and imaginary error functions, respectively.*

Proof. The average distances in expressions (3.6)-(3.8) can be determined from the corresponding pdfs of the distance d^* between t and r^* with $0 < d^* \leq d_{\max}$ for each hopping strategy. The derivation of such pdfs is based on Properties 2.2 and 2.3, considering the area of the circular sector instead of the complete circumference and assuming that the neighborhood set $\mathcal{N}_t$ is not empty. Then, the pdf of d^*, denoted as $f(x)$, for the furthest neighbor, closest neighbor and random neighbor hopping strategies are given by:

$$f_{\mathrm{f}}(x) = 2\lambda_{\mathrm{r}} z\pi x \, \frac{e^{\lambda_{\mathrm{r}} z\pi x^2}}{e^{\lambda_{\mathrm{r}} z\pi d_{\max}^2} - 1}, \tag{3.9}$$

$$f_{\mathrm{c}}(x) = 2\lambda_{\mathrm{r}} z\pi x \, \frac{e^{-\lambda_{\mathrm{r}} z\pi x^2}}{1 - e^{-\lambda_{\mathrm{r}} z\pi d_{\max}^2}}, \tag{3.10}$$

$$f_{\mathrm{r}}(x) = \frac{2\,x}{d_{\max}^2}, \tag{3.11}$$

where $0 < x \leq d_{\max}$.

We hence obtain the expressions (3.6)-(3.8) by evaluating the expected value of each one of the distributions above. □

Proposition 3.2 (density of active links)**.** *The density of active links λ_{a} can be approximated for the three hopping strategies studied in this chapter as*

$$\lambda_{\mathrm{a}} \approx \left(1 - \exp\left(-\frac{\lambda_{\mathrm{t}}}{\lambda_{\mathrm{r}} z} \, \left(1 - \exp(-\lambda_{\mathrm{r}} z\pi d_{\max}^2)\right)\right)\right) \, \lambda_{\mathrm{r}}. \tag{3.12}$$

Proof. Let us recall that each active receiver pairs up with only one transmitter to form a link. Then the number of active links is equal to the number of active receivers so the density of active links λ_{a} can be expressed as

$$\lambda_{\mathrm{a}} = P_{r,\mathrm{act}} \, \lambda_{\mathrm{r}} = (1 - \overline{P}_{r,\mathrm{act}}) \, \lambda_{\mathrm{r}}, \tag{3.13}$$

where $P_{r,\mathrm{act}}$ is the probability that a (typical) receiver r is active, and $\overline{P}_{r,\mathrm{act}}$ is its complement.

In order to obtain an expression for $\overline{P}_{r,\mathrm{act}}$, let us first denote by $P_{r,t}$ the probability that a receiver r is chosen by a transmitter t in the neighborhood set $\mathcal{N}_t$ of t. Next, we will assume that the processes of selecting a receiver performed by transmitters are independent of each other. Clearly, this is a simplification, as the selection processes are independent only if the neighborhood sets $\mathcal{N}_t$ of transmitters are disjoint. As we will show later, this independence assumption leads to good approximation for λ_{a} regardless of the hopping strategy considered.

Let us consider a receiver r, whose neighborhood set $\mathcal{N}_r$ has cardinality x_{t}, which is a Poisson random variable with mean $\lambda_{\mathrm{t}}\pi d_{\max}^2$. Therefore, the probability that r is not selected by any $t \in \mathcal{N}_r$ can be approximated by

$$\overline{P}_{r,\mathrm{act}} \approx \mathrm{E}[(1 - P_{r,t})^{x_{\mathrm{t}}}] = e^{-P_{r,t}\lambda_t \pi d_{\max}^2}, \tag{3.14}$$

where $\mathrm{E}[\cdot]$ denotes expectation taken over the distribution of x_{t}.

To determine $P_{r,t}$, we apply Theorems 2.2 and 2.3 as follows. Let us consider a transmitter t and a typical potential receiver r_0 included in the initial point process in the neighborhood set $\mathcal{N}_t$ of t. The probability that r_0 is the selected receiver depends on its distance d_0 to t and the hopping strategy

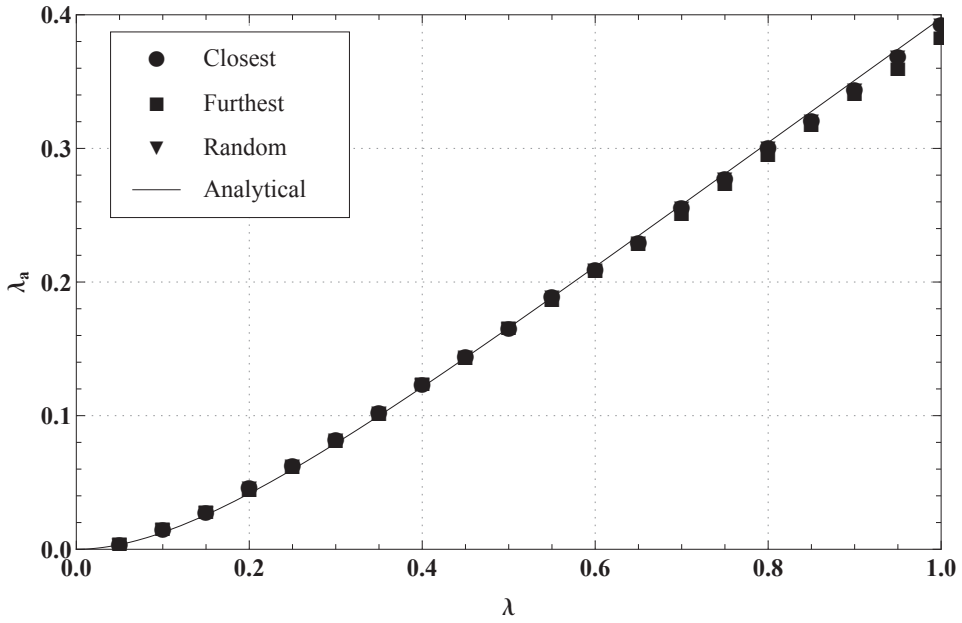

Fig. 3.2: Density of active links λ_{a} as a function of the node density λ (density of potential transmitters λ_{t} plus density of potential receivers λ_{r}) for the furthest neighbor, closest neighbor and random selection hopping strategies. The analytical curve was obtained from equation (3.12) and the points were computed via Monte-Carlo simulation assuming $\lambda_{\text{t}} = \lambda_{\text{r}} = \lambda/2$ and $d_{\text{max}} = 4$ [m].

adopted. Let us first consider the closest neighbor strategy. In this case, $P_{r,t}$ is the probability that no other receiver is closer to t than r_0. Thus,

$$P_{r,t} = \text{E}\left[e^{-\lambda_{\text{r}} z \pi d_0^2}\right] = \frac{1 - e^{-\lambda_{\text{r}} z \pi d_{\text{max}}^2}}{\lambda_{\text{r}} z \pi d_{\text{max}}^2}, \tag{3.15}$$

where the expectation is taken over the density function of d_0, given by $f_{d_0}(x) = 2x/d_{\text{max}}^2$ (uniform distribution of a point inside a circumference with radio d_{max}).

Following the same procedure for the furthest neighbor strategy and random selection, we can shown that the corresponding probabilities $P_{r,t}$ have exactly the same expression as (3.15). To conclude this proof, we insert (3.15) into (3.14) and then the resulting expression into (3.13), yielding (3.12). □

Fig. 3.2 presents density of active links λ_{a} as a function of the sum $\lambda_{\text{t}} + \lambda_{\text{r}}$, denoted by λ, for the three hopping strategies studied here. We can see a good agreement between the approximated expression (3.12) and numerical results obtained via Monte-Carlo simulation, regardless of the hopping strategy considered.

Proposition 3.3 (single-hop outage probability)**.** *Let β be the SIR threshold related to the coding-decoding scheme. Considering the outage event definition presented in Definition 2.5 and the dominant interferer approximation in Definition 2.6, the single-hop outage probability P_{o} for the furthest*

neighbor, closest neighbor and random selection hopping strategies can be approximated by

$$P_{\text{o,f}} \approx 1 - \lambda_{\text{r}} z \frac{1 - e^{-(\lambda_{\text{a}}\beta^{2/\alpha} - \lambda_{\text{r}} z)\pi d_{\max}^2}}{(\lambda_{\text{a}}\beta^{2/\alpha} - \lambda_{\text{r}} z)\left(e^{\lambda_{\text{r}} z \pi d_{\max}^2} - 1\right)}, \tag{3.16}$$

$$P_{\text{o,c}} \approx 1 - \lambda_{\text{r}} z \frac{1 - e^{-(\lambda_{\text{a}}\beta^{2/\alpha} + z\lambda_{\text{r}})\pi d_{\max}^2]}}{(\lambda_{\text{a}}\beta^{2/\alpha} + \lambda_{\text{r}} z)\left(1 - e^{-\lambda_{\text{r}} z \pi d_{\max}^2}\right)}, \tag{3.17}$$

$$P_{\text{o,r}} \approx 1 - \frac{1 - e^{-\lambda_{\text{a}} z \pi d_{\max}^2 \beta^{2/\alpha}}}{\lambda_{\text{a}} z \pi d_{\max}^2 \beta^{2/\alpha}}. \tag{3.18}$$

Proof. Let us consider the dominant interferer approximation. Then we can apply the outage probability stated in Proposition 2.1, but considering here that the transmitter-receiver distance d in equation (2.12) is now a random variable whose density function depends on the hopping strategy considered. Then the average probability of occurrence of outage event is given by

$$\Pr\left[\text{SIR} < \beta\right] = \int \Pr\left[\text{SIR} < \beta |\, x\right] f(x)\, dx, \tag{3.19}$$

where $f(\cdot)$ is the probability density functions of the transmitter-receiver distance d^*, determined according to the hopping strategy considered. Using each one of the pdfs given in (3.9), (3.10) and (3.11), we can obtain the single-hop outage probability for each hopping strategy. □

Remark 3.1. *The outage probability approximations stated above are lower bounds of the actual outage probabilities and hence the AMIE obtained with by them are upper bounds. As commented after Proposition 2.1, this approximation does not affect the exponential behavior of the outage probability if compared to the actual outage probability when Rayleigh fading is assumed (cf. Proposition 2.2). For this reason and due to the geometric nature of our proof (which is more intuitive), we prefer to use here the dominant interferer approximation. One can refer to [34] for a more detailed discussion of this approximation; the tightness of this bound for the hopping strategies used in this chapter can be found in [103].*

Note that the evaluation of the outage probability just presented still requires the SIR threshold β related to the coding-decoding scheme. We assume here a Gaussian point-to-point code and the IAN decoding rule as described in Section 2.1 such that Corollary 2.2 can be used to determine whether a rate is achievable.

Let us assume here that all transmitters use the same fixed coding rate R_{sh} to send their messages and the receivers employ the IAN decoding rule described in the previous chapter. Therefore, the target spectral efficiency of a single-hop link is also R_{sh} and can be related to the threshold β by computing the SIR required to achieve the channel capacity (upper bound in equation (2.6)), yielding

$$\beta = 2^{R_{\text{sh}}} - 1, \tag{3.20}$$

or, in other words, if the application requires a spectral efficiency of R_{sh}, then the SIR threshold that a packet is successfully received is $2^{R_{\text{sh}}} - 1$.

If we consider a fixed multi-hop distance d_{mh}, then the aggregate multi-hop information efficiency $\mathcal{M}$ given by (3.4) can be evaluated using equations (3.6)-(3.8) for the average single-hop TX-RX separation distance, equation (3.12) for the density of active links, equations (3.16)-(3.18), together with (3.20), for the outage probability and finally applying $k = d_{\text{mh}}/d_{\text{sh}}$ (perfect routing assumption) to compute the number of hops.

3.3 Numerical results

In this section, we apply the aggregate multi-hop information efficiency to investigate the spatial throughput of a wireless network for the three hopping strategies analyzed in this section. Table 3.1 shows the parameter values used to obtain the numerical results, except when otherwise stated. It is worth noting that the relative values between such values are more important than their absolute numbers themselves.

We first study the effects of the single-hop spectral efficiency on the AMIE by means of curves $\mathcal{M}$ versus R_{sh}, which are shown in Fig. 3.3. We can see that, regardless of the hopping strategy adopted, the curve $\mathcal{M}$ versus R_{sh} can be split into two regions: for small R_{sh}, where $\mathcal{M}$ is an increasing function of R_{sh}, and for large R_{sh}, where $\mathcal{M}$ is a decreasing function of R_{sh}. When R_{sh} is small, the required threshold β for correct reception is also small, since the communication links are robust, and outage events are unlikely to occur. Hence the AMIE of the network increases as R_{sh} increases. Since links are robust against interference when R_{sh} is small, single-hop links are allowed to have large TX-RX separation distances, reducing the number of hops k and decreasing the multi-hop error probability. When R_{sh} is small, the best hopping strategy is then to select the furthest neighbor, as evinced by Fig. 3.3.

When R_{sh} is large, the threshold β is large, and error events are more frequent since the links are now more vulnerable to interference. As R_{sh} increases, outages are more and more frequent, and $\mathcal{M}$ becomes a decreasing function of R_{sh}. Note that, if single-hop links are more vulnerable to interference, transmitter-receiver separation distance d^* should be made as small as possible, even if a small d^* leads to a large number of hops k. In fact, Fig. 3.3 shows that, when R_{sh} is large, the best hopping strategy is to select the closest neighbour.

Next, we investigate how the AMIE is affected by traffic intensity, measured in terms of the density of potential transmitters λ_{t}. Fig. 3.4 shows curves $\mathcal{M}$ versus λ_{t} for $R_{\text{sh}} = 2$ [bits/s/Hz] and different hopping strategies. All curves in Fig. 3.4 are similar to those presented in Fig. 3.3, and can be split into two different regions, now according to the traffic intensity. For small density of transmitters (i.e., low traffic intensity), the level of interference in the network is low, and the AMIE is not limited by interference, being an increasing function of the density of transmitters. Furthermore, since the level of interference is low, single-hop links can have large transmitter-receiver separation distances, reducing the number of hops and, consequently, decreasing the multi-hop outage probability. Therefore, as shown in Fig. 3.4, when the density of transmitters is small, the highest AMIE is obtained with the furthest neighbour hopping strategy.

Tab. 3.1: Parameter values used in the numerical analysis.

Parameter	Description	Value
α	Path loss exponent	4
d_{mh}	Multi-hop distance	3 m
d_{max}	Transmission range	1 m
λ_{r}	Density of receivers	1 RX/m^2
ϕ	Sector angle	$\pi/2$

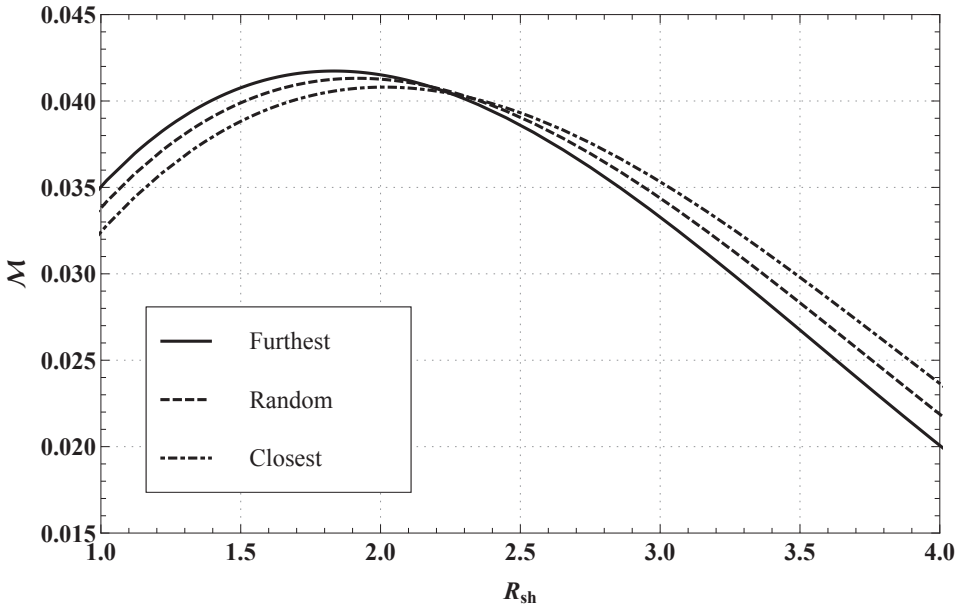

Fig. 3.3: AMIE $\mathcal{M}$ vs. the required spectral efficiency R_{sh} for $\lambda_{\mathrm{t}} = 0.05$ [TXs/m^2], considering the furthest, the closest and a random neighbor hopping strategies. The curves have been obtained using equations (3.4), (3.6)-(3.8), (3.12) and (3.16)-(3.18).

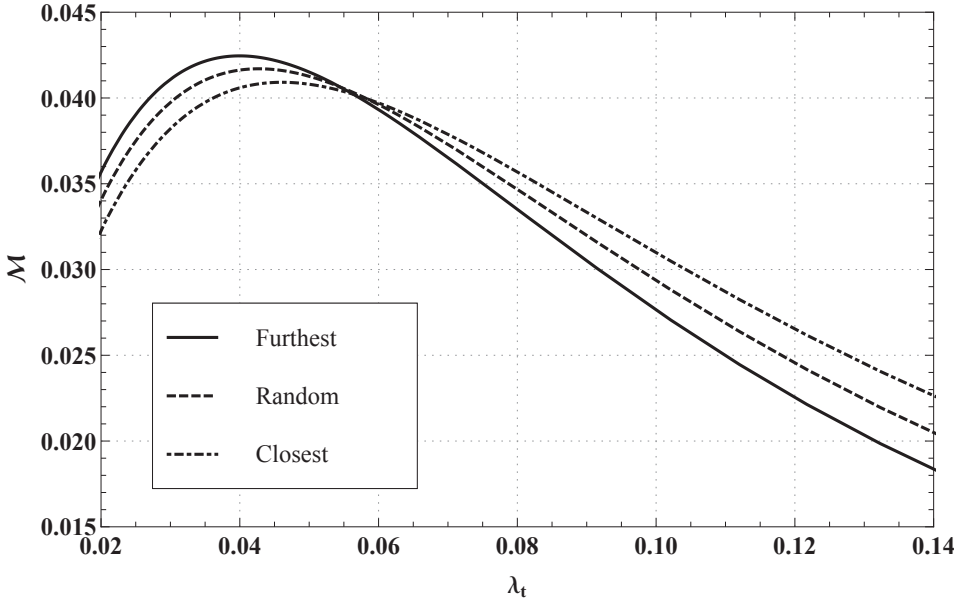

Fig. 3.4: AMIE $\mathcal{M}$ vs. density of potential transmitters λ_{t} for $R_{\mathrm{sh}} = 2$ [bits/s/Hz], considering the furthest, the closest and a random neighbor hopping strategies. The curves have been obtained using equations (3.4), (3.6)-(3.8), (3.12) and (3.16)-(3.18).

Based on the preceding discussion, we can conclude that the existence of two regions of behavior in Figs. 3.3 and 3.4 can help the network operator to assess whether a network is operating with its spatial throughput limited by interference for a given density of transmitters and single-hop spectral efficiency. For instance, according to the results shown in Fig. 3.4, a network operating with single-hop spectral efficiency $R_{\text{sh}} = 2$ [bits/s/Hz] has its performance limited by interference if the density of transmitters exceeds $0.04 - 0.05$ [nodes/m^2]. However, this scenario can be changed if the single-hop spectral efficiency (coding rate) is carefully reduced, resulting in more robust links and therefore higher AMIE, as suggested by the curves in Fig. 3.3.

3.4 Summary

In this chapter we have studied the performance of multi-hop wireless networks operating under different hopping strategies. We proposed here a metric called aggregate multi-hop information efficiency (AMIE) such that the efficiency of the information flow throughout the network can be assessed capturing the effect of communication in multiple hops.

Specifically three hopping strategies have been considered: furthest neighbor, closest neighbor and random selection. We derived closed-form equations to approximate several network parameters used to compute the AMIE, which include the average number of hops between source and destination, single-hop outage probability and single-hop spectral efficiency. Using our proposed formulation, we identified the network operating conditions under which a given hopping strategy outperforms the other options, providing guidelines on the optimal design setting for a given network condition.

Chapter 4

Analysis of packet retransmissions for different MAC protocols

In this chapter we investigate the transmission capacity (TmC) of a wireless network when packet retransmissions are allowed. We consider here a network operating under different MAC protocols, namely unslotted and slotted ALOHA, and CSMA with carrier sensing at the transmitter and with carrier sensing at the receiver. We then derive analytical expressions to compute the maximum allowed number of retransmissions attempts that leads to the optimal TmC. Numerical results show that CSMA with carrier sensing at the receiver (asynchronous transmissions) reaches the highest maximum transmission capacity when the traffic intensity is low, while slotted ALOHA (synchronous transmissions) is the best choice when the traffic intensity is high.

4.1 Network modeling

Let us assume a single-hop ad hoc network where transmitters (TXs) are located according to a 2-D homogeneous PPP Φ with density λ [TXs/m^2]. Every transmitter is associated with only one receiver that is located d [m] away in a random orientation following the bipolar model [10]. Packets of constant size associated with the time length T [s] arrive at the transmitters to be sent to their respective receivers according to independent Poisson processes with mean μ [packets/s/TX]. Applying the same approach described in [122], the spatial density λ_{a} [packets/m^2] active at some time during a given time period T is

$$\lambda_{\text{a}} = \lambda \, \mu \, T. \tag{4.1}$$

In this chapter we apply the same coding-decoding strategy as Chapter 3, where transmitters use G-ptp codes and receivers employ the IAN decoding rule introduced in Section 2.1. Considering that all transmitters code their messages using the same rate R, measured in [bits/s/Hz], we can apply the outage event stated in Definition 2.5, where the SIR threshold required for a successful reception β is computed based on the channel capacity, yielding

$$\beta = 2^R - 1. \tag{4.2}$$

We assume here two variations of the ALOHA, and the CSMA MAC protocols, which will be described later. In addition, packets that are not successfully decoded during a transmission attempt

can be retransmitted up to m times. If this limit of retransmissions is reached without success, the packet is then lost. The signaling between a transmitter and its receiver for retransmission requests occurs over an orthogonal error-free control channel, and the delay introduced by these requests is assumed to be negligible compared to the packet length.

We also assume a very dynamic network such that, at each retransmission attempt, the network topology changes and the spatial correlation between successive packet retransmissions can be neglected (high mobility random walking [10]). It is important to mention that, if the network is (quasi-)static, such an independence assumption does not hold and therefore spatial correlations [117, 123] plays a role in events under analysis (outage, retransmission and carrier sensing). In that case, it is hard or even impossible to obtain closed-form solutions to the optimal design setting. We argue that our results, even though relying on a somehow unrealistic modeling, are still valid and provide useful insights on the trade-offs that determine the network performance. In Chapter 7, we will come back to this point and compare the designing choices when the network is highly mobile or (quasi-)static.

In the next section, we redefine the TmC concept targeting the network analyzed in this chapter. We then cast an optimization problem to determine the maximum number of retransmission m^* that maximizes the TmC for a given maximum acceptable packet loss probability ϵ and density λ_{a}.

4.2 Optimizing the transmission capacity

Let us start this section by redefining the TmC metric to incorporate the specificities of the scenario studied in this chapter.

Definition 4.1 (transmission capacity)**.** *Let P_{pkt} be the packet loss probability after all retransmissions attempts. Then, the transmission capacity, denoted by $\mathcal{T}$ and measured in [bits/s/Hz/m^2], is defined as*

$$\mathcal{T} = \lambda_{\text{a}} \left(1 - P_{\text{pkt}}\right) \frac{R}{1 + \overline{m}}, \tag{4.3}$$

where $\overline{m}$ is the average number of retransmissions.

In the following subsections, we apply this definition to find the maximum number of retransmissions that leads to the optimal transmission capacity for different MAC protocols. As in the previous chapter, we use here the dominant interferer approximation and the distance dependent path loss channel modeling (refer to Section 2.2.2 for more details).

4.2.1 Slotted ALOHA protocol

When ALOHA protocol is used, packets are transmitted regardless of the channel status (busy or idle). In the slotted version of ALOHA, packet transmission begins at the first time slot after the packet arrival. If the packet is detected in error and not yet counted to be in outage, it waits an exponential distributed time according to the arrival process to be retransmitted in the first time slot after such random time (this maintains the proprieties of the Poisson distribution). We assume here that the time slot length T is equal to the packet duration.

It is important to mention that this assumption simplifies our analysis since the outage event in the packet reception can be related to the outage event in only one time slot. If, conversely, we assume

that a packet length is greater than one slot, then the success of a packet transmission will be related to reception errors in other slots, which makes assessment more complicated. In any case, our approach can be followed in this more realistic scenario.

In the following, we derive an expression for the allowed number of retransmissions m^* that maximizes the TmC for the slotted ALOHA protocol.

Proposition 4.1 (slotted ALOHA)**.** *The maximum number of retransmissions m^* that results in the optimal transmission capacity for the slotted ALOHA protocol when the target packet loss probability is ϵ is given by*

$$m^* = \max_{m \in \mathbb{N}} \left(1 - \epsilon^{\frac{1}{1+m}}\right) \log_2 \left(1 + d^{-\alpha} \left(\frac{1 - \epsilon^{\frac{1}{1+m}}}{1-\epsilon} \frac{1}{\lambda_{\mathrm{a}} \pi} \ln\left(\frac{1}{1 - \epsilon^{\frac{1}{1+m}}}\right)\right)^{\frac{\alpha}{2}}\right). \tag{4.4}$$

Proof. The idea behind this proof is to write the TmC expression given by (4.3)) in terms of m. We begin with the packet loss probability, remembering that a packet is lost if all $1 + m$ transmission attempts (one transmission and m retransmissions) have failed (outage events). Hence we can relate the target packet loss probability ϵ and the probability P_{o} that a packet is transmitted through a link in outage during a transmission attempt using the following expression:

$$\epsilon = P_{\mathrm{o}}^{1+m}. \tag{4.5}$$

We now turn our attention to the average number of transmission attempts $1 + \overline{m}$. Since a new transmission attempt occurs with probability P_{o} (i.e. an outage event occurred and the packet need to be retransmitted), we can write

$$1 + \overline{m} = \sum_{n=0}^{m} P_{\mathrm{o}}^n = \frac{1 - P_{\mathrm{o}}^{1+m}}{1 - P_{\mathrm{o}}} = \frac{1-\epsilon}{1 - \epsilon^{\frac{1}{1+m}}}. \tag{4.6}$$

To compute the TmC, we still need to write an expression for the spectral efficiency R in terms of m. As already mentioned, the SIR required β to achieve an outage probability P_{o} is related to R by the channel capacity formula (4.2). To obtain an expression for β, we begin by noting that packet retransmissions increase the interference level throughout the network, which can be modeled as an increase in the density of nodes in the network. Therefore, the *apparent* average density of nodes, as far as the effect of packet retransmission attempts on interference is concerned, can be written as

$$\lambda_{\mathrm{app}} = (1 + \overline{m})\, \lambda_{\mathrm{a}}. \tag{4.7}$$

If we consider here the dominant interferer approximation[1] and the distance dependent path loss channel modeling (cf. Section 2.2.2), we can apply Proposition 2.1 to state the following relation:

$$P_{\mathrm{o}} = 1 - e^{-\lambda_{\mathrm{app}} \pi d^2 \beta^{2/\alpha}}. \tag{4.8}$$

[1] As discussed in the previous chapters, it is worth remarking that this approximation is a lower bound on the actual outage probabilities. For more details, refer to [34]. The tightness of our approximation for the scenarios described in this paper can be found in [104, 122].

Inserting (2.12), (4.6) and (4.7) into (4.8), we have after some manipulation:

$$\beta = \left(\frac{1-\epsilon^{\frac{1}{1+m}}}{1-\epsilon} \frac{1}{\lambda \pi d^2} \ln\left(\frac{1}{1-\epsilon^{\frac{1}{1+m}}} \right) \right)^{\frac{\alpha}{2}}. \tag{4.9}$$

Here we insert expressions (4.5), (4.6), (4.2) and (4.9) into (4.3) to obtain the desired expression for TmC as a function of m:

$$\mathcal{T}(m) = \lambda_{\mathrm{a}} \left(1-\epsilon^{\frac{1}{1+m}}\right) \log_2 \left(1 + d^{-\alpha} \left(\frac{1-\epsilon^{\frac{1}{1+m}}}{1-\epsilon} \frac{1}{\lambda_{\mathrm{a}} \pi} \ln\left(\frac{1}{1-\epsilon^{\frac{1}{1+m}}} \right) \right)^{\frac{\alpha}{2}} \right). \tag{4.10}$$

Finally, we take the value of m that maximizes TmC to conclude the proof. □

Remark 4.1. In the preceding equation:

- One can easily show that (4.10) is a concave function in term of m so there always exists a $m \in \mathbb{N}$ that leads to the maximum TmC;
- The maximum number of retransmissions m is a natural number and typically small. Thus the search for the maximum TmC is computationally simple;
- If m is assumed to be a real number, it is possible to obtain the derivative of (4.10) in closed form and, then, compute m^* by solving $\mathcal{T}'(m) = 0$.

4.2.2 Unslotted ALOHA protocol

When the unslotted version of the ALOHA protocol is used, transmissions begin as soon as packets arrive and, in case of reception error, the packet waits an exponential distributed time according to the arrival process to be retransmitted (if retransmission is still possible). Therefore, a packet transmission initiated at time t_0 is interfered by transmissions initiated within the interval $[t_0 - T, t_0 + T)$. Based on this observation, we derive a proposition that gives the maximum number of retransmission for the unslotted ALOHA case.

Proposition 4.2 (unslotted ALOHA)**.** *The maximum number of retransmissions m^* that results in the optimal transmission capacity for the unslotted ALOHA protocol is given by given by*

$$m^* = \max_{m \in \mathbb{N}} \left(1-\epsilon^{\frac{1}{1+m}}\right) \log_2 \left(1 + d^{*-\alpha} \left(\frac{1-\epsilon^{\frac{1}{1+m}}}{1-\epsilon} \frac{1}{2\lambda_{\mathrm{a}} \pi} \ln\left(\frac{1}{1-\epsilon^{\frac{1}{1+m}}} \right) \right)^{\frac{\alpha}{2}} \right). \tag{4.11}$$

Outline of proof. The proof of this theorem basically follows the same steps as the proof of Proposition 4.1, with the difference that we now consider interfering transmissions in the interval $[-T, T)$. Therefore, the density of transmissions assumed in the unslotted ALOHA case is $\lambda_{\text{unslotted}} = 2\lambda_{\text{slotted}} = 2\lambda_{\mathrm{a}}$. □

4.2.3 CSMA with carrier sensing at the transmitter

When CSMA is used, packet transmissions occur only when the channel is assumed to be idle. The key mechanism of CSMA is the carrier sensing performed before each transmission attempt. If the channel is considered busy, i.e. if the SIR measured at the decision-making node (which can be either the transmitter or the receiver) is lower than a given threshold β_{sens}, then that transmission is backed off for an exponential distributed time period related to the arrival process. Otherwise, when the channel is considered idle, the packet transmission begins immediately. We will assume here that the back-off procedure may be repeated as many times as needed until the node finds the channel free and the packet is eventually transmitted, i.e. there is no constraint on the number of back-offs; this assumption can be easily relaxed [122] at expanse of more complicated mathematical formulation. Note that after a transmission begins, the receiver may experience SIR$< \beta$, leading to an outage event. We will also assume that the back-off procedure performed in each transmission attempts are independent of each other. As in the ALOHA protocol case, packets detected in error can be retransmitted up to m times before being dropped. If retransmission is required, the packet waits an exponential distributed time related to the arrival process to start the access procedure once again.

The channel sensing can be performed either at the transmitter node or at the receiver node. The former case is more usual and natural, as carrier sensing is typically triggered by packet arrivals at the transmitter. In this subsection, we will consider CSMA with carrier sensing at the transmitter side, while CSMA with carrier sensing at the receiver is considered in the next subsection.

Based on the transmission mechanism described above, we state the following proposition.

Proposition 4.3 (CSMA with carrier sensing at the transmitter)**.** *The maximum number of retransmissions m^* that results in the optimal transmission capacity for the CSMA protocol with sensing at the transmitter is given by*

$$m^* = \max_{m \in \mathbb{N}} \left(1 - \epsilon^{\frac{1}{1+m}}\right) \log_2 \left(1 + \frac{d^{-\alpha}}{s_m^{-\alpha}}\right), \tag{4.12}$$

where s_m is the sensing range required to achieve the required packet loss probability ϵ for a given m. The value of s_m is the s that is solution to the following equation:

$$A_s \left(1 + \exp\left(\lambda_{\text{a}} \frac{1 - \epsilon^{\frac{1}{1+m}}}{1-\epsilon} \pi s^2\right)\right) = \frac{1}{\lambda_{\text{a}}} \frac{1 - \epsilon^{\frac{1}{1+m}}}{1-\epsilon} \ln\left(\frac{1}{1 - \epsilon^{\frac{1}{1+m}}}\right), \tag{4.13}$$

where A_s is the area of the shaded region (portion of a disk of radius s centered at the receiver) shown in Fig. 4.1, and given by

$$A_s = \begin{cases} \pi s^2 & ; s \leq \dfrac{d}{2} \\ \pi s^2 + d\sqrt{s^2 - \dfrac{d^{*2}}{4}} - 2s^2 \cos^{-1}\left(\dfrac{d}{2s}\right) & ; s > \dfrac{d}{2} \end{cases}. \tag{4.14}$$

Proof. The proof is based on analyzing the transmission of a reference packet that begins at $t = 0$. Let $\mathcal{E}_1$ and $\mathcal{E}_2$ be the outage events associated with the interference caused by packets whose transmissions

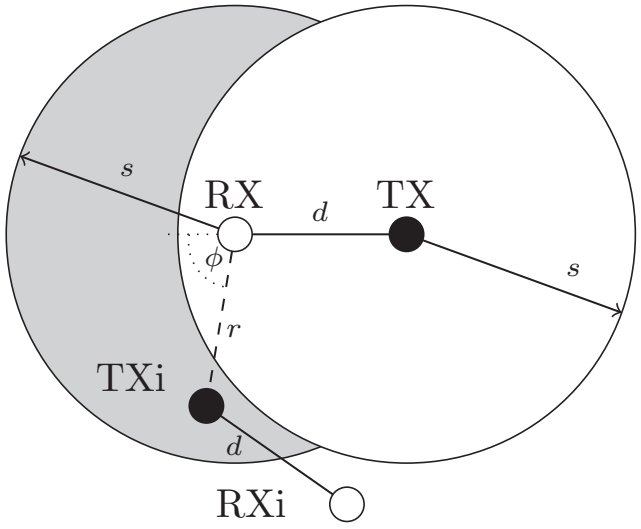

Fig. 4.1: Illustration of CSMA protocol with carrier sensing at the transmitter, where TX-RX is the reference link and TXi-RXi is an interferer link. An error event occurs whenever an active interfering transmitter lies inside the shaded area.

begin in the intervals $[-T, 0)$ and $[0, T)$, respectively. Thus, the outage probability P_{o} can be defined as

$$P_{\mathrm{o}} = \Pr\left[\mathcal{E}_1 \cup \left(\overline{\mathcal{E}_1} \cap \mathcal{E}_2\right)\right] = P_{\mathrm{o},1} + (1 - P_{\mathrm{o},1})\, P_{\mathrm{o},2}. \tag{4.15}$$

In this case, $P_{\mathrm{o},1}$ is the probability that there exists at least one active transmitter inside the area A_s (shaded area in Fig. 4.1) whose packet transmission initiated within interval $[-T, 0)$, while $P_{\mathrm{o},2}$ is the probability that at least one transmitter inside area A_s begins its transmission within interval $[0, T)$. Considering two distinct set of transmitters related, namely the set of active transmitters of density λ_{act} and the set of transmitters that are trying to access the channel of density λ_{csma}, we can compute the probabilities $P_{\mathrm{o},1}$ and $P_{\mathrm{o},2}$ based on Proposition 2.1 as

$$P_{\mathrm{o},1} = 1 - e^{-\lambda_{\mathrm{act}} A_s}, \tag{4.16}$$

$$P_{\mathrm{o},2} = 1 - e^{-\lambda_{\mathrm{csma}} A_s}. \tag{4.17}$$

Intuitively, the density of active links is equal to the density of transmitters trying to access the network that have not been backed off, i.e.

$$\lambda_{\mathrm{act}} = (1 - P_{\mathrm{b}})\, \lambda_{\mathrm{csma}}, \tag{4.18}$$

where P_{b} is the back-off probability. The back-off event corresponds to the event of having at least one active transmitter within the circular region of radius s centered at the transmitter. Therefore, P_{b} is given by

$$P_{\mathrm{b}} = 1 - e^{-\lambda_{\mathrm{act}} \pi s^2}. \tag{4.19}$$

The set of transmitters trying to access the network includes backed off links as well as links in retransmission mode. Thus, the density λ_{csma} is given by

$$\lambda_{\mathrm{csma}} = \lambda_{\mathrm{a}}\, \frac{1 - P_{\mathrm{o}}^{1+m}}{1 - P_{\mathrm{o}}} \sum_{i=0}^{\infty} P_{\mathrm{b}}^{i} = \lambda_{\mathrm{a}}\, \frac{1 - P_{\mathrm{o}}^{1+m}}{1 - P_{\mathrm{o}}}\, \frac{1}{1 - P_{\mathrm{b}}}, \tag{4.20}$$

Next, we insert (4.18), (4.20), (4.19), (4.16) and (4.17) into (4.15) and, then, we apply (4.5) to obtain (4.12) after some manipulations. The area A_s is computed using geometric arguments, which completes this proof. □

4.2.4 CSMA with carrier sensing at the receiver

In [122] the authors proposed a variant of CSMA in which the carrier sensing is performed at the receiver such that it senses the channel and reports to its associate transmitter whether the channel is busy or not. The communication between receiver and transmitter regarding the channel condition is over a control channel, assumed error-free. Based on this, we can state the following proposition.

Proposition 4.4 (CSMA with carrier sensing at the receiver)**.** *The maximum number of retransmissions m^* that results in the optimal transmission capacity for the CSMA with carrier sensing at the receiver is given by*

$$m^* = \max_{m \in \mathbb{N}} \left(1 - \epsilon^{\frac{1}{1+m}}\right) \log_2 \left(1 + \frac{d^{-\alpha}}{s_m^{-\alpha}}\right), \tag{4.21}$$

where s_m is the sensing range required to achieve the required packet loss probability ϵ for a given m. The value of s_m is the s that is solution to the equation:

$$I_s \ \exp\left(\lambda_{\mathrm{a}} \frac{1 - \epsilon^{\frac{1}{1+m}}}{1-\epsilon} \pi s^2\right) = \frac{1}{\lambda_{\mathrm{a}}} \ \frac{1 - \epsilon^{\frac{1}{1+m}}}{1-\epsilon} \ln\left(\frac{1}{1 - \epsilon^{\frac{1}{1+m}}}\right), \tag{4.22}$$

where I_s is given by

$$I_s = \begin{cases} \displaystyle\int_0^s \int_0^{2\pi} \left(1 - \frac{1}{\pi} \cos^{-1}\left(\frac{r^2+2d^2-s^2-2rd\cos\phi}{2d\sqrt{r^2+d^2-2rd\cos\phi}}\right)\right) r \ d\phi dr & ; s \leq d \\ \displaystyle\int_{s-d}^{s} \int_{\nu}^{2\pi-\nu} \left(1 - \frac{1}{\pi} \cos^{-1}\left(\frac{r^2+2d^2-s^2-2rd\cos\phi}{2d\sqrt{r^2+d^2-2rd\cos\phi}}\right)\right) r \ d\phi dr & ; s > d \end{cases}, \tag{4.23}$$

such that

$$\nu = \cos^{-1}\left(\frac{r^2 + 2ds - s^2}{2rd}\right). \tag{4.24}$$

Proof. The proof of this theorem is similar to the proof of Proposition 4.3, with some key differences, as commented next. Firstly, note that the interference caused by transmissions that begin within the interval $[-T, 0)$ is completely avoided when carrier sensing is performed at the receiver. During the interval $[0, T)$, however, interfering transmitters may still be present inside the sensing region (disk of radius s center at the receiver). This will happen if interfering transmissions begin within such interval and if the transmitter of the reference link is not located inside the sensing region of the interfering link (otherwise, the carrier sensing at the receiver of the interfering link would detect the transmission of the reference link).

Fig. 4.2 shows an example of such an event, where we can see that the occurrence of this event depends on a particular combination of relative positions (distance and angle) between the nodes

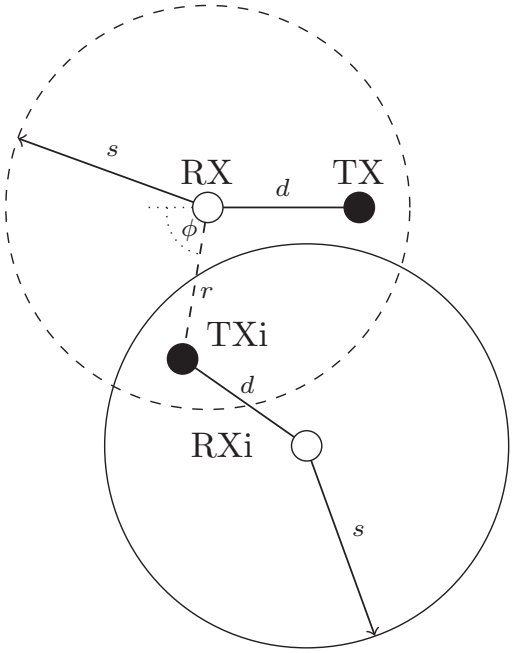

Fig. 4.2: Illustration of CSMA protocol with receiver sensing, where TX-RX is the reference link and TXi-RXi is an interferer link. An outage event occurs whenever an active interfering transmitter lies inside the area inside the dashed circumference and the reference transmitter is out of the range determined by the solid circle. The parameters ϕ and r are the integration variables.

of the reference link and the interfering link. The non-homogeneous Poisson process of interferers by-product of this sensing procedure has density $\lambda(r,\phi)$, which is computed as

$$\lambda(r,\phi) = \lambda_{\text{csma}} \Pr[\text{active}|\ (r,\phi)]. \tag{4.25}$$

Here we use the fact that the outage probability can be obtained in the non-homogeneous case as $1 - e^{-\text{E}[\#\text{ of interferers}]}$ [122], we can use Definition 2.3 to find the expected number of nodes in the area based on the intensity function $\lambda(r,\phi)$ and then

$$\begin{aligned} P_{\text{o}} &= 1 - \exp\left(- \iint\limits_{R} \lambda(r,\phi)\ r dr d\phi \right) \\ &= 1 - \exp\left(-\lambda_{\text{csma}} \iint\limits_{D} \Pr[\text{active}|\ (r,\phi)] r\ dr d\phi \right), \end{aligned} \tag{4.26}$$

where the integration region D and the probability $\Pr[\text{active}|\ (r,\phi)]$ are computed based on the geometry of the sensing procedure (see Fig. 4.2).

Now, we denote $\iint_D \Pr[\text{active}|\ (r,\phi)] r\ dr d\phi$ as I_s to finalize this proof[2]. □

[2]Refer to [122, Th. 7] for further details in the geometrical analysis of the sensing procedure.

4.3 Numerical results

In this section, we present a numerical analysis of the transmission capacity based on the expressions derived in the previous sections. We consider a network with transmitter-receiver separation distance equals to $d = 1$ [m], path-loss exponent $\alpha = 4$ and required packet loss probability $\epsilon = 0.02$.

Fig. 4.3 shows the transmission capacity TmC as a function of the maximum number of retransmissions m, for all four MAC protocols studied in this chapter, and for spatial density $\lambda_{\text{a}} = 0.05$ [packets/m^2]. We can see that all curves present the same behavior as the maximum number of retransmissions increases, regardless of the medium access scheme. Using a larger maximum number of retransmissions m allows for a larger outage probability P_{o} needed to achieve the required packet loss probability ϵ (as there will be more chances to transmit a packet until it is received without error). This higher outage probability means that information can be coded at higher rates R and thus the TmC increases.

On the other hand, a higher P_{o} leads to a larger average number of retransmissions $\overline{m}$, increasing the network traffic and reducing its efficiency since more channel usages are needed to eventually transmit a packet without error. The combination of these opposite effects explains the curve behavior as the maximum number of retransmission increases. Our analytical formulation provides the value of the maximum number of retransmissions that maximizes the TmC.

Next, using the proposition stated in the previous section, we analyze the optimal TmC obtained by setting of the maximum number of retransmission m^*. Fig. 4.4 shows the optimal TmC versus the packet density for all four MAC protocols investigated. We note that the both CSMA protocols outperform slotted ALOHA for lower λ_{a}, while the opposite happens when λ_{a} is large. For lower densities of packets, the contention resolution capability of CSMA protocols provides a considerable gain in the system efficiency (specially when carrier sensing is performed at the receiver[3]), evincing the benefits of carrier sensing and back-off procedures

When λ_{a} is further increased, clearly the traffic intensity throughout the network increases, regardless of the MAC protocol, causing more packet errors and backed off transmissions (for CSMA protocols). These in turn lead to a larger number of links trying to access the network (packets to be retransmitted and backed off), worsening the interference problem. Then, at higher levels of packet density, the synchronous nature of transmissions in the slotted ALOHA becomes a relevant feature for interference control. Consequently, such protocol has the highest transmission capacity when λ_{a} increases.

[3] Intuitively, CSMA with carrier sensing at the receiver performs better than that with carrier sensing at the transmitter, because interference is harmful at the receiver side.

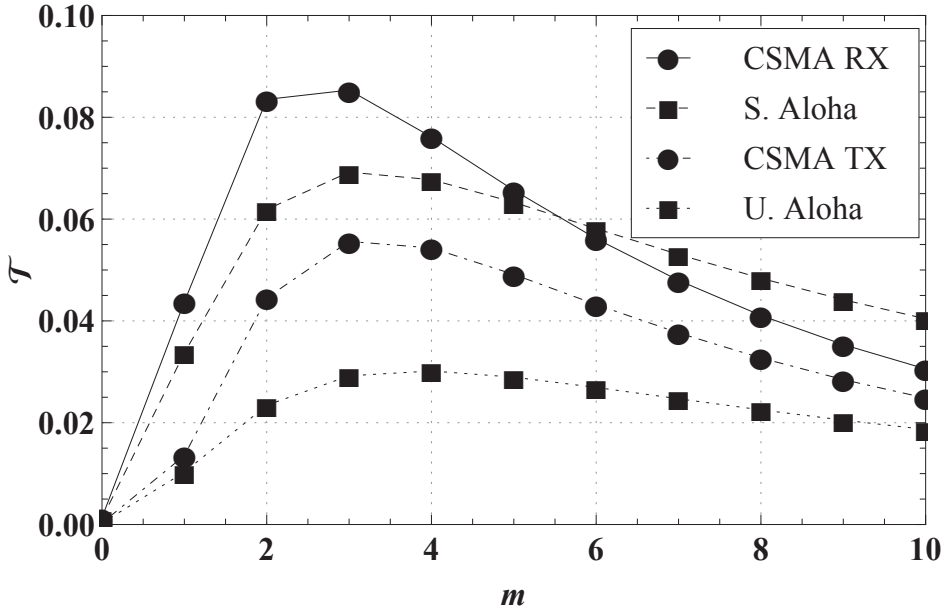

Fig. 4.3: Transmission capacity $\mathcal{T}$ given by (4.3) as a function of the maximum number of retransmissions m for slotted and unslotted ALOHA, and CSMA with sensing at transmitter and at the receiver. We assume that $\lambda_a = 0.05$ [packets/m^2].

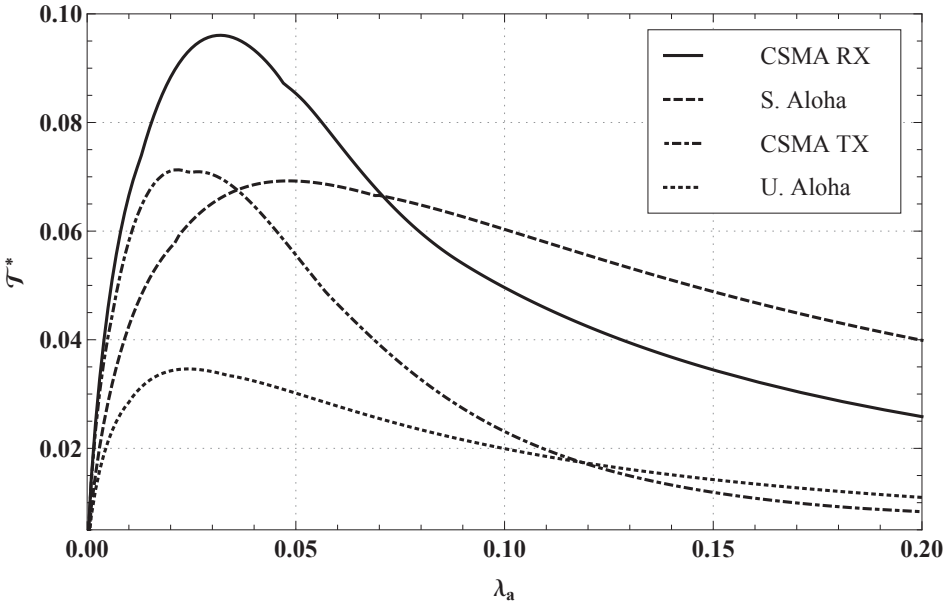

Fig. 4.4: Optimal transmission capacity $\mathcal{T}^*$ computed using Propositions 4.1 to 4.4 versus packet density λ_a for slotted and unslotted ALOHA, and CSMA with sensing at transmitter and at the receiver.

4.4 Summary

In this chapter we investigated the effects of packet retransmission on a revisited version of the transmission capacity (TmC) metric using the maximum number of allowed retransmission as the key parameter. Specifically, the formulation proposed here captures the trade-offs involving spectral efficiency, traffic intensity and transmission robustness, which will determine the system performance. Based on this new TmC definition, we derived analytical expressions to evaluate the maximum number of possible retransmissions that maximizes the TmC in networks operating under different variations of CSMA and ALOHA protocols.

Our numerical results show the traffic operating regions where the sensing capability of the CSMA protocol is preferable to the synchronous nature of the slotted ALOHA, and vice-versa. Specifically, when low packet densities are considered, the highest maximum transmission capacity is achieved by the CSMA protocol, while slotted ALOHA provides the best results for denser networks.

Chapter 5

Throughput optimization with queue stability and packet loss constraints

In this chapter, we extend the spatial throughput framework by studying single-hop networks with Poisson field of interferers and a limited number of retransmissions under a maximum packet loss probability and queue stability constraint. This provides another step towards a combined approach for addressing the longtime unconsumed union between information and networking theory [72]. Specifically, constrained maximization problems for the *effective link throughput* and the *network spatial throughput* of a random access network are cast, in which transmitters are located according to a PPP, packet inter-arrival time is geometrically distributed, and there is a limited number of retransmissions. In both optimization problems, we are interested in determining the operating points - access probability, coding rate and maximum number of retransmissions - that lead to the highest performance subjected to those constraints, given the packet arrival process and the density of transmitters in the network. Closed-form approximate solutions are then derived to both design settings as well as upper bounds of their highest achievable values based on the unconstrained optimization.

Our results show the effect of the network density and arrival rate on the network performance, indicating under which network parameters the optimal constrained performance converges to its unconstrained solution. Necessary conditions so that either effective link throughput or spatial throughput is achievable under the stability and packet loss constraints are also provided. Finally, we make evident the effect of selfish and collective decisions on the network efficiency, showing when selfish link optimization solutions can be also the best choice in terms of network-wide sum throughput performance.

5.1 System modeling and baseline definitions

5.1.1 Network modeling

We consider a single-hop ad hoc wireless network, in which the spatial locations of transmitters (TXs) at each time-slot $t \in \mathbb{N}_+$ are distributed according to a homogeneous Poisson point process $\Phi_0 \subset \mathbb{R}^2$ with non-null intensity λ_0 [TXs/m^2]. Each TX is associated with one receiver (RX) following a bipolar model [10] and packets arrive at the buffer of TX$_k$, $k \in \mathcal{A}_0$, according to a stochastic

arrival process $X_k(t)$, where $\mathcal{A}_0$ denotes the set of all TXs generated by Φ_0. The arrival process to transmitter TX_k is assumed to be stationary with an average rate μ_k packets/slot. We assume buffers of infinite capacity and time is slotted with slot duration equal to the packet duration.

At the end of each time slot t, the locations of the nodes are shuffled following a high mobility random walk as proposed in [85]. Due to this mobility model, the displacement theorem can be applied [10, Sec. 1.3.3] and hence the TXs' locations in each time slot t are generated as a different sample of the point process Φ_0. This assumption results in independence between the nodes' positions across time slots.

It is important to say that the high mobility random walk is somehow an artificial mobility model and practical scenarios should consider correlation between events that occur in different time slots [117, 123]. Nevertheless, such an approach is hard or impossible to lead to closed-form, analytical expressions due to the coupling between service rate and interference process. For that, in this work, we employ the high mobility random walk model in order to derive neat closed-form expressions, which in turn are still able to provide valuable and crisp insights on the network performance. We will further discuss these aspects related to mobility in Chapter 7.

Once again we assume that each TX_k employs Gaussian point-to-point (G-ptp) codes and its corresponding receiver RX_k employs the IAN decoding rule introduced in Section 2.1. We also apply Definition 2.5 to assess whether a given communication between TX_k-RX_k is in outage during a packet transmissions at time slot t. Assuming that the noise power is negligible in comparison to the interference and a channel modeling composed by a deterministic distance-dependent path loss with exponent $\alpha > 2$ and random channel gains h, we can rewrite equation (2.11) for time slot t as

$$\text{SIR}_k(t) = \frac{h_{kk}(t)d^{-\alpha}}{\sum\limits_{j\in\mathcal{A}(t)\setminus\{k\}} h_{kj}(t)(d_{kj}(t))^{-\alpha}} \geq \beta_k, \tag{5.1}$$

where d is the transmitter-receiver distance in [m], $d_{yx}(t)$ and $h_{yx}(t)$ are the distance and the random channel gain between TX_x and RX_y during a given time slot t, and $\mathcal{A}(t) \subseteq \mathcal{A}_0$ refers to the subset of active TXs in t. The SIR threshold β_k required by RX_k to successfully decode the packets is a system parameter that depends on the coding rate R_k [bits/s/Hz] employed by each TX_k. As in the previous chapters we can related the SIR threshold and the coding rate using the channel capacity, yielding $R_k = \log_2(1+\beta_k)$.

Likewise Chapter 4 we consider the ARQ retransmission protocol such that the success or failure (outage) of the packet detection at RX is reported back to TX through an error- and delay-free control channel. In that case, the undelivered packet returns to the head-of-line of the queue, waiting to be retransmitted in the next medium access. Assuming that a packet can be retransmitted through the TX_k–RX_k link at most m_k times, then there are two possible outcomes for packet departure from the queue of TX_k, namely (i) it is either correctly received or (ii) it is not successfully received after $1+m_k$ attempts and then dropped from the queue, declaring a packet loss event. Hence, the packet loss probability for TX_k–RX_k, denoted $P_{\text{pkt},k}$, is a function of the number of allowed retransmissions and the outage probability, i.e. $P_{\text{pkt},k} = f(P_{\text{o},k}, m_k)$, where the outage probability is given by $P_{\text{o},k} = \Pr[\text{SIR}_k < \beta_k]$.

5.1.2 Queue stability

Assuming here a single-server discrete-time queuing system, the backlog $Q_k(t)$ (queue length) for TX_k is evolving for $t \in \{0, 1, 2, \ldots\}$ as [84]:

$$Q_k(t+1) = \max[Q_k(t) - Y_k(t), 0] + X_k(t), \tag{5.2}$$

where $\{X_k(t)\}_{t=0}^{\infty}$ and $\{Y_k(t)\}_{t=0}^{\infty}$ are the arrival and the server process at TX_k in time slot t and the initial queue lengths $\{Q_k(0)\}$ are chosen independently across TXs according to some probability distribution. Note that packet arrival and channel access events are independent across sources and slots.

For the definition of queue stability, we resort to [124].

Definition 5.1 (stability)**.** *A multidimensional stochastic process (not necessarily Markovian)* $\mathbf{Q}(t) = (Q_1(t), \ldots, Q_1(t))$ *is stable if for* $\mathbf{x} \in \mathbb{N}_0^M$ *the following holds*

$$\lim_{t\to\infty} \Pr[\mathbf{Q}(t) < \mathbf{x}] = F(\mathbf{x}) \quad \text{and} \quad \lim_{\mathbf{x}\to\infty} F(\mathbf{x}) = 1, \tag{5.3}$$

where $F(\mathbf{x})$ *is the limiting distribution function and* $\mathbf{x} \to \infty$ *means that* $x_k \to \infty$, $\forall k$*. If a weaker condition holds, namely,*

$$\lim_{\mathbf{x}\to\infty} \liminf_{t\to\infty} \Pr[\mathbf{Q}(t) < \mathbf{x}] = 1, \tag{5.4}$$

then the process is called substable (tight or bounded in probability).

The queue stability evidently depends on both $\{X_k(t)\}_{t=0}^{\infty}$ and $\{Y_k(t)\}_{t=0}^{\infty}$. While the former is an input parameter that the network operator cannot always control, the latter is determined by the MAC protocol, the retransmission policy, and the probability that a packet is successfully received during a transmission attempt. Such a success probability is in fact a physical layer figure, which in turn is related to the decoding strategy, co-channel interference, noise power, and desired signal strength.

5.1.3 Performance metrics

Based on the system model presented above, we define next the performance measures of interest, which are the effective throughput of a point-to-point link and the spatial throughput of the network.

Definition 5.2 (effective link throughput)**.** *Given that the network is in a steady state, the effective link throughput of a given link* TX_k–RX_k*, denoted by* $\mathcal{R}_k$ *and measured in [bits/s/Hz], is defined as*

$$\mathcal{R}_k = (1 - P_{\text{pkt},k})\, p_k\, \rho_k\, \frac{R_k}{1 + \overline{m}_k}, \tag{5.5}$$

where ρ_k *is the probability that the queue of* TX_k *is not empty in a given time slot,* p_k *is the probability that* TX_k *is granted to access the radio channel in a given time slot, and* $\overline{m}_k$ *is the average number of packet retransmissions.*

Definition 5.3 (network spatial throughput)**.** *Given that the network is in a steady state, the spatial throughput, denoted by $\mathcal{S}$ and measured in [bits/s/Hz/m^2], is defined as the sum of the effective link throughputs $\mathcal{R}_k \; \forall \; k \in \mathcal{A}_0$ divided by the total network area A [m^2] where the points of process are distributed, i.e.*

$$\mathcal{S} = \frac{1}{A} \sum_{k \in \mathcal{A}_0} \mathcal{R}_k. \tag{5.6}$$

In the following sections, we use these definitions to assess and optimize the performance of decentralized networks where the transmitters' locations are spatially distributed according to a 2-D homogeneous PPP. Specifically, in Section 5.2, we study how the typical link tunes selfishly its access probability, its maximum number of retransmissions, and the SIR target as a mean of maximizing its own individual effective link throughput. In Section 5.3, on the other hand, we take on a different approach by considering the spatial network throughput, formulating a network-wide optimization problem, and showing under which conditions the selfish (local) behavior also maximizes the aggregate throughput.

5.2 Effective link throughput optimization

In this section, we aim at computing the maximum effective throughput that a link can support such that the packet loss probability is bounded by given maximum value and queue stability is guaranteed. Specifically, we show which design parameters achieve the maximum performance and then analyze how the effective throughput is related to the network density and the arrival rate.

5.2.1 Scenario description

Let Φ_0 be a homogeneous Poisson point process of intensity λ_0 [TXs/m^2] distributed over the infinite plane, i.e. the point process Φ_0 is analyzed in $\mathbb{R}^2$ and therefore the number K of TXs over the network tends to infinity. For convenience, we describe here a scenario in which there are K TXs distributed over the network area but always keeping in mind that $K \to \infty$.

Let us assume that at the beginning of each time slot t every TX$_k$ with $k \in \mathcal{A}_0$ is granted access to the network with probability p_k independently of other nodes (slotted ALOHA) and to its queue state. We define a vector $\mathbf{p} = (p_1, \ldots, p_K) \in [0,1]^K$ associated with the (constant) channel access probability of TX$_k$, $k = 1, \ldots, K$ with $K = |\mathcal{A}_0|$. Furthermore, if the queue system of all TXs is in the steady state, we can compute the probability that TX$_k$ does not have any packet to send in its buffer as $1 - \rho_k$, for $k \in \mathcal{A}_0$, and then we can similarly define the vector $\boldsymbol{\rho} = (\rho_1, \ldots, \rho_K) \in [0,1]^K$. The probability ρ_k is related to the offered load of TX$_k$ queue, as discussed next.

Let us consider that every TX$_k$ is subject to independent geometrical arrivals with rate $0 \leq \mu_k \leq 1$, allowing us to define the set of arrival rates $\boldsymbol{\mu} = (\mu_1, \ldots, \mu_K) \in [0,1]^K$. If the server process has finite average $\mathbb{E}[Y_k(t)] = \theta_k \leq 1$, which is a function of the access probability, the outage probability and number of allowed retransmissions, i.e. $\theta_k = f(p_k, P_{\mathrm{o},k}, m_k)$, the non-empty state probability, or the load of the queue system, ρ_k is defined as [125]

$$\rho_k \triangleq \frac{\mu_k}{\theta_k}. \tag{5.7}$$

From this, we can clearly see that $\boldsymbol{\rho}$ is a function of $\mathbf{p}$. In the steady state, the probabilities given by the vector $\boldsymbol{\rho}$ are also fixed regardless of which TXs are granted to access the network in a specific time slot. Once again it is important to remember that we consider here the high mobility random walk such that the nodes' position in every time slot can be viewed as a different and independent realization of the point process Φ_0. Therefore, we can identify two independent events related to every TX_k in a given time slot t assuming that the network has already reached its steady state: (i) access the network with a fixed probability p_k and (ii) have an empty queue with probability $1-\rho_k$.

Based on the above facts and the homogeneity of the PPP Φ_0, we can characterize the point process of the active TXs in network (i.e. the nodes that are awarded to access the network and have a packet to transmit in its queue) after the steady state is achieved applying two thinning transformations (cf. Property 2.5) associated to the events described above. Let us denote by Φ_{a} the point process byproduct of a thinning transformation of Φ_0 related to the network access defined by vector of probabilities $\mathbf{p}$. Hence we use Theorems 1.3 and 2.3 from [111] to verify that Φ_{a} also forms a homogeneous PPP of intensity $\lambda_{\text{a}} = \overline{p}\ \lambda_0$, where $\overline{x} = \|\mathbf{x}\|_1 / K$ with $\|\mathbf{x}\|_1$ being the L^1-norm of a vector $\mathbf{x}$. It is important to note that $\overline{p}$ can be interpreted as the average access probability that the TXs have.

Note that, in the steady state, the probability that an empty queue event occurs in a given slot t for every TX_k, $\forall k \in \mathcal{A}_0$, is independent of the event of TX_k being granted to access the network in that slot, even though the probability ρ_k is a function of p_k. Knowing this, we can characterize the process of the actual concurrent transmissions Φ, which is also a homogeneous PPP, as a thinning transformation of Φ_{a} in accordance with the probabilities characterized by $\boldsymbol{\rho}$. Then, we proceed as before to evaluate the intensity of the process Φ as $\lambda = \overline{p}\ \overline{\rho}\ \lambda_0$.

5.2.2 Analytical results

We focus on a typical link TX_0–RX_0 such that RX_0 is placed at the origin of Φ_0 and TX_0 is located at fixed distance d from it. Packets arrive at TX_0 queue system with rate μ_0, following a geometric distribution. We calculate the access probability p_0, the coding rate R_0, and the maximum number of retransmissions m_0, which lead to the maximum effective stable throughput (cf. Definition 5.2) for the typical link TX_0–RX_0.

We consider here that the small-scale fading channel gains $h_{yx}(t)$ between TX_x and RX_y are i.i.d. (across time and space) random variables with constant during time slot t. From these assumptions, we can rewrite the SIR equation (5.1) for the reference link as:

$$\text{SIR}_0(t) = \frac{h_{00}(t)\ d^{-\alpha}}{\sum\limits_{j \in \mathcal{A}(t)} h_{0j}(t)\ (d_{0j}(t))^{-\alpha}}, \tag{5.8}$$

such that the success probability is then given by $\Pr\left[\text{SIR}_0 \geq \beta_0\right]$, where β_0 is the SIR threshold required by TX_0–RX_0 in order to sustain a rate of $R_0 = \log_2(1+\beta_0)$ with arbitrarily low error probability using G-ptp codes and IAN decoding rule.

We assume in this chapter the outage probability for the Rayleigh fading case for exposition

convenience, i.e. h is an exponential random variable with unit mean[1]. Besides the time index is dropped whenever the quantities and the results are independent of the time slot t, i.e. in the steady state. From these assumptions, we can propose a variation of Proposition 2.2 for the scenario studied in this chapter as follows.

Proposition 5.1. *Given that all TXs have stable queue systems and the network is in the steady state, the outage probability $P_{\mathrm{o},0}$ experienced by TX_0–RX_0 is given by*

$$P_{\mathrm{o},0} = 1 - e^{-\overline{p}\,\overline{p}\,\lambda_0 \kappa\, d^2 \beta_0^{2/\alpha}} \tag{5.9}$$

where $\kappa = \pi\Gamma(1+2/\alpha)\Gamma(1-2/\alpha)$. In addition, if the maximum acceptable packet loss probability is bounded by a threshold ϵ, the following inequality has to be satisfied:

$$P_{\mathrm{o},0}^{1+m_0} \leq \epsilon. \tag{5.10}$$

Outline of proof. The proof of (5.9) follows the results presented in [10], noting that $\overline{p}$ and $\overline{p}$ are constants when all TXs have stable queues and the network is in its steady state. To prove (5.10), we use the fact that packets not successfully decoded by RX_0 can be retransmitted up to m_0 times before being dropped and that the outage events are independent across time slots, yielding that the packet loss probability is $P_{\mathrm{pkt},0} = P_{\mathrm{o},0}^{1+m_0}$. □

We proceed now with obtaining the probability that the buffer of a typical TX_0 is empty using similar arguments as in [85], under the assumption that a high mobility random walk model is considered and that the point process Φ is studied in $\mathbb{R}^2$. Consider that the system is in steady state and recall that the queue of the typical TX is subject to i.i.d. packet arrivals with probability μ_0 and i.i.d. departures with probability θ_0, the offered load is then $\rho_0 = \mu_0/\theta_0$. Using elements from the theory of G/G/1 queues, the probability that the queue is empty is shown to be $\max[0, 1-\rho_0]$ [125]. Furthermore, from the definition of ρ_0 and assuming stable queues for all TXs, we provide the following result.

Proposition 5.2 (service rate)**.** *Given that all TXs have stable queues and the network is in steady state, then the service rate θ_0 of a typical link is given by*

$$\theta_0 = p_0 \; \frac{e^{-\overline{p}\,\overline{p}\,\lambda_0 \kappa\, d^2 \beta_0^{2/\alpha}}}{1 - \left(1 - e^{-\overline{p}\,\overline{p}\,\lambda_0 \kappa\, d^2 \beta_0^{2/\alpha}}\right)^{1+m_0}}. \tag{5.11}$$

Proof. We first recall that the medium access process is independent of the outage events, which are independent across time slots. Therefore, we have that

$$\theta_0 = \frac{p_0}{1+\overline{m}_0}, \tag{5.12}$$

where $1+\overline{m}_0$ is the average number of transmission attempts available for a packet arriving at TX_0, given by

$$1 + \overline{m}_0 = 1 + P_{\mathrm{o},0} + P_{\mathrm{o},0}^2 + ... + P_{\mathrm{o},0}^{m_0} = \sum_{k=0}^{m_0} P_{\mathrm{o},0}^k = \frac{1 - P_{\mathrm{o},0}^{1+m_0}}{1 - P_{\mathrm{o},0}}. \tag{5.13}$$

Applying the sequence of equations (5.9) → (5.13) → (5.12), the proof is concluded. □

[1]Our results can be easily extended to either other general fading distributions or to the dominant interferer approximation used in the previous chapters.

The above proposition provided the server rate at TX_0 assuming that its queue is stable. We derive now a sufficient condition that guarantees queue stability at TX_0.

Proposition 5.3 (queue stability)**.** *Given that all TXs excluding TX_0 have stable queue systems and that the network is in steady state, a sufficient condition for stability in the queue system of TX_0 is given by*

$$\mu_0 < p_0 \left[\sum_{i=1}^{1+m_0} \binom{1+m_0}{i} (-1)^{i+1} \, e^{-\overline{p}\,\lambda_0 (i-1)\kappa d^2 \beta_0^{2/\alpha}} \right]^{-1}. \tag{5.14}$$

Proof. To provide a sufficient condition for stability in the queuing system of TX_0, we first assume the worst case scenario for interference, namely all TXs granted access the network transmit packets regardless of their backlog state (cf. *dominant network* [126]). In other words, transmitters with empty queues make dummy transmissions, yielding $\overline{p} = 1$ and that the density of active transmitters is $\lambda = \overline{p}\lambda_0$. Let $\theta_{0,\text{dom}}$ denote the server rate of TX_0 for the dominant network configuration. Based on the fact that the arrival and server processes are jointly ergodic and stationary (refer to [85] for more details), we can use the inequality $\mu_0 < \theta_{0,\text{dom}}$ as a sufficient condition for the stability of the typical link [125]. Then, applying the statements presented above into (5.11) yields

$$\mu_0 < \theta_{0,\text{dom}} = p_0 \, \frac{e^{-\,\overline{p}\,\lambda_0 \kappa \, d^2 \beta_0^{2/\alpha}}}{1 - \left(1 - e^{-\,\overline{p}\,\lambda_0 \kappa \, d^2 \beta_0^{2/\alpha}}\right)^{1+m_0}}. \tag{5.15}$$

To obtain equation (5.14), we manipulate the binomial expansion of the denominator of (5.15), which concludes this proof. □

Remark 5.1. *Following Definition 5.1, we can say that, when $\rho_0 = \dfrac{\mu_0}{\theta_0} \to 1$, the queue of TX_0 is in the boundary of stability.*

Before presenting the optimization problem that is the main target of this section, we rewrite the effective link throughput formulation stated in Definition 5.2 as:

$$\begin{aligned} \mathcal{R}_0 &= (1 - P_{\text{pkt},0}) \, p_0 \, \rho_0 \, \frac{R_0}{1 + \overline{m}_0} \\ &= (1 - P_{o,0}^{1+m_0}) \, p_0 \, \rho_0 \, \frac{R_0 \, (1 - P_{o,0})}{1 - P_{o,0}^{1+m_0}} \\ &= p_0 \, \rho_0 \, \log_2(1 + \beta_0) \, e^{-\overline{\rho}\,\overline{p}\,\lambda_0 \kappa \, d^2 \beta_0^{2/\alpha}}. \end{aligned} \tag{5.16}$$

Combining the above propositions with (5.16), we formulate the optimization problem which provides the highest effective link throughput the typical link TX_0–RX_0 can achieve while its packet loss probability is bounded by a maximum value ϵ and its queue is stable as follows[2]:

[2]It is interesting to say that in some applications there is a requirement of minimum coding rate R_0 and then an additional constraint regarding the threshold β_0 must be included. Clearly a different optimization formulation for this new scenario might be found, but in any case it will never outperform the solution without the minimum rate constraint, which in fact provides an upper bound to the new problem.

$$\begin{aligned}
\max_{(p_0,\beta_0,m_0)} \quad & p_0\ \rho_0\ \log_2(1+\beta_0)\ e^{-\overline{\rho}\,\overline{p}\,\lambda_0\kappa\ d^2\beta_0^{2/\alpha}} \\
\text{s.t.} \quad & \left(1-e^{-\overline{\rho}\,\overline{p}\,\lambda_0\kappa\ d^2\beta_0^{2/\alpha}}\right)^{1+m_0} \leq \epsilon, \\
& \theta_0 = p_0\ \frac{e^{-\overline{\rho}\,\overline{p}\,\lambda_0\kappa\ d^2\beta_0^{2/\alpha}}}{1-\left(1-e^{-\overline{\rho}\,\overline{p}\,\lambda_0\kappa\ d^2\beta_0^{2/\alpha}}\right)^{1+m_0}}, \\
& \theta_0 \geq p_0\ \left[\sum_{i=1}^{1+m_0}\binom{1+m_0}{i}(-1)^{i+1}\ e^{-\overline{p}\,\lambda_0(i-1)\kappa d^2\beta_0^{2/\alpha}}\right]^{-1} > \mu_0.
\end{aligned}$$

The above optimization problem is non-convex in general, hence it is hard to obtain an analytical solution. In order to gain some insight, we propose an approximate closed-form solution to determine the maximum constrained effective link throughput $\mathcal{R}_0^*$ by observing some properties of the problem.

Proposition 5.4 (highest constrained effective link throughput)**.** *Given that all TXs excluding TX$_0$ have stable queues, the packet loss constraint ϵ has a small value and the system reached a steady state, and assuming that the number of retransmissions m_0 is a non negative real number, the highest effective throughput $\mathcal{R}_0^*$ achieved by the typical link TX$_0$–RX$_0$ under queue stability and bounded packet loss can be approximated by*

$$\mathcal{R}_0^* \approx \mu_0\ (1-\epsilon)\ \log_2\left(1+\left(\frac{-\ln(\mu_0\ (1-\epsilon))}{\overline{\rho}\,\overline{p}\ \lambda_0\kappa\ d^2}\right)^{\alpha/2}\right), \tag{5.17}$$

where the system parameters $(p_0^*, \beta_0^*, m_0^*)$ that lead to the approximated optimal effective rate $\mathcal{R}_0^*$ are given by

$$\begin{aligned}
p_0^* &= 1, \\
\beta_0^* &= \left(\frac{-\ln(\mu_0\ (1-\epsilon))}{\overline{\rho}\,\overline{p}\ \lambda_0\kappa\ d^2}\right)^{\alpha/2}, \\
m_0^* &= \frac{1}{\log_\epsilon(1-\mu_0(1-\epsilon))} - 1.
\end{aligned}$$

Proof. The optimal values or functions of them are denoted below using *. Note first that the optimal solution should be in the boundary of stability (i.e. $\rho_0^* = \theta_0^*/\mu_0 \to 1$), indicating that whenever TX$_0$ is granted access to the medium, it has a packet to transmit. As the packet loss constraint ϵ is a small number, we can make the following approximation $P_{\text{pkt},0}^* = P_{\text{o},0}^{*1+m_0^*} \approx \epsilon$ for the optimal solution (i.e. $P_{\text{pkt},0}$ is approximated to its maximum acceptable value). From these observations, using equations (5.12) and (5.13), we have the following relation:

$$\mu_0 \approx \theta_0^* = p_0^*\ \frac{1-\epsilon^{\frac{1}{1+m_0^*}}}{1-\epsilon} \Rightarrow p_0^*\ \left(1-\epsilon^{\frac{1}{1+m_0^*}}\right) \approx \mu_0(1-\epsilon). \tag{5.18}$$

We also manipulate the outage constraint (5.10) knowing that $P_{\text{o},0}^* = \epsilon^{\frac{1}{1+m_0^*}}$, which yields

$$\epsilon \approx \left(1-e^{-\overline{\rho}\,\overline{p}\,\lambda_0\ \kappa\ d^2\ \beta_0^{*2/\alpha}}\right)^{1+m_0^*}. \tag{5.19}$$

Then we can combine (5.18) and (5.19) by isolating the term $1 - \epsilon^{\frac{1}{1+m_0^*}}$ to obtain the following relation:

$$1 - \epsilon^{\frac{1}{1+m_0^*}} \approx \frac{\mu_0}{p_0^*}(1-\epsilon) \approx e^{-\overline{\rho}\,\overline{p}\,\lambda_0\,\kappa\,d^2\,\beta_0^{*2/\alpha}},$$

from where, after an algebraic manipulation, we compute the SIR threshold β_0^* that leads to our approximation to the highest effective throughput as

$$\beta_0^* \approx \left(\frac{\ln(p_0^*) - \ln(\mu_0(1-\epsilon))}{\overline{\rho}\,\overline{p}\,\lambda_0\kappa d^2}\right)^{\alpha/2}. \tag{5.20}$$

Recalling that $R_0^* = \log_2(1+\beta_0^*)$, we then apply (5.18) and (5.20) into (5.16), which results in

$$\mathcal{R}_0^* \approx \mu_0\,(1-\epsilon)\log_2\left(1 + \left(\frac{\ln(p_0^*) - \ln(\mu_0(1-\epsilon))}{\overline{\rho}\,\overline{p}\,\lambda_0\kappa d^2}\right)^{\alpha/2}\right). \tag{5.21}$$

In order to optimize (5.21), the access probability p_0^* should be made as large as possible, resulting in $p_0^* = 1$, which proves (5.17). To conclude the proof, we apply $p_0^* = 1$ into (5.20) and (5.18), obtaining then the design parameters that maximize our approximated $\mathcal{R}_0^*$. □

From the equations presented in Proposition 5.4, we can state interesting properties of our proposed approximation to the optimal link effective throughput as follows.

Corollary 5.1. *The link throughput $\mathcal{R}_0^*$ and the system parameters $(p_0^*, \beta_0^*, m_0^*)$ stated in Proposition 5.4 have the following properties:*

- *$\mathcal{R}_0^*$ is a concave function of $\mu_0 \in [0,1]$ and a monotonically decreasing function of $\lambda_0 > 0$, $\bar{p} \in [0,1]$ and $\bar{\rho} \in [0,1]$;*
- *the arrival rate $\mu_0^* \in [0,1]$ that maximizes of $\mathcal{R}_0^*$ can be found as the $\mu_0 \in [0,1]$ that is solution[3] to the derivative equation: $d\mathcal{R}_0^*/d\mu_0 = 0$;*
- *p_0^* has a constant value regardless of $\mu_0 \in [0,1]$, $\lambda_0 > 0$, $\bar{p} \in [0,1]$ and $\bar{\rho} \in [0,1]$;*
- *β_0^* is a monotonically decreasing function of $\mu_0 \in [0,1]$, $\lambda_0 > 0$, $\bar{p} \in [0,1]$ and $\bar{\rho} \in [0,1]$.*
- *m_0^* is a monotonically decreasing function of $\mu_0 \in [0,1]$ and not affected by $\lambda_0 > 0$, $\bar{p} \in [0,1]$ and $\bar{\rho} \in [0,1]$.*

The proof for this corollary is straightforward by inspection of equations (5.17) and (5.18), and for this reason it is omitted here. Further discussions of such properties will be provided when analyzing the numerical results in Section 5.2.3. Next we obtain other important results derived from Proposition 5.4.

[3]Note that closed form solution is not possible in this case, but we can always resort to numerical procedures to find such a maximum.

Proposition 5.5 (upper bound of the effective link throughput)**.** *An upper bound of effective link throughput $\mathcal{R}_0^*$ stated in Proposition 5.4 is given by*

$$\mathcal{R}_0^* \leq \mathcal{R}_{0,\text{up}} = \log_2(1+\beta_{\text{up}})\ e^{-\overline{\rho}\,\overline{p}\,\lambda_0\,\kappa\,d^2\,\beta_{\text{up}}^{2/\alpha}}, \tag{5.22}$$

where β_{up} is found as the value of β_0 that is the solution to

$$\beta_0 = 2\,\overline{\rho}\,\overline{p}\,\lambda_0\,\kappa\,d^2\,\beta_0^{2/\alpha}\,(1+\beta_0)\,\ln(1+\beta_0). \tag{5.23}$$

Proof. We first use the fact that the effective throughput obtained by the unconstrained optimization of eq. (5.16) is always an upper bound of the constrained optimization given by (5.17). The unconstrained objective function (cf. eq. (5.16)) is maximized for $p_0 = 1$ and $\rho_0 \to 1$. Furthermore, it can be easily shown that (5.16) is a concave function of β_0 with $\beta_0 > 0$, hence taking the derivative $d\mathcal{R}_0/d\beta_0$ and after some manipulations, its optimal value is given by (5.23). To conclude the proof, we put this optimal value into (5.16), which yields (5.22). □

Theorem 5.1 (necessary condition for effective link throughput)**.** *Given that all TXs except TX_k have stable queues, the packet loss constraint ϵ has a small value and the network is in the steady state, a necessary condition so that the effective throughput $\mathcal{R}_k$, $k \in \mathcal{A}_0$, is achievable with bounded packet loss probability and queue stability is given by*

$$\mathcal{R}_k < \mu_k\,(1-\epsilon)\,\log_2\left(1+\left(\frac{-\ln(\mu_k\,(1-\epsilon))}{\overline{\rho}_{\mathcal{A}_0\setminus\{k\}}\overline{p}_{\mathcal{A}_0\setminus\{k\}}\,\lambda_0\kappa\,d^2}\right)^{\alpha/2}\right), \tag{5.24}$$

where μ_k is the arrival rate at TX_k and the subindex $_{\mathcal{A}_0\setminus\{k\}}$ indicates that the averages $\overline{\rho}$ and $\overline{p}$ do not take into account link k.

Proof. First, we use the fact that, in the steady state, the stochastic processes that determine the network behavior are stationary and isotropic over the time slots and links. Then, we apply Theorems 2.2 and 2.3 to evaluate the statistical proprieties of every link TX_k–RX_k with $k \in \mathcal{A}_0$ based on one typical link TX_0–RX_0 added in the generating point process so that the index 0 can be exchanged by k in (5.17) to obtain the maximum effective throughput $\mathcal{R}_k^*$ supported by TX_k–RX_k that satisfies the stability and packet loss constraints. Note that the averages $\overline{\rho}$ and $\overline{p}$ are related to the *interfering* TXs that are active in a given network realization and therefore the node in study, i.e. TX_k, should be excluded from the computation of such averages. Moreover, $\overline{\rho}$ and $\overline{p}$ have constant values since the network is assumed to have reached its steady state and all potential interfering TXs are assumed to have stable queues. To conclude this proof, we use the fact that $\mathcal{R}_k^*$ is by definition the highest possible effective throughput under the packet loss and queue stability constraints and then *every* throughput $\mathcal{R}_k$ that is subject to the same constraints should be lower than that maximum value. □

Remark 5.2. *It is worth noting that the theorem states a necessary condition, but not sufficient. This means that it is possible to have effective throughputs $\mathcal{R}_k < \mathcal{R}_k^*$ when the queue system of TX_k is unstable and/or the packet loss probability exceeds ϵ. Moreover, this maximum value $\mathcal{R}_k^*$ is surprisingly only a function of the arrival rate μ_k at TX_k and the network characteristics, and it does not depend on the specific system parameters employed to achieve it. In other words, $\mathcal{R}_k^*$ can be view as a limit of the system and the design setting says how to achieve it.*

Finally, we provide some consequent results for a system operating with optimal system parameters.

Corollary 5.2. *If all TX_k–RX_k links with $k \in \mathcal{A}_0$ employ the optimal strategy given by Proposition 5.4, then $\overline{p}_{\mathcal{A}_0\setminus\{k\}} \to 1$ and $\overline{p}_{\mathcal{A}_0\setminus\{k\}} = 1$, reducing the necessary condition given by Theorem 5.1 to*

$$\mathcal{R}_k < \mu_k\,(1-\epsilon)\,\log_2\left(1+\left(\frac{-\log(\mu_k\,(1-\epsilon))}{\lambda_0\kappa\,d^2}\right)^{\alpha/2}\right). \tag{5.25}$$

Corollary 5.3. *Let each design choice (p_k, β_k, m_k) be the individual strategy profile of a game amongst the $k \in \mathcal{A}_0$ links (players or agents) distributed over the network and effective link throughput $\mathcal{R}_k$ be the utility function of each link TX_k–RX_k. Then, if all k links employ the optimal individual design described in Proposition 5.4, the game is in a strict Nash equilibrium [127], i.e. an individual change cannot increase its own utility function when the other links continue using the same strategy.*

Corollary 5.4. *If a zero packet loss probability is required, i.e. $\epsilon = 0$, then the maximum number of retransmissions $m_k^* \to \infty,\ \forall k \in \mathcal{A}_0$.*

Corollary 5.5 (network spatial throughput of the optimal individual setting)**.** *If all TX_k–RX_k links with $k \in \mathcal{A}_0$ employ the optimal strategy described in Proposition 5.4 and all TXs are subject to the same arrival rates $\mu_k = \mu\ \forall k \in \mathcal{A}_0$ (symmetric case), then the spatial throughput $\mathcal{S}^*_{\text{ind}}$ for this scenario is computed as*

$$\mathcal{S}^*_{\text{ind}} = \lambda_0\,\mu\,(1-\epsilon)\,\log_2\left(1+\left(\frac{-\log(\mu\,(1-\epsilon))}{\lambda_0\kappa\,d^2}\right)^{\alpha/2}\right). \tag{5.26}$$

The proofs of these corollaries are straightforward and they are omitted here.

5.2.3 Numerical results

In this section, we use the analytical expressions previously derived to provide numerical results that help us to have a better understanding of the effective link throughput behavior as a function of the network parameters. These results also serve to illustrate the properties of the approximated solution to the link throughput optimization previously derived as well as assess the tightness of our approximation[4].

The design setting parameters employed by the typical link in order to maximize its effective throughput (cf. Proposition 5.4) are shown in Table 5.1 for different pairs of network densities λ_0 and arrival rates μ_0, which are the input parameters. Table 5.1 also contains such the optimal values computed using Proposition 5.4 and its upper bound as stated in Proposition 5.5.

[4]The numerical analysis carried out here can be extended to any link of the network, as previous argued.

Tab. 5.1: Optimal effective throughput design setting of TX_0–RX_0 for $\overline{p} = 1$, $\overline{\rho} \to 1$, $\alpha = 4$, $d = 1$ [m] and $\epsilon = 0.02$.

(λ_0, μ_0)	$(p_0^*, R_0^*, 1 + m_0^*)$	$\mathcal{R}_0^*$	$\mathcal{R}_{0,\text{up}}$
$(0.1, 0.2)$	$(1, 3.57, 17.9)$	0.700	0.865
$(0.1, 0.8)$	$(1, 0.31, 2.6)$	0.246	0.865
$(0.5, 0.2)$	$(1, 0.52, 17.9)$	0.102	0.102
$(0.5, 0.8)$	$(1, 0.014, 2.6)$	0.011	0.102

First, we analyze the scenario where $\lambda_0 = 0.1$ [TXs/m^2] and $\mu_0 = 0.2$. To achieve the highest effective throughput under packet loss and queue stability constraints, TX_0 should set its rate equal to $R_0^* = 3.57$ [bits/s/Hz] and $m_0^* = \lfloor 16.9 \rfloor$ possible retransmission attempts. These numbers show that TX_0 communicates with high coding rates, which increases the chance that the transmitted packet is not correctly decoded by RX_0 (outage event), thus a very large number of retransmissions should be allowed so that the packet loss constraint is not violated. By employing this setting, TX_0–RX_0 can reach an effective throughput of $\mathcal{R}_0^* = 0.700$ [bits/s/Hz], which is relatively close to its upper bound $\mathcal{R}_{0,\text{up}} = 0.865$ [bits/s/Hz], indicating some flexibility for the possible feasible solutions of our constrained optimization problem.

Second, we turn our attention to the scenario where the arrival rates are more frequent, namely $\mu_0 = 0.8$, still considering $\lambda_0 = 0.1$. From Table 5.1, one can clearly see that the effective throughput $\mathcal{R}_0^*$ decreases almost 65% as compared to the case where $\mu_0 = 0.2$, while the upper bound remains the same. This effective throughput is achieved when both coding rate and number of retransmissions heavily decrease, indicating that the combination of R_0^* and m_0^* is limited by the queue stability. In other words, when μ_0 is large, the outage events need to happen less frequently, decreasing the rate as well as the possible number of retransmissions so that both stability and packet loss requirements are respected.

In contrast, when the network has a density $\lambda_0 = 0.5$ and TX_0 experiences an arrival rate of $\mu_0 = 0.2$, the effective link throughput $\mathcal{R}_0^*$ achieves its upper bound $\mathcal{R}_{0,\text{up}}$. This indicates that low values of μ_0 do not impose a strict restriction to the feasible design options for the density λ_0. Hence the highest possible effective throughput can be reached by decreasing the coding rate R_0^* while the number of retransmissions can be still high, without violating the stability constraint. In any case, even though the effective throughput $\mathcal{R}_0^*$ is very close to its upper bound when $\lambda_0 = 0.5$, its value is much lower when $\lambda_0 = 0.1$, which evinces the harmful effects of the co-channel interference, i.e. the higher the density of active links, the lower the TX_0–RX_0 effective throughput.

Finally we study the case where a dense network with high rate of arrivals is considered, verifying the substantial loss of the effective throughput $\mathcal{R}_0^*$. As expected, the value of $\mathcal{R}_0^*$ presents a significant gap to its upper bound $\mathcal{R}_{0,\text{up}}$, indicating that the TX_0–RX_0 performance is severely limited by both the interference level observed by RX_0 and the restricting choice of feasible solutions due to the stability constraint. It is worth noticing that some of these facts have been already predicted by Corollary 5.1 and Table 5.1 helps us to visualize them.

Now in order to better assess the performance, we present in Fig. 5.1 how the arrival rates μ_0 affect the effective throughputs $\mathcal{R}_0^*$ for different values of $\overline{p}$.

First we observe that when the same arrival rate is considered, the higher the $\overline{p}$, the lower the $\mathcal{R}_0^*$. This behavior is indeed intuitive since $\overline{p}$ is related to the number of active links in the network and

thus it determines the interference experienced by RX_0.

We also see that the effective throughput $\mathcal{R}_0^*$ is a concave function of μ_0 (this statement can be easily proved from equation (5.17), considering $0 < \mu_0 \leq 1$). For low rate of arrivals, the design setting used to reach $\mathcal{R}_0^*$ should hold the packets more time in the queue in order to make $\rho_0 \to 1$. We also infer that low values of μ_0 also limit $\mathcal{R}_0^*$ due to its low value since the optimal design choice surprisingly yields a high outage probability in order to maintain the load of the queue close to one. Increasing μ_0, on the other hand, the effect of this limitation diminishes and thus the effective throughput $\mathcal{R}_0^*$ also increases until it reaches its maximum. After this inflection point, any increase of μ_0 degrades the link performance, indicating that high arrival rates are shrinking the feasible designing options, as discussed before.

Now, to study that maximum value, we present in Fig. 5.2 the effective throughput $\mathcal{R}_0^*$ and its upper bound $\mathcal{R}_{0,\,\mathrm{up}}$ as a function of μ_0 when $\overline{p} = 1$. From the curves, we can verify that the maximum $\mathcal{R}_0^*$ reaches its upper bound[5] given by (5.22), showing that, under certain circumstances, it is possible to obtain the unconstrained effective throughput $\mathcal{R}_{0,\mathrm{up}}$ even assuming strong requirements of queue stability and bounded packet loss probability.

In addition, we present in this figure together with the curves obtained using our analytical approximation the actual optimal values of $\mathcal{R}_0^*$ which are computed using standard numerical procedures of Mathematica software, namely NMaximize. As one can clearly verify, our approximation provides a good matching with the exact numerical solution[6], evincing that the assumptions used to derive Proposition 5.4 are fairly reasonable. Nevertheless, it is worth pointing out that our approximation works properly for small values of ϵ. When this condition is relaxed, the approximation $P_{\mathrm{pkt},0}^* = P_{\mathrm{o},0}^{*1+m_0^*} \approx \epsilon$ does not hold anymore and consequently our result becomes weaker.

Figs. 5.1 and 5.2 also evince a necessary condition for achieving the effective throughput. Theorem 5.1 states that all effective throughputs above the $\mathcal{R}_0^*$ curves cannot be achievable under the stability and packet loss constraints, determining then the boundary of stability for effective throughputs that the typical link TX_0–RX_0 can achieve with bounded packet loss for a given network specification. In other words, if any effective throughput $\mathcal{R}_0$ is stably achievable and the packet loss probability is at most ϵ, then the inequality $\mathcal{R}_0 < \mathcal{R}_0^*$ holds.

[5]Even though Fig. 5.2 only shows the results for $\overline{p} = 1$, the same analysis is still valid when other values of $\overline{p}$ are considered.

[6]To maintain the quality of the figures, we present the points obtained through numerical optimization only in some plots. In any case, the same good match is seen for other different network conditions.

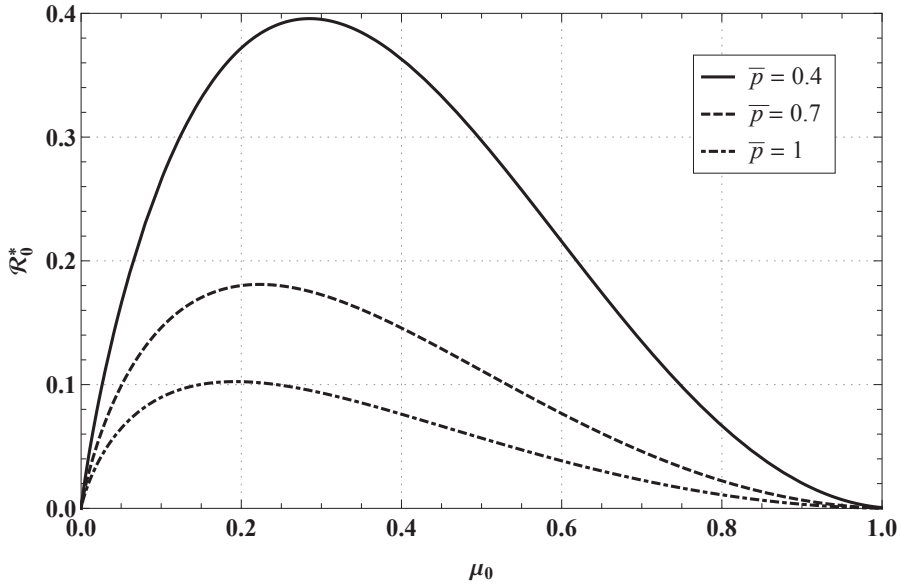

Fig. 5.1: Optimal effective link throughput $\mathcal{R}_0^*$ of the typical link TX_0–RX_0 (cf. Proposition 5.4) versus its arrival rate μ_0 for different $\overline{p}$ and considering $\overline{\rho} \to 1$, $\lambda_0 = 0.5$ [TXs/m^2], $\alpha = 4$, $d = 1$ [m] and $\epsilon = 0.02$.

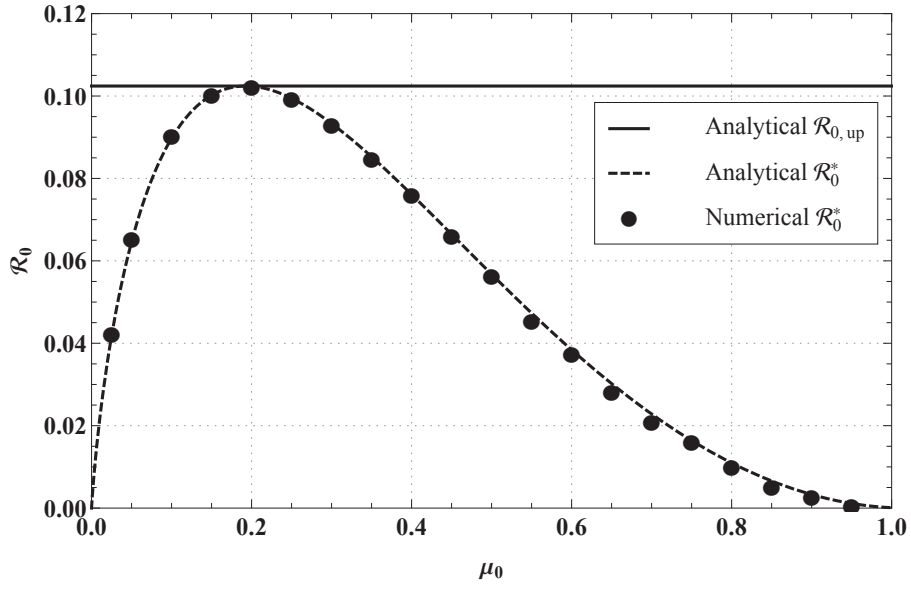

Fig. 5.2: Optimal effective link throughput $\mathcal{R}_0^*$ of the typical link TX_0–RX_0 and its upper bound $\mathcal{R}_{0,\text{up}}$ (cf. Proposition 5.5) as a function of the arrival rate μ_0 considering $\lambda_0 = 0.5$ [TXs/m^2], $\overline{p} = 1$, $\overline{\rho} \to 1$, $\alpha = 4$, $d = 1$ [m] and $\epsilon = 0.02$. The optimal throughput $\mathcal{R}_0^*$ is analytically assessed using Proposition 5.4 and via numerical optimization NMaximize using Wolfram Mathematica.

5.3 Spatial throughput optimization

In this section, we analyze the aggregate performance of the network using the spatial throughput metric introduced in Definition 5.3, i.e. stable achievable spatial throughput, such that the packet loss probability is bounded for all links. Specifically we consider the Poisson random network described in the previous section and formulate an optimization problem in order to maximize the spatial throughput under queue stability and bounded packet loss probability for all links. Note that the infinite Poisson network model is equivalent in distribution to the limit of a sequence of finite networks with a fixed density as the area increases to infinity. Using similar steps to the proof of Proposition 5.4, we derive an approximated closed-form solution for such a problem, which allows us to compare the optimal spatial throughput to the spatial throughput byproduct of the optimal individual decisions given by Corollary 5.5.

5.3.1 Analytical Results

We consider the symmetric case where all TX_k–RX_k, $\forall k \in \mathcal{A}_0$ are subject to the same arrival rates μ and employ the same design parameters, namely access probability p, rate R, and maximum number of retransmissions of packets decoded in error m, resulting in the server rate θ. Recalling that the set $\mathcal{A}_0$ refers to all TXs generated by the homogeneous PPP Φ_0 with density λ_0, we can rewrite the spatial throughput definition given by equation (5.6) as follows:

$$\mathcal{S} = \lambda_0 \, (1 - P_{\text{pkt}}) \, p \, \rho \, \frac{R}{1 + \overline{m}}, \tag{5.27}$$

where $\rho = \mu/\theta$, P_{pkt} is the packet loss probability and $\overline{m}$ is the average number of retransmissions.

To define the constrained spatial throughput maximization problem, we focus again on the typical link TX_0–RX_0, which characterizes the performance of any link TX_k–RX_k, $k \in \mathcal{A}_0$ (cf. Theorems 2.2 and 2.3). The constraints given by Propositions 5.1, 5.2, and 5.3 are applied, noticing though that in the symmetric case $\overline{\rho} = \rho_0 = \rho$ and $\overline{p} = p_0 = p$ as well as $\theta_0 = \theta$, $\beta_0 = \beta$ and $m_0 = m$. Furthermore, recall that $1 + \overline{m} = \frac{1 - P_{\text{o}}^{1+m}}{1 - P_{\text{o}}}$, where $P_{\text{o}} = 1 - e^{-p \, \frac{\mu}{\theta} \, \lambda_0 \, \kappa \, d^2 \beta^{2/\alpha}}$, and that $P_{\text{pkt}} = P_{\text{o}}^{1+m}$. Then the spatial throughput optimization problem under stability and packet loss constraints is formulated as follows:

$$\begin{aligned}
\max_{(p,\beta,m)} \quad & \lambda_0 \, p \, \frac{\mu}{\theta} \, \log_2(1+\beta) \, e^{-p \, \frac{\mu}{\theta} \, \lambda_0 \, \kappa \, d^2 \beta^{2/\alpha}} \\
\text{s.t.} \quad & \left(1 - e^{-p \frac{\mu}{\theta} \, \lambda_0 \, \kappa \, d^2 \beta^{2/\alpha}}\right)^{1+m} \leq \epsilon, \\
& \theta = p \, \frac{e^{-p \, \frac{\mu}{\theta} \, \lambda_0 \, \kappa \, d^2 \beta^{2/\alpha}}}{1 - \left(1 - e^{-p \, \frac{\mu}{\theta} \, \lambda_0 \, \kappa \, d^2 \beta^{2/\alpha}}\right)^{1+m}}, \\
& \theta \geq p \, \left[\sum_{i=1}^{1+m} \binom{1+m}{i} (-1)^{i+1} \, e^{-p \, \lambda_0 (i-1) \, \kappa d^2 \beta^{2/\alpha}} \right]^{-1} > \mu.
\end{aligned}$$

The above problem seems more intricate than the one in Section 5.2 as the parameters $\overline{\rho}$ and $\overline{p}$ are now variables, creating higher interdependence between the design parameters and the network

performance. Yet, to derive a closed-form approximate solution, we proceed in a similar way as before.

Proposition 5.6 (highest constrained spatial throughput)**.** *Given that the network is in the steady state and and assuming that m is a non-negative real number, the highest spatial throughput $\mathcal{S}^*$ such that every TX$_k$, $\forall k \in \mathcal{A}_0$, has stable queue and the packet loss probability of every TX$_k$–RX$_k$ link is bounded by ϵ, which has a small value, can be approximated by*

$$\mathcal{S}^* \approx \begin{cases} \mu\ \lambda_0\ (1-\epsilon)\ \log_2\left(1+\left(\dfrac{1}{\mu\ \lambda_0\ (1-\epsilon)\ \kappa\ d^2\ e}\right)^{\alpha/2}\right) \textit{ for } \mu(1-\epsilon) \le e^{-1} \\ \\ \mu\ \lambda_0\ (1-\epsilon)\ \log_2\left(1+\left(\dfrac{-\log(\mu\ (1-\epsilon))}{\lambda_0\ \kappa\ d^2}\right)^{\alpha/2}\right) \textit{ for } \mu(1-\epsilon) > e^{-1} \end{cases}, \tag{5.28}$$

where the optimal design parameters (p^*, β^*, m^*) used to achieve the approximated $\mathcal{S}^*$ when $\mu(1-\epsilon) \le e^{-1}$ are given by

$$\begin{aligned} p^* &= \mu(1-\epsilon)e, \\ \beta^* &= \left(\frac{1}{\mu\ \lambda_0\ (1-\epsilon)\ \kappa\ d^2\ e}\right)^{\alpha/2}, \\ m^* &= \frac{1}{\log_\epsilon(1-e^{-1})} - 1, \end{aligned}$$

while (p^*, β^*, m^*) for $\mu(1-\epsilon) > e^{-1}$ are computed as

$$\begin{aligned} p^* &= 1, \\ \beta^* &= \left(\frac{-\log(\mu_0\ (1-\epsilon))}{\lambda_0\ \kappa\ d^2}\right)^{\alpha/2}, \\ m^* &= \frac{1}{\log_\epsilon(1-\mu(1-\epsilon))} - 1. \end{aligned}$$

Proof. We apply similar steps as for the proof of Proposition 5.4 recalling that * refers either to the optimal parameter choice or to a function of it. We first use the fact that the optimal solution is achieved when all TXs' probability (in steady state) that their backlog is empty tends to 0, i.e. $\rho^* \to 1$ (boundary of stability). In addition, we consider that the packet loss constraint is low enough so that to achieve the spatial throughput $\mathcal{S}^*$ the packet loss probability reaches its maximum value, i.e. $P^*_{\text{pkt}} = P_{\text{o}}^{*1+m^*} = \epsilon$. Thus,

$$\mu \approx \theta^* = p^*\ \frac{1-P^*_{\text{o}}}{1-P_{\text{o}}^{*1+m^*}} = p^* \frac{1-\epsilon^{\frac{1}{1+m^*}}}{1-\epsilon} \Rightarrow p^*\ \left(1-\epsilon^{\frac{1}{1+m^*}}\right) \approx \mu(1-\epsilon). \tag{5.29}$$

Using this relation and recalling that in the optimal configuration the following equality should hold $1-P^*_{\text{o}} = e^{-p^*\ \lambda_0\ \kappa\ d^2 \beta^{*2/\alpha}}$, β^* can be computed as

$$\beta^* = \left(\frac{\log(p^*) - \log(\mu(1-\epsilon))}{p^*\ \lambda_0\ \kappa\ d^2}\right)^{\alpha/2}. \tag{5.30}$$

Manipulating the spatial throughput (5.27) based on the arguments stated above yields

$$\begin{aligned}\mathcal{S}^* &= \lambda_0\,(1-P^*_{\text{pkt}})\,p^*\,\rho^*\,\frac{R^*}{1+\overline{m}^*}\\ &= \lambda_0\,p^*\,R^*\,(1-P^*_{\text{o}})\\ &\approx \mu\,\lambda_0\,\,(1-\epsilon)\log_2\left(1+\left(\frac{\log(p^*)-\log(\mu(1-\epsilon))}{p^*\,\lambda_0\,\kappa\,d^2}\right)^{\alpha/2}\right),\end{aligned} \tag{5.31}$$

where $R^* = \log_2(1+\beta^*)$.

Note that the only design parameter in (5.31) is p^*, which can be thus computed as

$$p^* = \arg\max_x \frac{\log(x)-\log(\mu(1-\epsilon))}{x\,\lambda_0\,\kappa\,d^2} = \min(\mu(1-\epsilon)e, 1), \tag{5.32}$$

where $\mu < x \leq 1$.

Placing (5.32) in (5.31) results in (5.28), and in order to obtain the optimal design parameters, we apply (5.32) into (5.30) so as to obtain β^* and then manipulate (5.29) to find m^*. □

The solution to the optimization problem stated above provides the highest achievable spatial throughput constrained by queue stability and bounded packet loss requirements for all links. Similarly to the previous section, the following corollaries follow from properties of the above result.

Corollary 5.6. *The spatial throughput $\mathcal{S}^*$ and the system parameters $(p_0^*, \beta_0^*, m_0^*)$ stated in Proposition 5.6 have the following properties:*

- *$\mathcal{S}^*$ is a concave function of $\mu \in [0,1]$ and $\lambda_0 > 0$;*
- *The arrival rate $\mu^* \in [0,1]$ that maximizes of $\mathcal{S}^*$ can be found as the $\mu \in [0,1]$ that is solution to the derivative equation: $d\mathcal{S}^*/d\mu = 0$;*
- *The network density $\lambda_0 > 0$ that maximizes of $\mathcal{S}^*$ can be found as the $\lambda_0 > 0$ that is solution to the derivative equation: $d\mathcal{S}^*/d\lambda_0 = 0$;*
- *p^* is a monotonically increasing function of μ and is not affected by $\lambda_0 > 0$;*
- *β^* is a monotonically decreasing function of $\mu \in [0,1]$ and $\lambda_0 > 0$.*
- *m^* is a monotonically decreasing function of $\mu \in [0,1]$ and $\lambda_0 > 0$.*

The proof of this corollary comes directly from the analysis of the function stated in Proposition 5.6 and therefore it is not presented here.

Proposition 5.7 (upper bound of highest spatial throughput)**.** *An upper bound for the highest spatial throughput $\mathcal{S}^*$ given by Proposition 5.6 $\mathcal{S}_{\text{up}}$ is given by*

$$\mathcal{S}^* \leq \mathcal{S}_{\text{up}} = \begin{cases} \dfrac{\lambda_0 \log_2(1+\beta^*)}{e^{\lambda_0\,\kappa\,d^2\,\beta^{*2/\alpha}}} & \textit{for} \quad \beta^* \leq (\lambda_0 \kappa d^2)^{-\alpha/2} \\ \dfrac{\log_2(1+\beta^*)}{\kappa\,d^2\,\beta^{*2/\alpha}\,e} & \textit{for} \quad \beta^* > (\lambda_0 \kappa d^2)^{-\alpha/2} \end{cases}, \tag{5.33}$$

where β^* is found as the value of β that is the solution to

$$\beta = \begin{cases} \left(\frac{2}{\alpha}\ \lambda_0\ \kappa\ d^2\ (1+\beta)\ \log(1+\beta)\right)^{\frac{\alpha}{\alpha-2}} & \textit{for} \quad \beta \leq (\lambda_0 \kappa d^2)^{-\alpha/2} \\ -1 + e^{\mathcal{W}_0\left(-\frac{\alpha}{2}e^{-\alpha/2}\right)+\frac{\alpha}{2}} & \textit{for} \quad \beta > (\lambda_0 \kappa d^2)^{-\alpha/2} \end{cases}, \tag{5.34}$$

where $\mathcal{W}_0(\cdot)$ is the principal branch of the Lambert W function defined as $x = \mathcal{W}_0(x)e^{\mathcal{W}_0(x)}$ such that $x \geq -e^{-1}$ and $\mathcal{W}_0(x) \geq -1$.

Proof. To solve the unconstrained optimization, we first assume that the dominant network in which TXs have always packets to transmit (i.e. $\rho \to 1$). We then compute the values of the access probability p^* and the SIR threshold β^* that lead to a feasible equilibrium point, noting that the spatial throughput given by $\mathcal{S} = \lambda_0 p \log_2(1+\beta) e^{-p\lambda_0 \kappa d^2 \beta^{2/\alpha}}$ is a concave function of both β and p. From the derivative equations, we find the relation between p^* and β^* at the equilibrium point as

$$p^* = \frac{1}{\lambda_0\ \kappa\ d^2\ \beta^{*\frac{2}{\alpha}}}. \tag{5.35}$$

Note that since $0 \leq p \leq 1$ some equilibrium points given by (5.35) may not lie in the feasibility region of the problem, thus whenever $p^* > 1$, we set $p^* = 1$ and manipulate the equations accordingly. After some algebraic manipulations using (5.35), we obtain (5.33) and (5.34), concluding the proof[7]. □

Theorem 5.2 (necessary condition for spatial throughput)**.** *Given that the network is in steady state, a necessary condition so that any spatial throughput $\mathcal{S}$ is achievable with bounded packet loss probability and queue stability for all TXs is*

$$\mathcal{S} < \mathcal{S}^*, \tag{5.36}$$

where $\mathcal{S}^*$ is given by Proposition 5.6.

The proof of Theorem 5.2 is similar to the proof of Theorem 5.1 from the previous section and thus it will be omitted. Next we provide two important corollaries that identify how $\mathcal{S}^*$ is related to the spatial throughput $\mathcal{S}^*_{\text{ind}}$ reached when all links use the best individual design parameters stated in Corollary 5.5.

Corollary 5.7 (network optimal vs. per-link optimal spatial throughputs)**.** *Given that the network is in steady state, then in the symmetric case*

$$\mathcal{S}^*_{\text{ind}} \leq \mathcal{S}^*, \tag{5.37}$$

where $\mathcal{S}^*$ is given by Proposition 5.6 and $\mathcal{S}^*_{\text{ind}}$ by Corollary 5.5. Equality in (5.37) *happens whenever $p^* = 1$.*

Corollary 5.8 (tragedy of the commons)**.** *Given that the network is in steady state, then in the symmetric case the best individual design setting derived in Section 5.2 is not globally optimal for the aggregate network performance when $\mu(1-\epsilon) \leq e^{-1}$. In other words, the selfish behavior of the TXs leads to a poor use of the network resources, degrading its spatial throughput. This degradation in the aggregate performance due to selfish per-link decisions can be seen as a tragedy of the commons class of problem [128].*

[7] Note that the computation of $\mathcal{S}_{\text{up}}$ involves a simple numerical procedure to solve the first equation in (5.34).

Remark 5.3. *The ratio between $\mathcal{S}^*_{\text{ind}}$ and $\mathcal{S}^*$ can be directly obtained from equations* (5.26) *and* (5.28)*. From such ratio, one can verify that $\mathcal{S}^*_{\text{ind}} = \mathcal{S}^*$ when $\mu(1-\epsilon) > e^{-1}$, exactly when the access probability p^* that leads to $\mathcal{S}^*$ becomes 1. It is also interesting to note that the range of arrival rates where selfish decisions are not optimal is $\mu(1-\epsilon) \leq e^{-1}$. As our basic assumption is that the maximum acceptable packet loss probability ϵ is small, one can see that μ determines the feasibility region of our optimization regardless of the design setting used to achieve the optimal performance. In other words, by increasing μ, the probability p^* that is the spatial rate $\mathcal{S}^*$ optimizer monotonically increases up to $p^* = 1$, independently of other system variables (c.f. Corollary 5.6). Once p^* is determined, the other parameters must be optimally tuned in accordance with the system constraints.*

The proofs of these corollaries are straightforward and thus they are omitted.

5.3.2 Numerical Results

In this section, we provide numerical results in order to verify the aforementioned analytical results. Let us start presenting in Table 5.2 the design setting (p^*, β^*, m^*) that leads to the highest spatial throughput achieved when stability and packet loss constraints are required for all links, considering different combinations of the input parameters λ_0 and μ.

From Table 5.2, it is verified that in scenarios with low values of μ, e.g. $\mu = 0.2$, the access probability p^* is about 0.5, whereas when $\mu = 0.8$, it approaches the value of the link optimization case, i.e. $p^* = 1$. These facts indicate that, when the network is not limited by high arrival rates, it is important to have some kind of medium access control so that the effects of co-channel interference are weakened. On the other hand, increasing the arrival rates, the stability constraint makes the optimal access probability p^* become higher, reaching 1. This reflects that, in scenarios where the queue stability restriction is the dominant factor, the optimal link decisions are also optimal for the network point of view, i.e. $\mathcal{S}^* = \mathcal{S}^*_{\text{ind}}$. In any case, when $p^* = 1$, $\mathcal{S}^*$ is remarkably lower than its upper bound $\mathcal{S}_{\text{up}}$ given in Proposition 5.7.

Fig. 5.3 shows the spatial throughput $\mathcal{S}^*$ together with $\mathcal{S}_{\text{up}}$ and $\mathcal{S}^*_{\text{ind}}$ versus the arrival rate[8]. As argued before, we deduce that for lower values of μ, the performance gap between the spatial throughputs $\mathcal{S}^*$ and $\mathcal{S}^*_{\text{ind}}$ is big, reaching 100% for some values of μ. This gap closes for increasing arrival rates μ. More interestingly, we can see from Fig. 5.3 that the constrained spatial throughput $\mathcal{S}^*$ can achieve values very close to its upper bound given by the unconstrained spatial throughput optimization.

Tab. 5.2: Optimal spatial throughput design setting for $\alpha = 4$, $d = 1$ [m] and $\epsilon = 0.02$.

(λ_0, μ)	$(p^*, R^*, 1+m^*)$	$\mathcal{S}^*_{\text{ind}}$	$\mathcal{S}^*$	$\mathcal{S}_{\text{up}}$
$(0.1, 0.2)$	$(0.53, 3, 95, 8.5)$	0.070	0.077	0.0865
$(0.1, 0.8)$	$(1, 0.31, 2.6)$	0.025	0.025	0.0865
$(0.5, 0.2)$	$(0.51, 0.66, 8.5)$	0.051	0.065	0.0865
$(0.5, 0.8)$	$(1, 0.014, 2.6)$	0.005	0.005	0.0865

[8]Once again we can see the good matching between our approximation and the results obtained via numerical optimization.

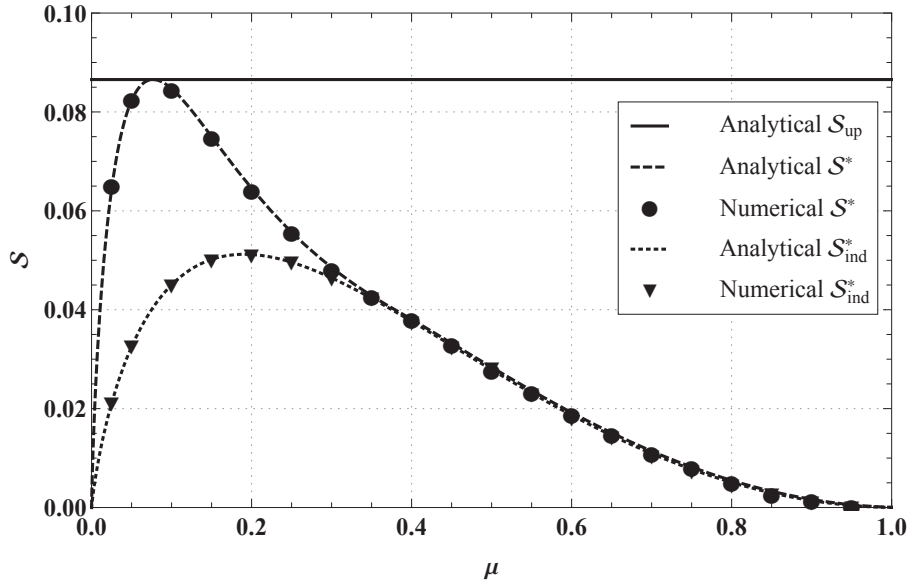

Fig. 5.3: Optimal spatial throughput $\mathcal{S}^*$, its upper bound $\mathcal{S}_{\text{up}}$ (cf. Proposition 5.7) and the spatial throughput $\mathcal{S}^*_{\text{ind}}$ obtained with the best individual choice versus the arrival rate μ for $\lambda_0 = 0.5$ [TXs/m^2], $\alpha = 4$, $d = 1$ [m] and $\epsilon = 0.02$. $\mathcal{S}^*$ and $\mathcal{S}^*_{\text{ind}}$ are analytically assessed using Proposition 5.5 and Corollary 5.5, and numerically solved via the NMaximize function from Wolfram Mathematica.

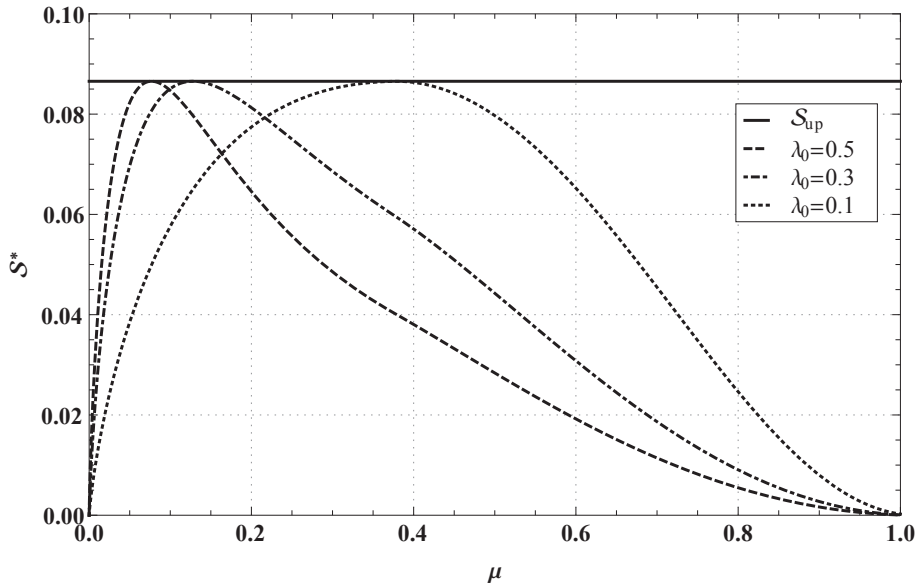

Fig. 5.4: Optimal spatial throughput $\mathcal{S}^*$ (cf. Proposition 5.6) and its upper bound $\mathcal{S}_{\text{up}}$ (cf. Proposition 5.7) versus the arrival rate μ for different densities λ_0, considering $\alpha = 4$, $d = 1$ [m] and $\epsilon = 0.02$.

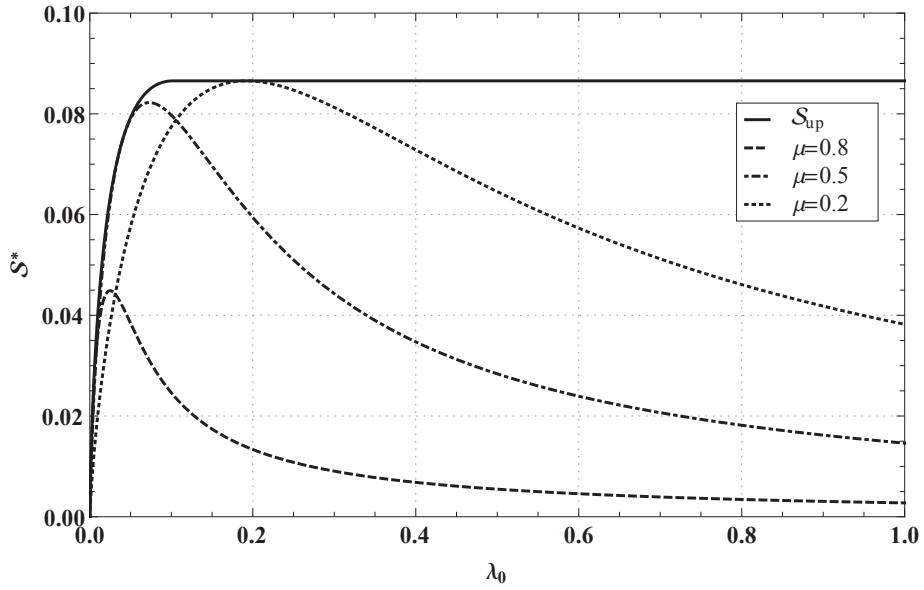

Fig. 5.5: Optimal spatial throughput $\mathcal{S}^*$ (cf. Proposition 5.6) and its upper bound $\mathcal{S}_{\text{up}}$ (cf. Proposition 5.7) versus the network density λ_0 for different arrival rates μ, considering $\alpha = 4$, $d = 1$ [m] and $\epsilon = 0.02$.

As discussed in Section 5.2.3, to reach the optimal performance under queue stability constraint, all TXs must transmit with high probability when the arrival rate increases. When the unconstrained optimization problem is considered, however, the opposite happens: the optimal performance is achievable by *decreasing* the access probability, thus controlling the interference level by contention (see equation (5.35)). In other words, increasing the arrival rates μ, the stability constraint makes the access probability be far away from its optimal unconstrained value. Nevertheless, $\mathcal{S}^*$ can still reach the unconstrained spatial throughput for some specific combinations of μ and λ_0, as shown by Figs. 5.4 and 5.5.

Fig. 5.4 presents how $\mathcal{S}^*$ behaves as a function of the arrival rates μ for different values of density λ_0. For low values of μ, $\mathcal{S}^*$ increases as μ increases until it reaches $\mathcal{S}_{\text{up}}$. At lower densities, λ_0 can be viewed as the limiting factor of $\mathcal{S}^*$ due to the poor spatial reuse and, therefore, such an inflection point is reached at higher arrival rates μ for lower densities λ_0. After its maximum value, $\mathcal{S}^*$ decreases as μ increases, approaching zero when μ goes to 1, regardless of the density considered. This once again corroborates the intuition that high arrival rates degrade the network efficiency.

In Fig. 5.5 we see that increasing the node density λ_0, the values of $\mathcal{S}^*$ and $\mathcal{S}_{\text{up}}$ increase up to a maximum, which indicates that the network is limited by the low spatial density of TXs. Conversely, once such maximum point is reached, which is at lower densities λ_0 for higher arrival rates μ (justified by the same arguments used before), $\mathcal{S}^*$ becomes a decreasing function of λ_0 while $\mathcal{S}_{\text{up}}$ is able to maintain its best performance regardless of λ_0 due to contention, reflecting that the interference from the concurrent transmissions starts dominating the network performance when the constraints are imposed.

Interestingly, for lower values of λ_0, $\mathcal{S}^*$ is very close to its upper bound $\mathcal{S}_{\text{up}}$ when arrival rates $\mu = 0.5$ and $\mu = 0.7$ are considered, while the network has poorer performance for $\mu = 0.2$. These

facts indicate that a sparse network subject to low traffic conditions operate below its limit, which is achievable when the arrival rates are higher. On the other hand, when denser network scenarios are considered, $\mu = 0.2$ leads to higher $\mathcal{S}^*$ than the other arrival rates studied here. All in all, these facts reinforce our argument that, under certain conditions, it is possible to achieve the unconstrained performance via a suitable parameter design, even though strong requirements in terms of packet loss and stability are imposed.

5.4 Summary

In this chapter, we investigated the performance of random spatial networks in terms of effective link throughput and the network-wide spatial throughput under queue stability constraint and bounded packet loss probability. Considering an ad hoc network in which transmit nodes are located according to a Poisson point process and are subjected to geometric packet arrivals, we showed under which conditions it is possible to achieve the unconstrained throughput performance and also established a necessary condition so that both throughputs are achievable under the above constraints. Furthermore, we proved that the link design parameters that lead to the highest effective link throughput are not always a wise choice for maximizing the network spatial throughput and we also identified when the solutions of both optimization problems coincide.

Chapter 6

Spatial throughput under different decoding rules

In this chapter we deal with the problem of characterizing the highest spatial throughput – or spatial capacity – of wireless single-hop ad hoc networks for the two decoding rules presented in Section 2.1: *treating interference as noise* – the IAN rule – and *joint detection of the strongest interferers' messages and treating the others as noise*[1] – the OPT rule. It is important to say that we do not assume any *interference cancellation* (IC) technique as in [34], [129, 130, 131] since the OPT rule used in this paper always performs better than IC, as discussed in [71, 132]; we will return to this topic later in this chapter. Besides no kind of strong coordination between the active links is considered so that *interference alignment* [68] is unfeasible; a detailed discussion about it can be found in [71].

We then use Theorems 2.2 and 2.3 to obtain approximations and bounds of the highest approximate achievable spatial throughput for the IAN and OPT rules based on the performance of a typical link for a given network density, naming this maximum value as *spatial capacity*. For comparison purposes, we also evaluate the highest approximate spatial throughputs achieved when all links use fixed (symmetric) coding rates (which is the most usual approach in the literature, also used in the previous chapters). We then proceed with an unconstrained optimization of the *average* spatial throughput over different spatial realizations, where the optimization variable is the rate that the transmitters code their messages.

Differently from the spatial-capacity-achieving scenario where the coding rates are tuned to be the highest achievable rates given the relative nodes' positions for each spatial realization, the fixed rate scheme only cares about the average behavior of the network, resulting in decoding errors (outage events) for links whose capacity is below that predetermined rate. We prove that, under the same assumptions, such a strategy performs worse than the spatial-capacity-achieving one. Our numerical results illustrate this difference as well as the advantages of using OPT instead of IAN. We then discuss the feasibility of the decoding rules and optimization strategies for different mobility patterns: for (quasi-)static topologies, the spatial capacity can be achieved; for highly mobile topologies, it cannot and the fixed rate optimization with IAN turns out to be the most appropriate choice.

[1] This rule splits the set of interferers into two mutually exclusive subsets: one contains the strongest interferers whose messages will be joint decoded with the desired one, and the other contains the transmitters with weaker detected power that will be treated as noise.

6.1 Spatial capacity of Poisson networks

Before we start, let us first define the spatial throughput metric.

Definition 6.1 (spatial throughput)**.** *Let A [m^2] be the network area. Then the spatial throughput, denoted by $\mathcal{S}$ and measured in [bits/s/Hz/m^2], is defined as*

$$\mathcal{S} = \frac{1}{A} \sum_{i=0}^{K} R_i. \tag{6.1}$$

Now, based on this definition and the capacity region stated in Theorem 2.1, we can define the spatial capacity as the highest achievable spatial throughput such that all rates are achievable.

Definition 6.2 (spatial capacity of a given spatial realization)**.** *The spatial capacity, denoted by $\mathcal{S}^*$, is defined as the maximum spatial throughput of the network such the rate tuple is achievable – $\mathbf{R} = (R_0, ..., R_K) \in \mathcal{H}$. Then,*

$$\mathcal{S}^* = \max_{\mathbf{R} \in \mathcal{H}} \mathcal{S}. \tag{6.2}$$

The spatial capacity reflects the highest sum of achievable rates over a given area and it may have a huge variation depending on the network topology (i.e. the number and/or position of the transmitter–receiver pairs). To deal with this issue, we opt for studying Poisson distributed networks that are analytically tractable, allowing us to derive approximate expressions for the expected spatial capacity $\mathcal{S}^*$ (over different spatial realizations).

Now let Φ be a 2-D homogeneous PPP with density λ [nodes/m^2] that characterizes the spatial distribution of transmitters (TXs) over $\mathbb{R}^2$. We assume that each TX is associated with one receiver (RX) located at a fixed distance d [m] from it in a random orientation following the bipolar modeling [10]. In addition, we consider that all TXs transmit information to their intended RXs using the G-ptp codes described in Section 2.1.

For each realization of Φ, the network may have a different capacity region $\mathcal{H}$ and consequently a different spatial capacity $\mathcal{S}^*$. Even worse, when the network area is the infinite plane (i.e. $\mathbb{R}^2$), the capacity region given by equation (2.4) becomes impossible to be computed. Knowing these limitations, we define the average spatial capacity as the expected value of the highest achievable spatial throughputs, which allows us to approximate the performance of infinite networks over different spatial realizations of Φ based on a typical link.

Definition 6.3 (average spatial capacity)**.** *Let $\mathbf{R} = (R_0, ..., R_K)$ be a tuple rate and $\mathcal{H}$ be the capacity region for a given network realization, then the average spatial capacity $\mathcal{C}$ is defined as*

$$\mathcal{C} = \mathrm{E}\left[\mathcal{S}^*\right] = \mathrm{E}\left[\max_{\mathbf{R} \in \mathcal{H}} \frac{1}{A} \sum_{i=0}^{K} R_i\right]. \tag{6.3}$$

We can now apply properties from the point process theory to compute an approximation to the spatial capacity of this class of Poisson networks as follows.

Proposition 6.1 (average approximate spatial capacity)**.** *The average spatial capacity $\mathcal{C}$ can be approximate for the Poisson network described here as*

$$\mathcal{C} \approx \lambda \, \mathrm{E}[R^*], \tag{6.4}$$

where R^* is the random variable that characterizes the spatial-capacity achievable rates of a typical link over the different network realizations.

Proof. Reminding that the spatial process Φ takes place in $\mathbb{R}^2$, then $A \to \infty$, $K \to \infty$ and $\mathbf{R} = (R_0, R_1, ...)$. Therefore:

$$\mathcal{C} = \mathrm{E}\left[\max_{\mathbf{R}\in\mathcal{H}} \lim_{A\to\infty} \frac{1}{A} \sum_{i=0}^{K} R_i\right], \tag{6.5}$$

$$\overset{(a)}{=} \mathrm{E}\left[\lim_{A\to\infty} \frac{1}{A} \sum_{i=0}^{K} R_i^*\right], \tag{6.6}$$

$$\overset{(b)}{\approx} \lambda \, \mathrm{E}[R^*]. \tag{6.7}$$

Specifically, equality (a) considers the value of $\mathbf{R}^* = (R_0^*, R_1^*, ...) \in \mathcal{H}$ that leads to the maximum spatial throughput for a given network realization, resulting in the spatial capacity $\mathcal{S}^*$. Since the PPP under analysis is homogeneous, we can apply Theorem 2.3 to determine the statistical proprieties of any node in Φ over different spatial realizations based on a typical link (receiver node added at the origin, whose transmitter node is d meters away from it). Denoting the optimal coding rate employed by such a transmitter as R^*, we can make the approximation (b) by multiplying the network density λ and R^*, which concludes this proof. □

Remark 6.1. *Equality in (b), instead of approximation in equation* (6.7)*, is not possible since we cannot guarantee that the limit in equation* (6.6) *exists. It is also worth saying that, in this case, neither the spatial ergodic theorem nor the Campbell's theorem can be applied due to the interdependence between the elements of the optimal rate set $\mathbf{R}^*$ in each specific spatial realization. As presented in the following sections, we are still able to assess the performance of a typical link over different realizations of the network based on closed-form expressions, which, we believe, makes valid our proposed approximation* (6.4)*.*

From equation (6.4), one can see that the main problem is now to derive the distribution of the spatial-capacity achievable rates R^*, which is our focus in the next two sections. We would like to mention that Baccelli and Blaszczyszyn have presented in [11, Sec. 16.2.3] a general closed-form solution to the average rate of the typical link using Laplace transforms. Nevertheless, we argue that our forthcoming derivations also contribute to the field due to their geometric appeal, where we explicitly compute an approximate pdf of the Shannon rates of the typical link solely based on the distance from the typical receiver to its closest interferer treated as noise.

6.2 IAN decoding rule

In this section we assess the spatial capacity using the decoding rule where the receivers treat the interference as noise – or IAN decoders. The following corollary shows its achievable rates.

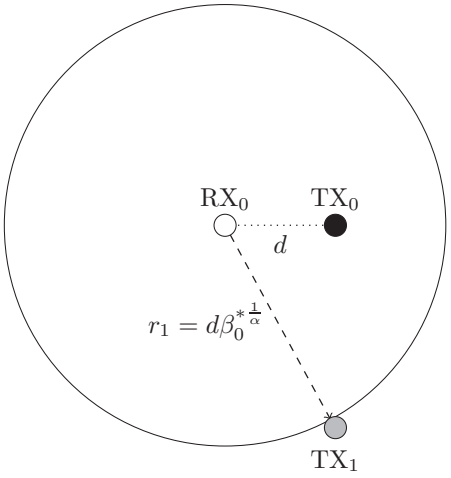

Fig. 6.1: Illustrative example of the typical link TX_0–RX_0 employing the IAN decoding rule, where TX_1 represents the closest interferer to RX_0. To reach the highest achievable rate R_0^*, the relation $r_1 = d\beta_0^{*\frac{1}{\alpha}}$ must be respected such that r_1 is the random variable that denotes the distance between RX_0 and TX_1.

Let us apply Corollary 2.2 to the scenario described in Section 6.1 to assess the spatial capacity of Poisson networks when receivers use IAN decoders. We consider as a channel modeling only the distance-dependent path-loss modeling with exponent $\alpha > 2$ so the channel gain between TX_j and RX_i is proportional to $x_{ij}^{-\alpha}$, where x_{ij} denotes the distance between them. We also assume the noise power is negligible in comparison to the interference power (interference-limited regime) and the dominant interferer approximation (cf. Definition 2.6) so that the aggregate interference experienced by RX_k can be approximated by power $P_{k,\text{clo}}$ related to its closest interferer. Mathematically we have: $1 + \sum_{j \in \mathcal{A}\setminus\{k\}} P_{kj} \approx P_{k,\text{clo}}$.

Based on these assumptions, we can derive an approximation of the probability density function (pdf) of the spatial-capacity-achieving rates for IAN decoders as presented next.

Proposition 6.2 (approximate pdf of the spatial-capacity-achieving rates for IAN)**.** *Let* $\mathbf{R}^* = (R_0^*, R_1^*, ...) \in \mathcal{H}$ *be the rate tuple that achieves the spatial capacity for the network described in Section 6.1. The pdf of* R_i^*, $\forall\ i \in \mathcal{A}$ *over the different spatial realizations is equivalent to the pdf* $f_{R^*}(x)$ *of a typical rate* R^**, which is approximated by*

$$f_{R^*}(x) \approx \ln 4\ \frac{2^x \lambda \pi d^2 \left(2^x - 1\right)^{\frac{2}{\alpha}}}{\alpha \left(2^x - 1\right)}\ e^{-\lambda \pi d^2 \left(2^x - 1\right)^{\frac{2}{\alpha}}}, \tag{6.8}$$

where $x > 0$.

Proof. Let us analyze a typical link TX_0–RX_0 added to the PPP Φ. From Theorem 2.3, this inclusion does not affect the distribution of Φ. Without loss of generality, we assume that the origin of the plane is located at RX_0 and label the interferers TX_i accordingly to their distances to RX_0, i.e. TX_1 is the closest, TX_2 is the second closest and so on. From our assumptions, we have $1 + \sum_{k=1}^{\infty} P_k \approx P_1$. We

then apply the path-loss model to the IAN decoder presented in equation (2.6), considering that the distances from TX_0 and TX_1 to RX_0 are respectively $d > 0$ and $r_1 > 0$, resulting in

$$R_0 \leq \log_2\left(1 + \frac{d^{-\alpha}}{r_1^{-\alpha}}\right), \tag{6.9}$$

where r_1 is a random variable.

To compute the pdf of r_1, we use the definition of contact zone [111] (the distance between a typical point and its first neighbor) to obtain the pdf of r_1, resulting in (cf. Property 2.2):

$$f_{r_1}(x) = 2\lambda\pi x e^{-\lambda\pi x^2}, \tag{6.10}$$

such that $x > 0$. Defining $\beta_0^* = d^{-\alpha}/r_1^{-\alpha}$ such that inequality (6.9) still holds, then we have the following relation $r_1 = d{\beta_0^*}^{\frac{1}{\alpha}}$ (see Fig. 6.1). We now apply this variable transformation to (6.10) and hence the pdf of $\beta_0^* > 0$ can be obtained as

$$f_{\beta_0^*}(x) = \frac{2\lambda\pi d^2 x^{\frac{2}{\alpha}}}{\alpha x} e^{-\lambda\pi d^2 x^{\frac{2}{\alpha}}}. \tag{6.11}$$

To conclude this proof, we proceed with the transformation $R_0^* = \log_2(1 + \beta_0^*)$ remembering that PPPs are stationary so we can characterize any node of the network based on a typical node, dropping the index 0. □

The result just stated provides us an approximation[2] of pdf of the spatial-capacity-achieving rates using IAN decoders over an infinite plane and over different spatial realizations of the process Φ. Then, we apply (6.8) to approximate the spatial capacity given by (6.4), resulting in

$$\mathcal{C}_{\text{IAN}} \approx \lambda \int_0^\infty x f_{R^*}(x)\, dx, \tag{6.12}$$

which does not have a closed-form solution and a numerical integration is required. For this reason, next we derive some proprieties[3] of (6.12) that help us to understand the $\mathcal{C}_{\text{IAN}}$ behavior.

Property 6.1 (concavity of the spatial capacity)**.** *A function $f(\cdot)$ is said to be* quasi concave *if, and only if, $f\left(px_1 + (1-p)x_2\right) \geq \min\{f(x_1), f(x_2)\}$, where $0 \leq p \leq 1$. Considering that the rate that leads to the spatial capacity, R^*, is a function of the density λ (i.e. $R^* = f(\lambda)$), then $\mathcal{C}_{\text{IAN}}$ given by* (6.12) *is* quasi concave *in terms of λ, where R^* is a random variable characterized by the pdf* (6.8)*.*

Proof. Let us first consider two different network densities λ_1 and λ_2 such that $\lambda_1 < \lambda_2$. Then, defining that $\lambda = p\lambda_1 + (1-p)\lambda_2$ with $0 \leq p \leq 1$, we proceed with the following manipulation

$$\begin{aligned}
\mathcal{C}_{\text{IAN}}(\lambda) &= (p\lambda_1 + (1-p)\lambda_2)\ \mathrm{E}[f\left(p\lambda_1 + (1-p)\lambda_2\right)] && (6.13)\\
&\overset{(a)}{\geq} \lambda_1\, \mathrm{E}[f\left(p\lambda_1 + (1-p)\lambda_2\right)] && (6.14)\\
&\overset{(b)}{=} \lambda_1\, \mathrm{E}[f(\lambda_1)] \ = \ \mathcal{C}_{\text{IAN}}(\lambda_1) && (6.15)\\
&\overset{(c)}{\geq} \lambda_2\, \mathrm{E}[f(\lambda_2)] \ = \ \mathcal{C}_{\text{IAN}}(\lambda_2). && (6.16)
\end{aligned}$$

[2] We discuss the tightness of the closest interferer approximation later in Section 6.5.

[3] Such properties rely on the closest interferer approximation that will be discussed later on. For simplicity we hereafter refer to the approximate average spatial capacity as spatial capacity.

Inequality (a) comes from the fact that $\lambda_1 \leq p\lambda_1 + (1-p)\lambda_2$ whereas equality (b) is obtained by setting $p = 1$ since the first inequality holds for all $0 \leq p \leq 1$. This proves the quasi concavity of the analyzed function when $\lambda_1 \mathrm{E}[f(\lambda_1)] < \lambda_2 \mathrm{E}[f(\lambda_2)]$. Finally, inequality (c) is straight when $\lambda_1 \mathrm{E}[f(\lambda_1)] \geq \lambda_2 \mathrm{E}[f(\lambda_2)]$, which concludes this proof. □

Property 6.2 (highest spatial capacity)**.** *The network density λ^* that leads to the highest spatial capacity given by* (6.12) *is obtained as the density $\lambda > 0$ which is solution to the following equation:*

$$\int_0^{\infty} x^{\frac{2}{\alpha}-1} \log_2(1+x) e^{-\lambda \pi d^2 x^{\frac{2}{\alpha}}} dx = \int_0^{\infty} x^{\frac{2}{\alpha}-1} \left(\lambda \pi d^2 x^{\frac{2}{\alpha}} - 1\right) \log_2(1+x) e^{-\lambda \pi d^2 x^{\frac{2}{\alpha}}} dx. \tag{6.17}$$

Proof. Let us first rewrite the spatial capacity formulation using the pdf $f_{\beta^*}(x)$ given by (6.11), yielding

$$\mathcal{C}_{\text{IAN}} = \lambda \int_0^{\infty} \log_2(1+x) f_{\beta^*}(x)\, dx. \tag{6.18}$$

Then, we recall that the $\mathcal{C}_{\text{IAN}}$ is quasi-concave in terms of λ (Property 6.1) to find its maximum value based on the derivative equation $d\mathcal{C}_{\text{IAN}}/d\lambda = 0$. After some algebraic manipulation, we obtain (6.17), which concludes this proof. □

Property 6.3 (lower bound)**.** *A lower bound of the spatial capacity given by* (6.12) *is computed as*

$$\mathcal{C}_{\text{IAN}} \geq \lambda y e^{-\lambda \pi d^2 (2^y - 1)^{\frac{2}{\alpha}}}, \tag{6.19}$$

where $y > 0$.

Proof. To prove this property, we apply the Markov inequality as presented below:

$$\Pr[R^* \geq y] \leq \frac{\mathrm{E}[R^*]}{y} \Rightarrow \mathrm{E}[R^*] \geq y e^{-\lambda \pi d^2 (2^y - 1)^{\frac{2}{\alpha}}}, \tag{6.20}$$

where $\Pr[R^* \geq y] = 1 - \int_0^y f_{R^*}(x)\, dx$ and $2^y - 1 > 0$.

Then, we multiply both sides by λ, resulting in (6.19). □

Property 6.4 (upper bound)**.** *An upper bound of the spatial capacity given by* (6.12) *is computed as*

$$\mathcal{C}_{\text{IAN}} \leq \lambda \log_2 \left(1 + \left(\frac{1}{\lambda \pi d^2}\right)^{\frac{\alpha}{2}} \Gamma\left(1 + \frac{\alpha}{2}\right)\right). \tag{6.21}$$

where $\Gamma(\cdot)$ is the Euler gamma function.

Proof. Let us apply Jensen's inequality based on the concavity of (6.12) (refer to Property 6.1), yielding

$$\mathcal{C}_{\text{IAN}} = \lambda\, \mathrm{E}[R^*] \tag{6.22}$$

$$\stackrel{(a)}{=} \lambda\, \mathrm{E}[\log_2(1+\beta^*)] \tag{6.23}$$

$$\stackrel{(b)}{\leq} \lambda\, \log_2(1 + \mathrm{E}[\beta^*]), \tag{6.24}$$

where equality (a) comes from the fact that $R^* = \log_2(1+\beta^*)$ and inequality (b) is the Jensen inequality for quasi-concave functions. Then, we compute the expectation of the random variable β^* using (6.11), which proves (6.21). □

Property 6.5 (asymptotic equivalence)**.** *Let $\sim$ denote asymptotic equivalence of two functions, then*

$$\mathcal{C}_{\text{IAN}} \sim c\, \lambda^{1-\frac{\alpha}{2}}, \tag{6.25}$$

when $\lambda \to \infty$ and $c = \left(\frac{1}{\pi d^2}\right)^{\frac{\alpha}{2}} \Gamma\left(1+\frac{\alpha}{2}\right)$.

Proof. To prove that two functions $f(x)$ and $g(x)$ are asymptotically equivalent, i.e. $f(x) \sim g(x)$, we should show that $\lim_{x\to\infty} f(x)/g(x) = 1$. Let us first consider the behavior of the random variable β^*, characterized by (6.11) when $\lambda \to \infty$, yielding

$$\lim_{\lambda\to\infty} f_{\beta^*}(x) = \delta(x), \tag{6.26}$$

where $\delta(x)$ is the Dirac impulse function.

This indicates that the random variable β^* tends to have the value 0 with high probability when the network density increases. Now, let us consider that $\beta^* \to 0$, then we have the following limit

$$\lim_{\beta^*\to 0} \frac{\log_2(1+\beta^*)}{\beta^*} = \frac{1}{\ln 2}. \tag{6.27}$$

Using these limits, we can manipulate the expression of the spatial capacity $\mathcal{C}_{\text{IAN}}$ as follows.

$$\lim_{\lambda\to\infty} \mathcal{C}_{\text{IAN}} = \lim_{\lambda\to\infty} \lambda\, \mathrm{E}[\log_2(1+\beta^*)] = \lim_{\lambda\to\infty} \lambda\, \frac{\mathrm{E}[\beta^*]}{\ln 2}. \tag{6.28}$$

Proceeding similarly with the upper bound, we have

$$\lim_{\lambda\to\infty} \lambda\ \log_2(1+\mathrm{E}[\beta^*]) = \lim_{\lambda\to\infty} \lambda\, \frac{\mathrm{E}[\beta^*]}{\ln 2}. \tag{6.29}$$

Now, we recall that the division of limits is the limit of the division, then

$$\lim_{\lambda\to\infty} \frac{\lambda\, \mathrm{E}[\log_2(1+\beta^*)]}{\lambda\ \log_2(1+\mathrm{E}[\beta^*])} = 1. \tag{6.30}$$

From this fact, we can state

$$\mathcal{C}_{\text{IAN}} \sim \lambda \log_2\left(1+\left(\frac{1}{\lambda\pi d^2}\right)^{\frac{\alpha}{2}} \Gamma\left(1+\frac{\alpha}{2}\right)\right), \tag{6.31}$$

when $\lambda \to \infty$.

Finally we verify that $\left(\frac{1}{\lambda\pi d^2}\right)^{\frac{\alpha}{2}} \Gamma\left(1+\frac{\alpha}{2}\right) \to 0$ when $\lambda \to \infty$ and apply the approximation $\log(1+x) \approx x$, valid when $x << 1$, into (6.31) yielding (6.25). □

Fig. 6.2 illustrates the behavior of the spatial capacity $\mathcal{C}_{\text{IAN}}$ and its proposed bounds as a function of the network density λ. Firstly, one can notice that the spatial capacity has a maximum point which is expected from its concavity stated in Property 6.1 and the density λ^* that achieves the optimal is

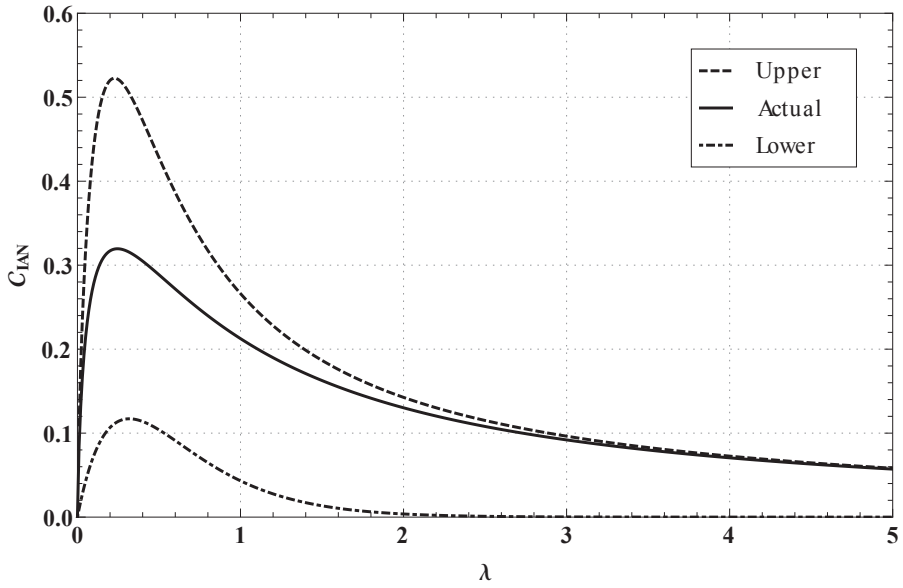

Fig. 6.2: Actual values, lower and upper bounds of the spatial capacity, $\mathcal{C}_{\text{IAN}}$, versus the network density λ for $\alpha = 4$ and $d = 1$ [m]. The lower bound is obtained using $y = 1$ in equation (6.19). The actual values and upper bound are computed using equations (6.12) and (6.21), respectively.

given by equation (6.17)[4]. When densities lower than this maximum are considered, the network is spatially not saturated and the spatial capacity of the network is still not in its highest value. In this situation, any increase of λ leads to an increase of $\mathcal{C}_{\text{IAN}}$ until such an inflexion point is achieved. After that point, on the other hand, the network spatial throughput degrades due to the proximity of the interferers, strongly reducing the average of the link rates R^*. Consequently, $\mathcal{C}_{\text{IAN}}$ becomes a decreasing function of λ.

From Fig. 6.2, we can also evaluate the proposed upper and lower bounds of the spatial capacity. As one can notice the lower bound proposed in Property 6.3 is loose, regardless of λ. In fact, the main use for this bound is to prove the relation between the spatial capacity and the maximum spatial throughput achieved with fixed rates, as discussed later on. Regarding the upper bound introduced in Property 6.4, when λ increases, the upper bound become tighter and tighter, as predict by Property 6.5. In other words, the upper bound has the same value as the spatial capacity $\mathcal{C}_{\text{IAN}}$ when $\lambda \to \infty$ as shown in Fig. 6.2.

Next we apply the same approach used here to derive the approximate spatial capacity and its properties when OPT decoders are employed.

6.3 OPT decoding rule

In this section we deal with OPT decoders, described Section 2.1. As before, we focus on the statistical characterization of the achievable rates, which are stated in Theorem 2.1, over different

[4]A closed-form solution is unknown for this equation but standard numerical methods solve it. In our case, we use FindRoot from Wolfram Mathematica.

spatial realizations using the OPT decoding rule. We then assess the average approximate spatial capacity of the network described in Section 6.1, which is given by equation (6.3).

For the scenario used throughout this section, though, the analysis is more complicated since the receiver node should choose the subset of messages that will be jointly decoded and then verify whether the coding rate of its own transmitter is achievable, given all other coding rates. By construction, all receivers proceed in the same way and hence the analysis becomes a very intricate combinatorial problem. For this reason, in order to derive the pdf of the achievable rates for the OPT decoders, we resort to some approximations that will be justified afterwards.

Before we start, we believe that is important to discuss about successive interference cancellation (SIC) strategies, under which the strongest interefers are successively subtracted from the desired signal, and why we do not consider them in this chapter. For example, in [34, Sec.5.2], Weber and Andrews described their SIC model, also considering challenges of the physical layer issues of the receiver designing (e.g. imperfect channel estimation and signal reconstruction, processing delays etc), dividing the interferers as partially cancellable nodes and uncancellable nodes. In [132], Blomer and Jindal have explicitly assessed the differences between joint decoding (JD) and SIC strategies in wireless networks, evincing the advantages of the first due to its coding-decoding construction. The scheme of JD presented therein is the basis of the OPT rule presented in [71], where the authors illustrate in an elegant way both the capacity region plots (cf. [71, Fig.1]) and the detection boundary regions using IAN, SIC, JD and OPT (cf. [71, Sec. V]), evincing how OPT outperforms SIC and the pure JD.

As in the previous section, we only consider the deterministic path-loss and that the sum of the interfering signals observed by RX_k that are treated as noise can be approximated by the signal from the closest interferer amongst them, whose power is denoted $P_{k,\mathrm{clo}}$. If the noise power is negligible compared to $P_{k,\mathrm{clo}}$, then $1+\sum_{j\in\bar{\mathcal{A}}^*{}_k} P_{kj} \approx P_{k,\mathrm{clo}}$. Based on these assumptions, we can state the following proposition.

Proposition 6.3 (approximate pdf of the spatial-capacity-achievable rates for OPT)**.** *Let us denote the rate tuple that achieves the spatial capacity for the network described in Section 6.1 as* $\mathbf{R}^* = (R_0^*, R_1^*, ...) \in \mathcal{H}$*. Then, the pdf of* $R_k^*, \forall\ k \in \mathcal{A}$ *follows the pdf of a typical rate* R^**, denoted by* $f_{R^*}(x)$ *and approximated as*

$$f_{R^*}(x) \approx \sum_{i=0}^{\infty} \frac{(\lambda\pi d^2)^i}{\Gamma(i)}\, e^{-\lambda\pi d^2} f_{R^*|n}(x|n=i) \tag{6.32}$$

where $f_{R^*|n}(x|n)$ *is the pdf of* R^* *given that* $1+n$ *messages are jointly decoded and is approximated by*

$$f_{R^*|n}(x|n) \approx \ln 4\ \frac{2^{(1+n)x}\lambda\pi d^2}{\alpha}\ \left(\frac{2^{(1+n)x}-1}{1+n}\right)^{\frac{2}{\alpha}-1}\ e^{-\lambda\pi d^2\left(\left(\frac{2^{(1+n)x}-1}{1+n}\right)^{\frac{2}{\alpha}}-1\right)}, \tag{6.33}$$

such that $x > \frac{\log(2+n)}{1+n}$.

Proof. Let us first deal with the typical link TX_0–RX_0. Without loss of generality, we place the origin of the Cartesian plane at RX_0 and assume that all nodes that are closer to RX_0 than TX_0 have their messages jointly decoded with TX_0 message (see Fig. 6.3). From the distance-dependent path-loss modeling, the closer the TX, the higher the power, and then this choice of the subset $\mathcal{A}_0^*$ is justified.

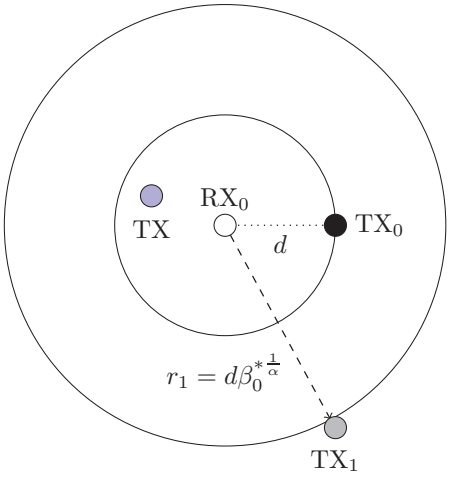

Fig. 6.3: Illustrative example of the typical link TX$_0$–RX$_0$ employing the OPT decoding rule. The blue TX has its message jointly decoded with TX$_0$ message and TX$_1$ is the closest interferer to RX$_0$ whose signal is treated as noise. The random variable r_1 denotes the distance between RX$_0$ and TX$_1$ such that $r_1 > d$.

For each network spatial realization, we consider that a number n associated with the transmitters whose messages are decoded by RX$_0$ is known, which yields the following inequality

$$\log\left(1+\frac{(1+n)P_{00}}{P_{0,\text{clo}}}\right) < \log\left(1+\frac{P_{00}+\sum_{i=1}^{n}P_{0i}}{P_{0,\text{clo}}}\right). \tag{6.34}$$

One can see from (2.5) and (6.34) that rate tuples that satisfy $R_0+\sum_{i=1}^{n}R_i < \log\left(1+\frac{(1+n)P_{00}}{P_{0,\text{clo}}}\right)$ are always achievable. Defining $\beta_0^* = P_{00}/P_{0,\text{clo}}$, we use similar steps to the ones used in the proof of Proposition 6.2, but considering now that $r_1 > d$ to compute the pdf $f_{\beta_0^*}(x)$ as

$$f_{\beta_0^*}(x) = \frac{2\lambda\pi d^2 x^{\frac{2}{\alpha}}}{\alpha x} e^{-\lambda\pi d^2\left(x^{\frac{2}{\alpha}}-1\right)}, \tag{6.35}$$

where $x > 1$ and $f_{\beta_0^*}(x) = 0$ when $x \leq 1$.

Then, we assume that $R_0+\sum_{i=1}^{n}R_i \approx (1+n)R_0$ to obtain $(1+n)R_0^* = \log(1+(1+n)\beta_0^*)$. By applying such a transformation, we can find the pdf of R_0^* given n. Here we use Theorem 2.3 and then the index 0 can be dropped, resulting in equation (6.33). To unconditioned the pdf $f_{R^*|n}(x|n)$, we apply the definition of Poisson process to compute the probability that $n = i$ points lie in the area πd^2, concluding this proof. □

Remark 6.2. *In addition to the closest interferer treated as noise approximation, this proposition is based on other two main assumptions: (i) the detected power at RX$_0$ related to the $1+n$ jointly decoded messages is equal to $(1+n)P_{00}$ and (ii) the sum rate associated with those messages is given by $(1+n)R_0$. In assumption (i), we use the lower bound given by* (6.34)*, which indicates that we underestimate the aggregate power, while in (ii) we approximate the sum of $1+n$ random variables that follows the same distribution by one random variable multiplied by $1+n$. We argue that*

the underestimation byproduct of assumption (i) leaves us some room for variations in the sum rate approximation used in (ii). In addition, due to the homogeneity of the spatial process, $R_0+\sum_{i=1}^{n} R_i \approx (1+n)R_0$ *leads to a reasonable approximation. Simulations results are presented in Section 6.5 where we discuss such approximations.*

Here we can compute the approximate average spatial capacity[5] $\mathcal{C}_{\text{OPT}}$ when the OPT decoding rule is employed as

$$\mathcal{C}_{\text{OPT}} \approx \lambda \int_0^{\infty} x f_{R^*}(x)\, dx, \tag{6.36}$$

where $f_{R^*}(x)$ is given in Proposition 6.3.

The integral in (6.36) is analytically unsolvable (we can rely on numerical solutions, though). To gain more insights on the system performance, we next derive some properties of the spatial capacity.

Property 6.6 (concavity)**.** *Considering that the rate* R^* *is a function of the network density* λ*, then* $\mathcal{C}_{\text{OPT}}$ *given by* (6.36) *is* quasi concave *in terms of* λ*, where* R^* *is a random variable given by* (6.32)*.*

Property 6.7 (lower bound)**.** *A lower bound of the spatial capacity given by* (6.36) *is computed as*

$$\mathcal{C}_{\text{OPT}} \geq \lambda \sum_{i=0}^{\infty} \frac{(\lambda\pi d^2)^i}{\Gamma(i)} y e^{-\lambda\pi d^2\left(\frac{2^{(1+i)y}-1}{1+i}\right)^{\frac{2}{\alpha}}}, \tag{6.37}$$

where $y > \frac{\log_2(2+i)}{1+i}$ *for all* $i \geq 0$*.*

Property 6.8 (upper bound)**.** *A upper bound of the spatial capacity given by* (6.36) *is computed as*

$$\mathcal{C}_{\text{OPT}} \leq \lambda \sum_{i=0}^{\infty} \frac{(\lambda\pi d^2)^i}{\Gamma(i)} \frac{e^{-\lambda\pi d^2}}{1+i} \times \\ \times \log_2\left(1 + (1+i)\left(\frac{1}{\lambda\pi d^2}\right)^{\frac{2}{\alpha}} \Gamma\left(1+\frac{2}{\alpha}, \lambda\pi d^2\right) e^{\lambda\pi d^2}\right), \tag{6.38}$$

where $\Gamma(\cdot,\cdot)$ *is the incomplete Gamma function, which is defined as* $\Gamma(z,a) = \int_a^{\infty} t^{z-1}e^{-t}\, dt$*.*

Property 6.9 (asymptotic equivalence)**.** *Let* $\sim$ *denote asymptotic equivalence of two functions, then*

$$\mathcal{C}_{\text{OPT}} \sim \lambda \sum_{i=0}^{\infty} \frac{(\lambda\pi d^2)^i}{\Gamma(i)} \frac{e^{-\lambda\pi d^2}}{1+i} \times \\ \times \log_2\left(1 + (1+i)\left(\frac{1}{\lambda\pi d^2}\right)^{\frac{2}{\alpha}} \Gamma\left(1+\frac{2}{\alpha}, \lambda\pi d^2\right) e^{\lambda\pi d^2}\right), \tag{6.39}$$

when $\lambda \to \infty$*.*

[5] As in the previous section we use the term spatial capacity to refer to the approximate average spatial capacity.

The proofs of these properties follow the same principles used before so we omit them here. It is worth pointing out that the proofs of (6.37)-(6.39) begin by assuming that the number $1+n$ of jointly decoded messages is known. Then, we use the fact that the unconditioned spatial capacity is a linear combination of the conditioned capacities with weights given by the Poisson probabilities such that $n=i$ nodes lie in a area of πd^2 computed as $\frac{(\lambda\pi d^2)^i}{\Gamma(i)}\, e^{-\lambda\pi d^2}$.

Next, we present a proposition that states that the OPT decoding rule always leads to a better performance than the IAN rule.

Proposition 6.4 ($\mathcal{C}_{\text{OPT}}$ vs. $\mathcal{C}_{\text{IAN}}$)**.** *For any given network density λ,*

$$\mathcal{C}_{\text{OPT}} \geq \mathcal{C}_{\text{IAN}}. \tag{6.40}$$

Proof. To prove this proposition, we first use the identity $a\log_2(1+x) \leq \log_2(1+ax)\ \forall\ a \geq 1$ to verify that

$$\int_1^{\infty} x^{\frac{2}{\alpha}-1} \frac{\log_2(1+(1+n)x)}{1+n} e^{-\lambda\pi d^2 x^{\frac{2}{\alpha}}} dx \geq \int_0^{\infty} x^{\frac{2}{\alpha}-1} \log_2(1+x) e^{-\lambda\pi d^2\left(x^{\frac{2}{\alpha}}-1\right)} dx, \tag{6.41}$$

where $n \in \mathbb{N}$ represents the number of jointly decoded messages by the typical link TX_0-RX_0. Recalling that all TXs that are located closer to RX_0 than TX_0 have their messages jointly decoded by RX_0, then the number n follows a Poisson distribution over an area of πd^2. Using this fact and multiplying both sides of (6.41) by $\frac{2\lambda\pi d^2}{\alpha}$, we have the following inequality:

$$\begin{aligned}\sum_{i=0}^{\infty} \frac{(\lambda\pi d^2)^i}{\Gamma(i)} e^{-\lambda\pi d^2} \int_1^{\infty} f_{\beta^*}^{\text{OPT}}(x)\ \frac{\log_2(1+(1+i)x)}{1+i}\ dx \geq \\ \geq \sum_{i=0}^{\infty} \frac{(\lambda\pi d^2)^i}{\Gamma(i)} e^{-\lambda\pi d^2} \int_0^{\infty} f_{\beta^*}^{\text{IAN}}(x)\ \log_2(1+x)\ dx,\end{aligned} \tag{6.42}$$

where $f_{\beta^*}^{\text{OPT}}(x)$ and $f_{\beta^*}^{\text{IAN}}(x)$ are given by (6.35) and (6.11), respectively.

Finally we multiply both sides of (6.42) by λ, obtaining then (6.40). □

In Fig. 6.4, we present the spatial capacity $\mathcal{C}_{\text{OPT}}$ given by (6.36) as a function of λ together with its proposed upper and lower bounds. One can observe that the lower bound given by Property 6.7 is very loose for the value of the constant y that was arbitrarily chosen ($y=2$). This bound, however, can be improved by tuning the constant y in accordance to the number of jointly decoded messages. Such an improvement in the proposed bound will be discussed in the next section when we apply it to analytically assess the performance of networks where predetermined fixed rates are imposed.

Turning your attention to the values of $\mathcal{C}_{\text{OPT}}$ given by (6.36), one can easily see that it is an increasing function of λ. For lower densities, $\mathcal{C}_{\text{OPT}}$ increases faster since the probability that an interfering TX has its message jointly decoded is also low and, consequently, the rate is constrained by the interferers that are treated as noise, indicating that $\mathcal{C}_{\text{OPT}}$ is limited by the low spatial reuse. When λ increases, on the other hand, more messages from interfering TXs start being jointly decoded, which diminishes the $\mathcal{C}_{\text{OPT}}$ rate of increase. Furthermore, we can observe that the upper bound proposed in Property 6.8 is a good approximation to $\mathcal{C}_{\text{OPT}}$ for all densities λ especially when $\lambda \to \infty$, corroborating Property 6.9.

By comparing the results shown in Fig. 6.2 (IAN) and Fig. 6.4 (OPT), one can see that the OPT decoding rule provides higher spatial capacities, regardless of the network density, as predicted by

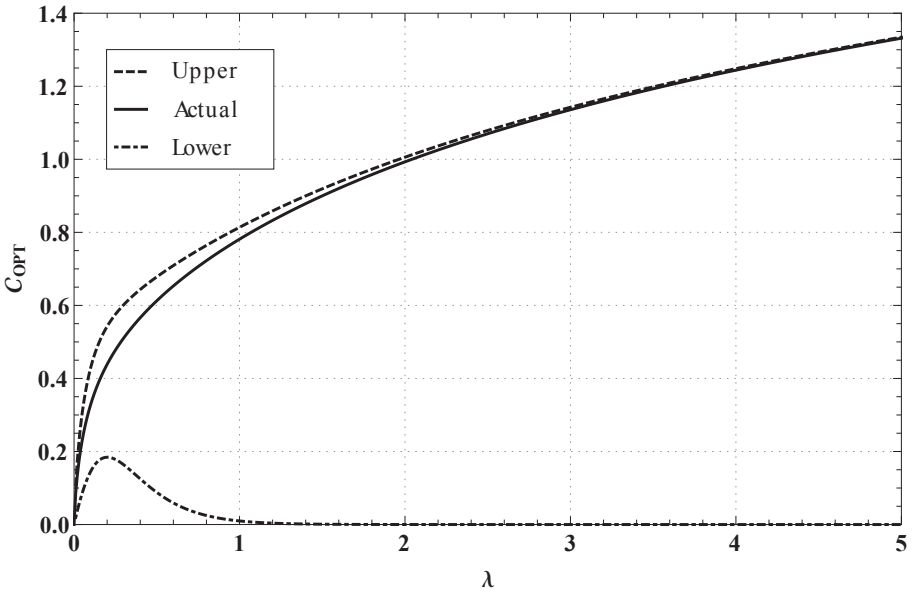

Fig. 6.4: Actual values, lower and upper bounds of the spatial capacity, $\mathcal{C}_{\mathrm{OPT}}$, versus the network density λ for $\alpha = 4$ and $d = 1$ [m]. The lower bound is obtained using $y = 2$ in equation (6.37). The actual values and upper bound are computed using equations (6.36) and (6.38), respectively.

Proposition 6.4. The performance gain obtained with the OPT decoder in comparison with the IAN decoder indicates that the mechanism of joint detection used here is a good way to deal with the strongest interferers. A more detailed comparative analysis between OPT and IAN decoding rules is presented later.

In the following section, we compare the results obtained so far with the most usual approach found in the literature (e.g. [34]): coding rates are fixed for a given network density and set to optimize the average spatial throughput regardless of a specific network topology, leading to outage events (i.e. some pairs use coding rates above their channel capacity).

6.4 Spatial throughput optimization using predetermined fixed rates

We now focus our attention on scenarios where TXs set their coding rates to the fixed values that leads to the highest average spatial throughput, given that the TXs are aware of how many messages are jointly decoded by their RXs. Using this scheme, groups of TXs use the same fixed coding rates and then an optimization problem is formulated to find these rates such that the average spatial throughput is maximized. As a consequence the optimal choice of coding rates, as discussed later on, is not in the network capacity region, stated in Theorem 2.1, leading to outage events for some links. Next, we present the definition of the aforementioned optimization problem.

Definition 6.4 (highest spatial throughput)**.** *The spatial throughput optimization problem for a net-*

work where TXs have fixed coding rates is defined as[6]*:*

$$\mathcal{T} = \max_{\mathbf{R}} \ \mathrm{E}[\mathcal{S}], \tag{6.43}$$

where $\mathcal{T}$ is the maximum spatial throughput, $\mathbf{R} = (R_0, R_1, ...)$ represents the set of fixed coding rates R_i used by the TXs such that i is the number of jointly decoded messages in addition to the desired one, and $\mathcal{S}$ is the spatial throughput given by (6.1)*, where only the successful transmissions are taking into account.*

When the IAN decoding rule is used, there is no jointly decoded message and then the optimization is only related to one fixed coding rate[7]. We now present two propositions that state the highest spatial throughputs for IAN and OPT decoders applying the network modeling used before[8].

Proposition 6.5 (highest spatial throughput for IAN)**.** *The highest spatial throughput $\mathcal{T}_{\text{IAN}}$ achieved when IAN decoders are used is given by*

$$\mathcal{T}_{\text{IAN}} = \lambda \log_2(1+\beta^*) e^{-\lambda\pi d^2 \beta^{*\frac{2}{\alpha}}}, \tag{6.44}$$

where β^* is the value of $\beta > 0$, which is solution of

$$\beta = \left(\frac{2}{\alpha} \lambda\pi d^2 (1+\beta) \ln(1+\beta) \right)^{\frac{\alpha}{\alpha-2}}. \tag{6.45}$$

Proof. Let us write the spatial throughput given by (6.1) for this scenario as

$$\mathcal{S} = \lambda(1-P_{\text{o}})R, \tag{6.46}$$

where R is the fixed coding rate used by all TXs and P_{o} is the outage probability associated with R (cf. Definition 2.5).

We proceed here similarly to the proof of Proposition 6.2 and then apply the relation $R = \log_2(1+\beta)$, where $R, \beta > 0$. From Proposition 2.12, we can write $P_{\text{o}} = 1 - e^{-\lambda\pi d^2 \beta^{\frac{2}{\alpha}}}$ and hence:

$$\mathcal{S} = \lambda \log_2(1+\beta) e^{-\lambda\pi d^2 \beta^{\frac{2}{\alpha}}}, \tag{6.47}$$

which is a concave function of β. We compute β^* as the solution of the derivative equation $d\mathcal{S}/d\beta = 0$, resulting after some manipulation in (6.45). To conclude this proof, we use β^* into equation (6.47), obtaining (6.44). □

Proposition 6.6 (highest spatial throughput for OPT)**.** *The highest spatial throughput $\mathcal{T}_{\text{OPT}}$ achieved when OPT decoders are used is given by*

$$\mathcal{T}_{\text{OPT}} = \lambda \sum_{i=0}^{\infty} \frac{(\lambda\pi d^2)^i}{\Gamma(i)} \frac{e^{-\lambda\pi d^2}}{1+i} \log_2(1+(1+i)\beta_i^*) \, e^{-\lambda\pi d^2 \left(\beta_i^{*\frac{2}{\alpha}} - 1\right)} \tag{6.48}$$

where, for each $i = 0, 1, 2, ...$, β_i^* is found as the value of $\beta_i > 1$, which is solution of

$$\beta_i = \left(\frac{2}{(1+i)\alpha} \lambda\pi d^2 (1+(1+i)\beta_i) \ln(1+(1+i)\beta_i) \right)^{\frac{\alpha}{\alpha-2}}. \tag{6.49}$$

[6] This can be also viewed as the transmission capacity without outage constraint.

[7] This is the usual approach as in [34] or in the previous chapters of this thesis.

[8] Once again we use the closest intereferer treated as noise approximation. Besides, the term highest spatial throughput refers to the highest approximate spatial throughput.

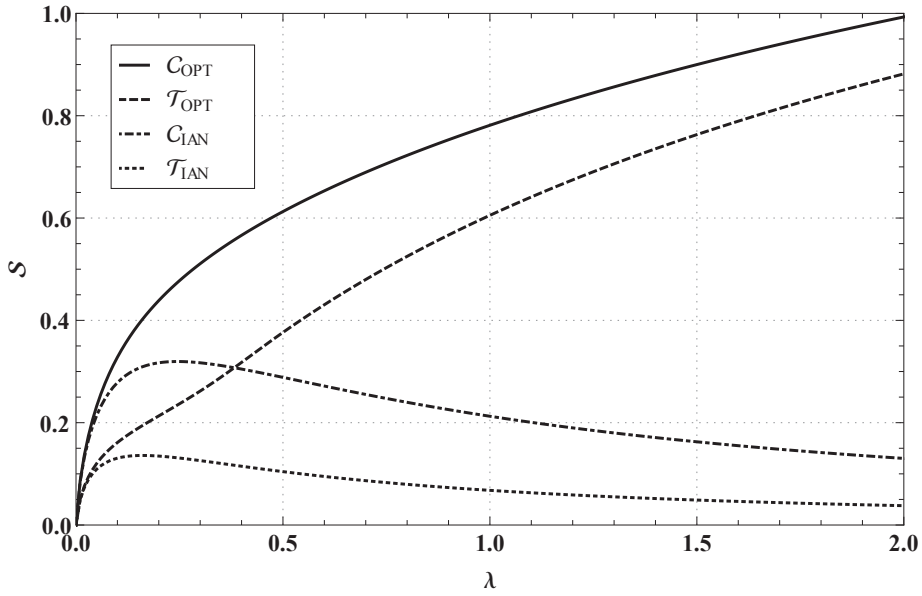

Fig. 6.5: The highest spatial throughputs $\mathcal{T}$ using fixed coding rates given by (6.44) and (6.48), and the spatial capacities $\mathcal{C}$ given by (6.12) and (6.36) as a function of the network density λ for IAN and OPT decoding rules, $d = 1$ [m] and $\alpha = 4$.

Outline of proof. To prove this proposition, we follow the same steps used in the proof of Proposition 6.5, considering these basic differences: $\beta_i = d^{-\alpha}/r_1^{-\alpha} > 1$ (since messages from TXs closer to a given RX than its own TX are jointly decoded and then $r_1 > d$) and the optimization is proceeded for each $i = 0, 1, 2, ...$ which yields (6.49). To conclude this outline, we average the spatial throughputs by the Poisson probabilities that i nodes lie in the area πd^2, resulting in (6.48). □

Here we apply Properties 6.3 and 6.7 to obtain an analytical relation between the spatial capacity $\mathcal{C}$ and the highest spatial throughput $\mathcal{T}$ using fixed rates for either decoding rules.

Proposition 6.7 ($\mathcal{C}$ vs. $\mathcal{T}$)**.** *For a given density λ and assuming that all links use the same decoding rule (either IAN or OPT), then*

$$\mathcal{C} \geq \mathcal{T}. \tag{6.50}$$

Proof. This statement is a consequence of Property 6.3, when we set the constant $y = \log(1 + \beta^*)$ in (6.19), yielding (6.44). Similarly, we use Property 6.7, applying for each different $i \in \mathbb{N}$ a different constant y in (6.37) such that $y_i = \frac{\log(1+(1+i)\beta_i^*)}{1+i}$, which yields (6.48), concluding this proof. □

Fig. 6.5 shows the maximum spatial throughput following the formulation derived in this section. As proved in Proposition 6.7, $\mathcal{T}$ is always lower than or equal to $\mathcal{C}$ for the same density and the same decoding rule. This is justified by the methodology used to derive the spatial capacity, which allows for a coding rate setting based on the relative positions of the nodes for each different realization of the spatial process. When fixed rates are used, the transmitters code their messages using a fixed rate that depends only on the number of other messages that are jointly decoded by their own receivers. By optimizing based only on the average behavior of the network, some RXs cannot successfully decode their messages for specific topologies, which decreases the spatial throughput. Therefore, the

spatial-capacity-achieving strategy has always a better performance. Besides given the decoding rule employed, the curves of $\mathcal{T}$ and $\mathcal{C}$ have a similar shape.

Fig. 6.5 also shows that the spatial capacity obtained when OPT is used has a huge gain if compared with the IAN option. As predicted by Proposition 6.4, this result reflects that the OPT rule is able to avoid the strongest interferers by jointly decoding their messages.

When λ is low, both OPT and IAN decoders have approximately the same performance since the probability that a interferer is closer to a given RX than its own TX is very low. Increasing λ, such a probability also increases and then the differences between the strategies become apparent as the closest interferer is the limiting factor for IAN, while such node may have its message jointly decoded when OPT is used, what decreases the effects of the nearby interferers.

6.5 Discussion

So far we have showed that, for same network density, (i) OPT decoders outperform IAN, and (ii) the spatial-capacity-achieving strategy outperforms the average spatial throughput optimization when receivers employ the same decoding rule. Nevertheless we still need to discuss some possible limitations of our finds, namely the tightness of our approximations and the feasibility of each decoding rule for practical implementations. In the following subsections we deal with both aspects, identifying why our results are important even when our approximation is poor and for which circumstances the design setting that provides the worst performance is more suitable than the optimal.

6.5.1 Tightness of our approximation

Here we discuss the validity of the "closest interferer treated as noise approximation" used to derive the approximate performance of both decoding rules. Fig. 6.6 shows the average spatial capacity $\mathcal{C}$ computed using our analytical approximation and Monte Carlo simulation as a function of the network density λ for both decoders[9]. For both IAN and OPT, the lower the density is, the better our approximation works. Conversely, increasing the density, our approximate spatial capacity gets looser and looser.

The closest interferer approximation is in fact a lower bound of the aggregate interference [34], leading then to an upper bound of the actual spatial capacity. This bound have been proved to be asymptotically equivalent to the actual values when $\lambda \to 0$ [129, 34][10]. For higher densities, the closest interferer treated as noise tends to contribute less to the aggregate interference experienced by the receivers, worsening our approximation.

Yet, the comparison between the IAN and OPT decoders is fair since the results presented in Sections 6.2 and 6.3 rely on the same approximation[11]. We further argue that our approximation has no effect in the trade-off analysis done in this chapter and Fig. 6.6 illustrates this fact by showing that

[9] The results for the highest average spatial throughput presented in Section 6.4 follows the same trends and thus we exclude them from this thesis.

[10] In our point of view this asymptotic analysis is unsuitable for the study carried out here; we assume an interference-limited network, which opposes the idea of very low density of interferers. When $\lambda \to 0$, we see the network in its noise-limited regime.

[11] We can argue in the same way to say that the analysis presented in Section 6.4 is also fair.

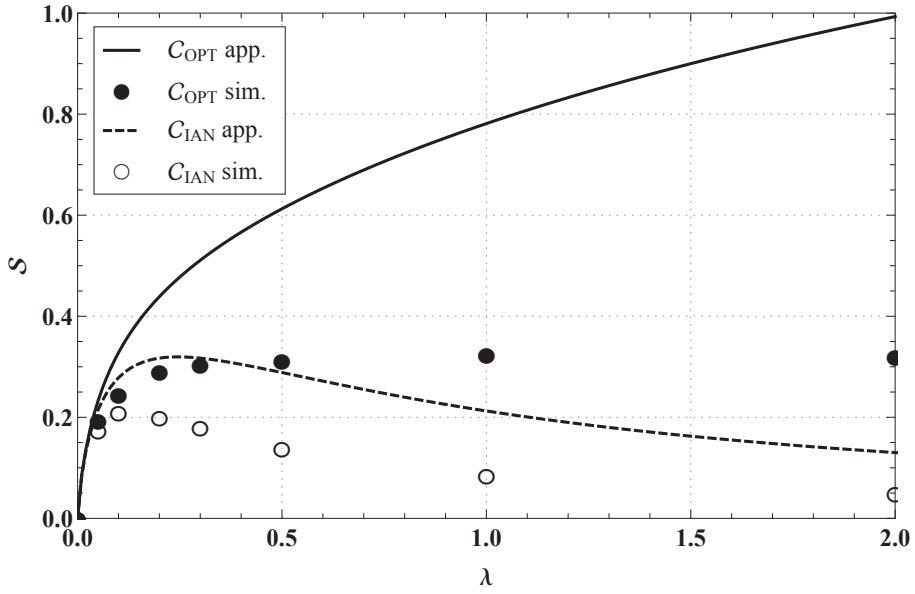

Fig. 6.6: Spatial capacities $\mathcal{C}$ for IAN and OPT as a function of the network density λ , $d = 1$ [m] and $\alpha = 4$. Approximate results given by equations (6.12) and (6.36), and simulations.

the OPT always outperforms IAN in similar scales: the ratios $\mathcal{C}_{\text{IAN}}/\mathcal{C}_{\text{OPT}}$ obtained via simulation or via our approximations have similar values when considering the same λ. As the proposed formulation provides a much simpler way to assess the network performance than numerical simulations, we reinforce the contribution of this paper even when our approximations provide poor bounds.

All in all, we believe that our main messages – OPT is better than IAN, and spatial-capacity achieving strategy is better than the best fixed rate one – are unaffected by our approximations. Despite of these facts, the optimal strategy is many times unfeasible for practical implementation as discussed in the following.

6.5.2 Design setting and mobility pattern

Throughout this chapter we have shown that the best design option in terms of spatial throughput is to employ OPT decoders and apply the spatial-capacity achieving scheme. This solution, however, has drawbacks: (i) RXs require the knowledge of the codebooks of the jointly decoded messages and (ii) OPT decoders are computationally more complex than IAN.

Knowing them, we argue that the use of either/both OPT and/or spatial-capacity achieving strategy is unfeasible for (highly) mobile topologies. Under this topology, the neighbors of any given receiver vary very fast, making impossible the joint decoding procedure. Shopping malls and streets where people frequently come and go can exemplify this scenario. If this is the case, even though the design setting employing IAN decoders with fixed rate optimization is far from the optimal performance, it is a more suitable choice.

Conversely, when (quasi-)static networks are considered, the optimal strategy becomes possible. In this case, receiver nodes must known the codebooks of their strongest interfering nodes and jointly decode their messages. In addition, the links must coordinate their coding rates to be in the network

capacity region. Smart homes, industry plants and other kind of machine-to-machine communications can exemplify this mobility pattern.

Besides, there are other aspects that may be prohibitive for OPT. For instance, many applications require secrecy and then the codebook knowledge makes OPT unfeasible even for static topologies. Other applications need fast processing time, which is also unfeasible when many interfering messages are jointly decoded. Anyway, this dependence on the topology must be taken into account when the network is designed. Furthermore, the mobility pattern of the network can also change over time – for example, offices during the night are quasi-static, while highly dynamic during parts of the working hours. We will return to this discussion once again in the next chapter, also including other results presented throughout this thesis.

6.6 Summary

In this chapter we studied the spatial throughput of interference networks using Gaussian point-to-point codes for two different decoding rules: (i) treating all interfering messages as noise – IAN, and jointly decoding the messages whose detected power is higher than the desired message power while treating the others as noise – OPT. We proposed an approximation of the highest spatial throughput for Poisson distributed networks such that all links work in their capacity region (spatial-capacity achieving strategy). We then stated several properties of our approximation using either decoders and prove that, when the same network density is assumed, (i) the OPT always outperforms IAN, and (ii) the spatial-capacity-achieving strategy is always better than the predetermined fixed rate optimization, where transmitters code their messages in order to optimize the average spatial throughput.

Chapter 7

Discussion

In this section we discuss how the lessons learned from Chapter 3 to 6 can be put together. First we are going to identify which are the internal and external factors to each node that may affect the overall system performance for two different cases, namely quasi-static network and highly mobile network. For each case, we will make claims about how the communication system should be designed to improve its efficiency. Finally, we apply those claims to make a guideline on the implementation of an adaptive algorithm that each node should run in an ad hoc fashion.

7.1 Internal and external factors

Let us start by defining internal and external factors for the ad hoc network under analysis as follows. Internal factors are the constraints that each network element has to satisfy due to its own quality requirement. We can cite as example of possible internal factors a minimum coding rate or spectral efficiency, a bounded outage probability, a minimum required effective throughput, a maximum packet loss probability after back-offs and retransmissions, queue stability and so on.

In a similar way we can relate the external factors to the constraints imposed by the network. For example, we can list the fairness of the medium access across different links (i.e. nodes should have similar opportunities of access the medium), a maximum transmit power used by transmitters in order to control the interference level and a floor level of spatial throughput. It is important noting that, differently from the internal factors, the items listed above are not controlled by the link or any other entity, but rather they are product of the interactions among links that in turn are subject to their own internal factors.

Clearly, how to cope with such interactions while preserving the overall network requirements and at the same time satisfying the internal factors of each individual link can be viewed as the biggest design challenge that engineers should deal with. To complicate even more this picture, the network should be robust enough to variations of the scenario itself. For example, traffic conditions can vary during the day, mobility of nodes causes changes in the network topology etc; even under these wide range of different, many times unpredictable, external conditions, the system should work properly.

To understand how our results indicate the basis of a robust adaptive communication system for ad hoc networks, we present next two scenarios where the conditions of mobility are extreme - highly mobile and quasi-static topologies. Then we will make claims regarding how the system should be

designed to improve the information flow based on the analysis carried out in this thesis. Using those claims, we will discuss the construction of ad hoc procedures that should be functional, working similarly to intelligent humans in the "chatting in a party problem" presented in Section 1.2.

7.2 Network design

As mentioned before, we assess in this section ad hoc networks under two extreme mobility conditions, namely quasi-static and high-mobile. For each one of these scenarios, we will make claims regarding the design setting looking at the network conditions, and the internal and external factors that its nodes face. Here it is worth pointing out that we are not going to present formal proofs of the claims, which are in fact conclusions that one can infer from the previous chapters as well as other works available in the literature such as [34, 71].

7.2.1 Quasi-static network

Let us assume here a network where the elements are either quasi-static or static, which indicates its topology changes very slow. Examples of this can be an office with desktop computers, electro-electronics devices in a house or machines in an industrial plant. For this scenario, we consider that the channel gains are dominated by the distance-dependent path loss (i.e. channel gains related to slow and fast fading are neglected) and that all transmitters are subject to the same power constraint imposed by the network. Based on these mild assumptions and considering that all transmitters are able to estimate the distances between its own receiver and the interfering nodes, we can make the following claims.

Claim 7.1 (achievable rate)**.** *The transmitters can individually code their messages such that the coding rate is achievable for (quasi-)static topology regardless of the decoding rule used (refer to Corollaries 2.1 and 2.2).*

Claim 7.2 (decoding rules)**.** *If the network is sparsely populated (lower densities), IAN and OPT decoders perform similarly in terms of spatial throughput. Conversely, if the network is densely populated, OPT significantly outperforms IAN.*

Remark 7.1. *The advantage of OPT is obtained at expanse of computationally complex decoder. In addition, to jointly decode some messages, the receivers must know the codebook of other interfering transmitters, which is not always feasible or desirable.*

Claim 7.3 (access protocol and retransmissions)**.** *The design choices conditioned by the network conditions are stated below.*

- *If all nodes are able to transmit with achievable rates (i.e. the network operates within its capacity region given by Theorem 2.1) and there is no minimum coding rate requirement, there is no need for retransmissions or medium access protocols.*
- *If there exist a minimum required coding rate, then distributed time-division (synchronous transmissions) should be used to achieve such a rate.*

- *If the network is densely populated, then distributed time-division (synchronous transmissions) should be used to increase the spatial throughput.*

- *If the traffic conditions are heavy and there is no minimum required coding rate, the transmitters should find the best coding rate for the time-division employed such that each transmitter is able to maintain the stability of its own queue system.*

- *When a feasible combination does not exist for such heavy traffic conditions, the network will operate outside its capacity region. Therefore, distributed time-division schemes should be implemented together with a limited number of retransmissions, allowing for a bounded packet loss probability.*

- *In multi-hop systems, the nodes should act as a relay if its own traffic condition allows, i.e. this new incoming traffic can be introduced without causing instability.*

- *If a node is acting as a relay, it should choose the next relay node based on the relative distance, the coding rate used and the density of the network. For dense networks, links should be more robust against interference so that lower coding rates together to closest-neighbor hopping strategy (more hops) increase the network efficiency. Conversely, sparsely populated networks allow for higher coding rates and furthest-neighbor hopping strategy (less hops).*

All these claims provide us some intuition of the design setting that static or quasi-static ad hoc networks should have under different conditions. It is important to mention that these claims hold only when every network element has the knowledge of: (i) the distances to the other transmitters, (ii) its own traffic conditions and (iii) network density. Therefore, all transmitters must have the capability of *sensing* the available signals to then compute *estimations* of the network state and traffic conditions. With these estimations of the external conditions in hand, the elements must find solutions that satisfy their own internal and external factors. But before going further into implementation issues, which will be our focus later on Section 7.3, we still need to analyze highly mobile topologies as presented next.

7.2.2 Highly mobile network

Here we consider a network where its elements are highly mobile such that their positions change very fast so properties of Poisson point process can be applied using tools of stochastic geometry based on the high mobility random walking model (cf. Section 2.2). We can see such a situation in shopping malls, streets, coffee houses or wherever place with intense flux of people using mobile devices. We assume that channel gains are a composition of distance-dependent path loss and fast fading[1]. As before, all transmitters are subject to the same power constraint imposed by the network. Then, we can make the following claims considering that every transmitter knows the distance to its own receiver as well as the density of interfering nodes.

[1]It is worth remembering here the last paragraph of Chapter 2, where we point out that the distance-dependent path loss using the dominant-interferer and the Rayleigh fast fading cases have a similar formulation. In this way, the results obtained using one modeling can be extended to the other.

Claim 7.4 (achievable rate)**.** *Every transmitter can individually code its messages so that the outage probability given by Definition 2.5 can be bounded.*

Remark 7.2. *Due to the high mobility of the nodes, the network is always working out of its capacity region. Yet, it is possible to bound the link outage probability by properly setting the coding rate.*

Claim 7.5 (decoding rules)**.** *The OPT decoder is an unfeasible option for highly mobile networks, while IAN is still functional under such conditions.*

Remark 7.3. *A necessary condition to the OPT decoding rule is the knowledge of the coding book of other transmitters. As the network topology changes very fast, it is not feasible to have such a knowledge. Moreover, when transmitters move during the transmissions, the subset of messages that are jointly decoded and treated as noise may also change. All in all, it is very difficult, or even impossible, to employ OPT decoders in highly mobile scenarios.*

Claim 7.6 (access protocol and retransmissions)**.** *The design choices conditioned by the network conditions are stated below.*

- *A limited number of retransmissions for packets detected in error improves the system performance regardless of the medium access procedure.*
- *The only kind of distributed time-division for highly mobile networks (synchronous transmissions) is slotted ALOHA.*
- *If the network is sparsely populated, then random access protocols that employ carrier sensing (e.g. CSMA) tend to outperform slotted ALOHA schemes.*
- *If the network is densely populated and the traffic conditions are not heavy, the synchronous transmissions required by the slotted ALOHA improve both individual link and spatial throughputs.*
- *If the traffic conditions are heavy and the network is densely populated, the transmitters should find the best combination of access probability under slotted ALOHA protocol, coding rate and number of allowed retransmissions per packet such that every transmitter is able to maintain the stability of its own queue system and have a bounded packet loss probability.*
- *In multi-hop systems, the nodes should act as a relay if its own traffic condition allows, i.e. this new incoming traffic can be introduced without causing instability.*
- *If a node is acting as a relay, it should choose the next relay node based on the relative distance (if it is possible estimate), the coding rate used and the density of the network. For dense networks, links should be more robust against interference so that lower coding rates together to closest-neighbor hopping strategy (more hops) increase the network efficiency. Conversely, sparsely populated networks allow for higher coding rates and furthest-neighbor hopping strategy (less hops).*

Here, once again, one can see that every network element must be able to sense and estimate the network and traffic conditions, using them to assess the feasibility of possible design setting based on their internal and external pressures. Using these claims and the ones proposed in the previous section, we will discuss in the following how a robust ad hoc adaptive algorithm that allows should be designed for interference networks under different conditions of density, traffic and mobility.

7.3 Implementation aspects

In the previous subsections we stated several claims describing how the design of ad hoc networks should be for two extreme mobility scenarios based on the results obtained in this thesis. In any case, we still have a small understanding of the deployment of more practical scenarios where the network condition varies (i.e. during some time the network can be high mobile while during some other periods it can be quasi-static or neither one). We can visualize this condition in, for instance, smart homes where there are equipments communicating that are static and there might be people using other communication devices as well; sometimes there is no one around or people are sleeping and then only machines communicate. In contrast, during other periods they are awake using their wireless devices, walking around and generating traffic.

Our aim here is to guide the design of a possible adaptive algorithm to improve the network efficiency while the constraints associated to internal and external factors can be satisfied.

7.3.1 Variable to be optimized

In Chapter 5 we indicated that if all links optimize their own effective throughput given by Definition 5.2 in a selfish way, then the common resource might be overused, leading to similar effects to the tragedy of the commons problem [128]. There, we also showed that if all links optimize the network spatial throughput given by Definition 5.3, then they can reach link effective throughputs at least as high as in the selfish optimization case.

The reason of this is the following. While the former procedure optimizes the link performance for a *given* network state which is in turn considered independent of its own decision, the latter assumes that the designing choice of every transmitter affects the others and then also modifies the actual network state. Therefore, by optimizing the network spatial throughput assuming that all links proceed in the same way, the setting that is the optimal for the network is also the optimal for each individual link. Motivated by this result, we argue that the spatial throughput is the measure to be optimized by the most efficient algorithms designed for interference networks since it provides incentives to collaborative behavior, avoiding then prisoner dilemma kind of loses [133].

7.3.2 Variables required to proceed with the optimization

Now that the maximization target is defined, we should determine what each network element should know to optimize its performance. First of all, they should assess their own internal factors as their basic constraints. For example, every transmitter should infer its arrival process, which is an external factor, to determine the conditions that guarantee its own queue stability and therefore it will be able to determine the feasibility of possible solutions.

Then they should also estimate the mobility pattern of the network to evaluate how its topology changes[2]. Once the mobility pattern is identified, the nodes should quantify the network density and/or the distances from each other using procedures as the ones presented in [134] and [135], respectively. Clearly, it is important that all nodes assume in their calculations that the external factors experienced by other nodes are similar (e.g. the same power constraint).

[2]If the node is moving itself, it will see a mobile network around it and will decide to design its communication system accordingly.

Given that such elements locally estimate those information about the network state, they can start optimizing their own design setting based on the claims stated before. In other words, given the internal and external factors, the mobility pattern and the knowledge of the distances and/or the network spatial density, each node will set, for example, the coding rate employed, the decoding rule, the medium access procedure and the maximum number of packet retransmissions that jointly maximize the network spatial throughput, which is locally computed from the estimated network state, while all constraints are satisfied. If the link starts facing problems in satisfying its own constraints or after a given period of time, the procedure should be repeated to adapt its setting to the new state of the network.

As one can notice, this algorithm somehow mimics the way that humans solve the chatting in a party problem defined in Section 1.2. It is also worth saying that we choose here to not go into the specificities of algorithms or signal processing schemes; rather we prefer to provide more general guidelines on the algorithm design.

Chapter 8

Conclusions

In this thesis, we studied the spatial throughput of wireless ad hoc networks from different perspectives using concepts of stochastic geometry, communication theory and information theory. Particularly, we applied a statistical-based analysis to quantify how efficiently the information bits are transmitted through communication links that are spatially distributed over a given area.

We showed that the aggregate performance of the network is closely related to the trade-offs involving density of concurrent transmissions, co-channel interference, required quality of service, link robustness and traffic conditions. In the following sections, we first summarize the contributions of this thesis chapter by chapter and then indicate possible research directions that the work done in this thesis can take.

8.1 Contributions

- **Chapter 2:** We introduced the capacity region of Gaussian point-to-point codes for interference networks, which is the basis of the coding-decoding strategy employed in this thesis. We also reviewed some properties of Poisson point processes that are applied together with the coding-decoding scheme to model wireless ad hoc networks, assessing then their performance.

- **Chapter 3:** We extended the information efficiency metric to incorporate the aspects of multi-hopping, proposing a new metric denominated aggregate multi-hop information efficiency (AMIE). We then used it to investigate under which conditions transmitting to the closest-neighbor (more hops; more reliable links) or to the furthest-neighbor (less hops; less reliable links) is the most adequate hopping strategy in multi-hop transmissions. Our results indicated that such a decision is closely related to the interference level of the network and the link spectral efficiency, which jointly determine the reliability of the links.

- **Chapter 4:** We modified the transmission capacity framework to allow for MAC protocols that use asynchronous transmissions and packet retransmissions. We derived the maximum number of allowed retransmissions such that the transmission capacity metric is optimized for unslotted and slotted ALOHA, and CSMA with carrier sensing at the transmitter and with carrier sensing at the receiver. Using this formulation, we also showed that, under mild traffic conditions, the CSMA protocol outperforms ALOHA. On the other hand, when the network is

facing high traffic conditions, our results evince that the synchronous nature of slotted ALOHA is preferable than the sensing capability of CSMA.

- **Chapter 5:** We analyzed two different throughput optimization problems under packet loss and queue stability constraints. Particularly we computed a closed-form approximation of the setting access probability (slotted ALOHA), coding rate, and maximum number of retransmissions that maximizes the effective link throughput and the spatial throughput, considering that packets arrive at the transmitters following a geometrical distribution. We also discuss when, and when not, the per-link throughput optimization also provides the optimal solution in terms of the network spatial throughput.

- **Chapter 6:** We studied the expected maximum spatial throughput, or spatial capacity, of ad hoc networks based on two decoding rules, namely (i) treating interference as noise, and (ii) jointly detecting the strongest interfering signals, treating the others as noise. We then compared these results against a system where transmitters code their messages at fixed rate set to optimize the average spatial throughput regardless of particular realizations of the network. We proved that, for the same decoding rule and network density, the spatial-capacity-achieving strategy achieves values of spatial throughputs higher than when the fixed rate strategy is employed.

- **Chapter 7:** We arose some lessons that can be learned from the analytical results derived in the other chapters. More specifically we stated some claims about the design setting that each node should follow to improve the information flow throughout the network based on internal and external factors as well as the network conditions. We also applied these claims to discuss the implementation of adaptive ad hoc algorithms to improve the network performance and robustness.

8.2 Future directions and final remarks

We can identify many possible future directions for the work carried out during this thesis. For example, the results about queue stability presented in Chapter 5 only deals with slotted-ALOHA, while in Chapter 4 we have completely neglected the existence of queues to assess the performance of different MAC protocols. Hence one can extend those results by looking at a scenario where both aspects are incorporated.

We can also take multi-hopping into account. In this case, relay packets insert additional traffic flows in the network, increasing the arrival rates in the queues. Clearly this adds another variable in the throughput optimization when stability constraints are required. Besides, for this new scenario, are the finds about different hopping strategies presented in Chapter 3 still valid? And when different MAC protocols are considered? Which are the trade-offs involved now? Answering these questions is another possible future direction of our work.

Another option is to make use of the discussion presented in Chapter 7 to design an adaptive algorithm to build functional interference networks that may be subject to dynamical conditions of mobility and traffic. In this context, a possible future work is to further develop those ideas employing tools from complexity science [136], which, we believe, provides powerful tools to better understand cognitive radio networks [137].

All in all, we are sure that the work presented in this thesis has a great potential to be extended in different lines, considering either mathematical insights of optimal designing choices or algorithmic implementations of cognitive solutions.

Bibliography

[1] R. E. Kahn, "The organization of computer resources into a packet radio network," in *Proceedings of the May 19-22, 1975, national computer conference and exposition on - AFIPS '75*. ACM Press, 1975, p. 177.

[2] B. Leiner, D. Nielson, and F. Tobagi, "Issues in packet radio network design," *Proceedings of the IEEE*, vol. 75, no. 1, pp. 6–20, 1987.

[3] C. Murthy and B. Manoj, *Ad Hoc Wireless Networks: Architectures and Protocols*. Prentice Hall, 2004.

[4] V. Chandrasekhar, J. Andrews, and A. Gatherer, "Femtocell networks: A survey," *IEEE Communications Magazine*, vol. 46, no. 9, pp. 59–67, Sep. 2008.

[5] A. Ghosh, J. G. Andrews, N. Mangalvedhe, R. Ratasuk, B. Mondal, M. Cudak, E. Visotsky, T. A. Thomas, P. Xia, H. S. Jo, H. S. Dhillon, and T. D. Novlan, "Heterogeneous cellular networks: From theory to practice," *IEEE Communications Magazine*, vol. 50, no. 6, pp. 54 –64, Jun. 2012.

[6] J. Andrews, S. Shakkottai, R. Heath, N. Jindal, M. Haenggi, R. Berry, D. Guo, M. Neely, S. Weber, S. Jafar, and A. Yener, "Rethinking information theory for mobile ad hoc networks," *IEEE Communications Magazine*, vol. 46, no. 12, pp. 94–101, 2008.

[7] Goldsmith, Andrea and Effros, Michelle and Koetter, Ralf and Medard, Muriel and Ozdaglar, Asu and Zheng, Lizhong, "Beyond Shannon: the quest for fundamental performance limits of wireless ad hoc networks," *IEEE Communications Magazine*, vol. 49, no. 5, pp. 195–205, May 2011.

[8] M. Haenggi and R. K. Ganti, "Interference in Large Wireless Networks," *NOW Foundations and Trends in Networking*, vol. 3, no. 2, pp. 127–248, 2008.

[9] M. Haenggi, J. Andrews, F. Baccelli, O. Dousse, and M. Franceschetti, "Stochastic geometry and random graphs for the analysis and design of wireless networks," *IEEE Journal on Selected Areas in Communications*, vol. 27, no. 7, pp. 1029–1046, 2009.

[10] F. Baccelli and B. Blaszczyszyn, "Stochastic geometry and wireless networks: Theory," *NOW Foundations and Trends in Networking*, vol. 3, no. 3-4, pp. 249–449, 2009.

[11] ——, "Stochastic geometry and wireless networks: Applications," *NOW Foundations and Trends in Networking*, vol. 4, no. 1-2, pp. 1–312, 2009.

[12] J. Andrews, R. Ganti, M. Haenggi, N. Jindal, and S. Weber, "A primer on spatial modeling and analysis in wireless networks," *IEEE Communications Magazine*, vol. 48, no. 11, pp. 156–163, 2010.

[13] M. Haenggi, *Stochastic Geometry for Wireless Networks*. Cambridge University Press, 2012.

[14] L. Kleinrock and J. Silvester, "Optimum transmission radii for packet radio networks or why six is a magic number," in *Proceedings of the IEEE National Telecommunications Conference*, vol. 4. Birimingham, USA, 1978.

[15] H. Takagi and L. Kleinrock, "Optimal transmission ranges for randomly distributed packet radio terminals," *IEEE Transactions on Communications*, vol. 32, no. 3, pp. 246–257, 1984.

[16] R. Nelson and L. Kleinrock, "The spatial capacity of a slotted ALOHA multi-hop packet radio network with capture," *IEEE Transactions on Communications*, vol. 32, no. 6, pp. 684–694, 1984.

[17] T.-C. Hou and V. Li, "Transmission range control in multi-hop packet radio networks," *IEEE Transactions on Communications*, vol. 34, no. 1, pp. 38–44, 1986.

[18] L. Kleinrock and J. Silvester, "Spatial reuse in multi-hop packet radio networks," *Proceedings of the IEEE*, vol. 75, no. 1, pp. 156–167, 1987.

[19] E. Sousa and J. Silvester, "Optimum transmission ranges in a direct-sequence spread-spectrum multi-hop packet radio network," *IEEE Journal on Selected Areas in Communications*, vol. 8, no. 5, pp. 762–771, 1990.

[20] M. Zorzi and S. Pupolin, "Optimum transmission ranges in multi-hop packet radio networks in the presence of fading," *IEEE Transactions on Communications*, vol. 43, no. 7, pp. 2201–2205, 1995.

[21] M. W. Subbarao and B. L. Hughes, "Optimal transmission ranges and code rates for frequency-hop packet radio networks," *IEEE Transactions on Communications*, vol. 48, no. 4, pp. 670–678, 2000.

[22] P. Liang and W. Stark, "Transmission range control and information efficiency for FH packet radio networks," in *21st Century Military Communications Conference Proceedings*. Los Angeles, USA, 2000.

[23] M. Chandra and B. Hughes, "Optimizing information efficiency in a direct-sequence mobile packet radio network," *IEEE Transactions on Communications*, vol. 51, no. 1, pp. 22–24, 2003.

[24] M. Souryal, B. Vojcic, and R. Pickholtz, "Information efficiency of multi-hop packet radio networks with channel-adaptive routing," *IEEE Journal on Selected Areas in Communications*, vol. 23, no. 1, pp. 40–50, 2005.

[25] H. Sui and J. Zeidler, "Information efficiency and transmission range optimization for coded MIMO FH-CDMA ad hoc networks in time-varying environments," *IEEE Transactions on Communications*, vol. 57, no. 2, pp. 481–491, 2009.

[26] P. H. J. Nardelli and P. Cardieri, "Aggregate information efficiency and packet delay in wireless ad hoc networks," in *Proceedings of 2008 IEEE Wireless Communications and Networking Conference*. Las Vegas, USA, 2008.

[27] ——, "Aggregate information efficiency in wireless ad hoc networks with outage constraints," in *Proceedings of 2008 IEEE International Workshop on Signal Processing Advances in Wireless Communications*. Recife, Brazil, 2008.

[28] S. Weber, X. Yang, J. Andrews, and G. de Veciana, "Transmission capacity of wireless ad hoc networks with outage constraints," *IEEE Transactions on Information Theory*, vol. 51, no. 12, pp. 4091–4102, 2005.

[29] S. Weber, J. Andrews, X. Yang, and G. de Veciana, "Transmission capacity of wireless ad hoc networks with successive interference cancellation," *IEEE Transactions on Information Theory*, vol. 53, no. 8, pp. 2799–2814, 2007.

[30] S. Weber, J. Andrews, and N. Jindal, "The effect of fading, channel inversion, and threshold scheduling on ad hoc networks," *IEEE Transactions on Information Theory*, vol. 53, no. 11, pp. 4127–4149, 2007.

[31] N. Jindal, J. Andrews, and S. Weber, "Bandwidth partitioning in decentralized wireless networks," *IEEE Transactions on Wireless Communications*, vol. 7, no. 12, pp. 5408–5419, 2008.

[32] N. Jindal, S. Weber, and J. Andrews, "Fractional power control for decentralized wireless networks," *IEEE Transactions on Wireless Communications*, vol. 7, no. 12, pp. 5482–5492, 2008.

[33] A. Hunter, J. Andrews, and S. Weber, "Transmission capacity of ad hoc networks with spatial diversity," *IEEE Transactions on Wireless Communications*, vol. 7, no. 12, pp. 5058–5071, 2008.

[34] S. Weber and J. Andrews, "Transmission capacity of wireless networks," *NOW Foundations and Trends in Networking*, vol. 5, no. 2-3, pp. 109–281, 2012.

[35] J. Andrews, S. Weber, M. Kountouris, and M. Haenggi, "Random access transport capacity," *IEEE Transactions on Wireless Communications*, vol. 9, no. 6, pp. 2101–2111, 2010.

[36] R. Vaze, "Throughput-delay-reliability tradeoff with ARQ in wireless ad hoc networks," *IEEE Transactions on Wireless Communications*, vol. 10, no. 7, pp. 2142–2149, 2011.

[37] R. Ganti, J. Andrews, and M. Haenggi, "High-SIR transmission capacity of wireless networks with general fading and node distribution," *IEEE Transactions on Information Theory*, vol. 57, no. 5, pp. 3100–3116, 2011.

[38] C.-h. Liu and J. Andrews, "Multicast outage probability and transmission capacity of multi-hop wireless networks," *IEEE Transactions on Information Theory*, vol. 57, no. 7, pp. 4344–4358, 2011.

[39] J. Lee, J. Andrews, , and D. Hong, "Spectrum-sharing transmission capacity," *IEEE Transactions on Wireless Communications*, vol. 10, no. 9, pp. 3053 – 3063, september 2011.

[40] F. Baccelli, B. Blaszczyszyn, and P. Muhlethaler, "An Aloha protocol for multihop mobile wireless networks," *IEEE Transactions on Information Theory*, vol. 52, no. 2, pp. 421–436, 2006.

[41] ——, "Stochastic analysis of spatial and opportunistic Aloha," *IEEE Journal on Selected Areas in Communications*, vol. 27, no. 7, pp. 1105 – 1119, Sep. 2009.

[42] P. Gupta and P. Kumar, "The capacity of wireless networks," *IEEE Transactions on Information Theory*, vol. 46, no. 2, pp. 388–404, 2000.

[43] L.-L. Xie and P. Kumar, "A network information theory for wireless communication: scaling laws and optimal operation," *IEEE Transactions on Information Theory*, vol. 50, no. 5, pp. 748–767, 2004.

[44] F. Xue, L.-L. Xie, and P. Kumar, "The transport capacity of wireless networks over fading channels," *IEEE Transactions on Information Theory*, vol. 51, no. 3, pp. 834–847, 2005.

[45] L.-L. Xie and P. Kumar, "On the path-loss attenuation regime for positive cost and linear scaling of transport capacity in wireless networks," *IEEE Transactions on Information Theory*, vol. 52, no. 6, pp. 2313–2328, 2006.

[46] F. Xue and P. Kumar, "Scaling laws for ad hoc wireless networks: An information theoretic approach," *NOW Foundations and Trends in Networking*, vol. 1, no. 2, pp. 145–270, 2006.

[47] M. Grossglauser and D. N. C. Tse, "Mobility increases the capacity of ad hoc wireless networks," *IEEE/ACM Transactions on Networking*, vol. 10, no. 4, pp. 477–486, 2002.

[48] A. El Gamal, J. Mammen, B. Prabhakar, and D. Shah, "Optimal throughput-delay scaling in wireless networks - part I: the fluid model," *IEEE Transactions on Information Theory*, vol. 52, no. 6, pp. 2568–2592, 2006.

[49] ——, "Optimal throughput-delay scaling in wireless networks - part II: : constant-size packets," *IEEE Transactions on Information Theory*, vol. 52, no. 11, pp. 5111–5116, 2006.

[50] M. Neely and E. Modiano, "Capacity and delay trade-offs for ad hoc mobile networks," *IEEE Transactions on Information Theory*, vol. 51, no. 6, pp. 1917–1937, 2005.

[51] A. Jovicic, P. Viswanath, and S. Kulkarni, "Upper bounds to transport capacity of wireless networks," *IEEE Transactions on Information Theory*, vol. 50, no. 11, pp. 2555–2565, 2004.

[52] A. Ozgur, O. Leveque, and D. Tse, "Hierarchical cooperation achieves optimal capacity scaling in ad hoc networks," *IEEE Transactions on Information Theory*, vol. 53, no. 10, pp. 3549–3572, 2007.

[53] D. Gesbert and M. Kountouris, "Rate scaling laws in multicell networks under distributed power control and user scheduling," *IEEE Transactions on Information Theory*, vol. 57, no. 1, pp. 234–244, 2011.

[54] M. Franceschetti, M. D. Migliore, and P. Minero, "The capacity of wireless networks: Information-theoretic and physical limits," *IEEE Transactions on Information Theory*, vol. 55, no. 8, pp. 3413–3424, 2009.

[55] M. Franceschetti, M. Migliore, P. Minero, and F. Schettino, "The degrees of freedom of wireless networks via cut-set integrals," *IEEE Transactions on Information Theory*, vol. 57, no. 5, pp. 3067–3079, May 2011.

[56] C. E. Shannon, "Two-way communication channels," in *Proceedings of 4th Berkeley Symposium of Mathematical Statistics Probability*. Berkeley, USA, 1961.

[57] A. Carleial, "A case where interference does not reduce capacity," *IEEE Transactions on Information Theory*, vol. 21, no. 5, pp. 569–570, 1975.

[58] ——, "Interference channels," *IEEE Transactions on Information Theory*, vol. 24, no. 1, pp. 60–70, 1978.

[59] T. Han and K. Kobayashi, "A new achievable rate region for the interference channel," *IEEE Transactions on Information Theory*, vol. 27, no. 1, pp. 49–60, 1981.

[60] H. Sato, "The capacity of the Gaussian interference channel under strong interference," *IEEE Transactions on Information Theory*, vol. 27, no. 6, pp. 786–788, 1981.

[61] A. Gamal and M. Costa, "The capacity region of a class of deterministic interference channels," *IEEE Transactions on Information Theory*, vol. 28, no. 2, pp. 343–346, 1982.

[62] M. Costa, "On the Gaussian interference channel," *IEEE Transactions on Information Theory*, vol. 31, no. 5, pp. 607–615, 1985.

[63] M. Costa and A. Gamal, "The capacity region of the discrete memoryless interference channel with strong interference," *IEEE Transactions on Information Theory*, vol. 33, no. 5, pp. 710–711, 1987.

[64] G. Kramer, "Outer bounds on the capacity of Gaussian interference channels," *IEEE Transactions on Information Theory*, vol. 50, no. 3, pp. 581–586, 2004.

[65] I. Sason, "On achievable rate regions for the Gaussian interference channel," *IEEE Transactions on Information Theory*, vol. 50, no. 6, pp. 1345–1356, 2004.

[66] R. H. Etkin, D. N. C. Tse, and H. Wang, "Gaussian interference channel capacity to within one bit," *IEEE Transactions on Information Theory*, vol. 54, no. 12, pp. 5534–5562, 2008.

[67] A. S. Avestimehr, H. El Gamal, S. A. Jafar, S. Ulukus, and S. Vishwanath, "Introduction to the special issue on interference networks," *IEEE Transactions on Information Theory*, vol. 57, no. 5, pp. 2545–2547, 2011.

[68] V. Cadambe and S. Jafar, "Interference alignment and degrees of freedom of the K-user interference channel," *IEEE Transactions on Information Theory*, vol. 54, no. 8, pp. 3425–3441, 2008.

[69] R. A. Berry and D. N. C. Tse, "Shannon meets Nash on the interference channel," *IEEE Transactions on Information Theory*, vol. 57, no. 5, pp. 2821–2836, 2011.

[70] A. Gamal and Y. Kim, *Network Information Theory*. Cambridge University Press, 2012.

[71] F. Baccelli, A. El Gamal, and D. N. C. Tse, "Interference networks with point-to-point codes," *IEEE Transactions on Information Theory*, vol. 57, no. 5, pp. 2582–2596, 2011.

[72] A. Ephremides and B. Hajek, "Information theory and communication networks: An unconsummated union," *IEEE Transactions on Information Theory*, vol. 44, no. 6, pp. 2416–2434, 1998.

[73] R. Gallager, "Basic limits on protocol information in data communication networks," *IEEE Transactions on Information Theory*, vol. 22, no. 4, pp. 385–398, 1976.

[74] V. Anantharam and S. Verdu, "Bits through queues," *IEEE Transactions on Information Theory*, vol. 42, no. 1, pp. 4–18, 1996.

[75] J. Thomas, "On the Shannon capacity of discrete time queues," in *Proceedings of 1997 IEEE International Symposium on Information Theory*. IEEE, 1997.

[76] A. Bedekar and M. Azizoglu, "The information-theoretic capacity of discrete-time queues," *IEEE Transactions on Information Theory*, vol. 44, no. 2, pp. 446–461, 1998.

[77] E. Arikan, "On the reliability exponent of the exponential timing channel," *IEEE Transactions on Information Theory*, vol. 48, no. 6, pp. 1681–1689, 2002.

[78] J. Giles and B. Hajek, "An information-theoretic and game-theoretic study of timing channels," *IEEE Transactions on Information Theory*, vol. 48, no. 9, pp. 2455–2477, 2002.

[79] A. Ephremides and S. Verdu, "Control and optimization methods in communication network problems," *IEEE Transactions on Automatic Control*, vol. 34, no. 9, pp. 930–942, 1989.

[80] L. Tassiulas and A. Ephremides, "Stability properties of constrained queueing systems and scheduling policies for maximum throughput in multihop radio networks," *IEEE Transactions on Automatic Control*, vol. 37, no. 12, pp. 1936–1948, 1992.

[81] ——, "Dynamic server allocation to parallel queues with randomly varying connectivity," *IEEE Transactions on Information Theory*, vol. 39, no. 2, pp. 466–478, 1993.

[82] L. Tassiulas, "Adaptive back-pressure congestion control based on local information," *IEEE Transactions on Automatic Control*, vol. 40, no. 2, pp. 236–250, 1995.

[83] L. Georgiadis, M. Neely, and L. Tassiulas, "Resource allocation and cross-layer control in wireless networks," *NOW Foundations and Trends in Networking*, vol. 1, no. 1, pp. 1–144, 2005.

[84] M. Neely, "Stochastic network optimization with application to communication and queueing systems," *Synthesis Lectures on Communication Networks*, vol. 3, no. 1, pp. 1–211, 2010.

[85] K. Stamatiou and M. Haenggi, "Random-access Poisson networks: Stability and delay," *IEEE Communications Letters*, vol. 14, no. 11, pp. 1035–1037, 2010.

[86] ——, "Delay characterization of multi-hop transmission in a Poisson field of interference," *IEEE/ACM Transactions on Networking*, submitted. [Online]. Available: http://www.nd.edu/~mhaenggi/pubs/ton11b.pdf

[87] M. Haenggi, "The local delay in Poisson networks," *IEEE Transactions on Information Theory*, accepted. [Online]. Available: http://www.nd.edu/~mhaenggi/pubs/tit12.pdf

[88] ——, "Delay-based connectivity of wireless networks," in *Proceedings of International Symposium on Mathematical Theory of Networks and Systems*. Budapest, Hungary, 2010.

[89] ——, "Local delay in Poisson networks with and without interference," in *Proceedings of 2010 Allerton Conference on Communication, Control and Computing*. Monticello, USA, 2010.

[90] S. Srinivasa and M. Haenggi, "Throughput-delay-reliability tradeoffs in multi-hop networks with random access," in *Proceedings of 2010 Allerton Conference on Communication, Control and Computing*. Monticello, USA, 2010.

[91] K. Stamatiou, M. Haenggi, and A. Network, "Optimal spatial reuse in Poisson multi-hop networks," 2010.

[92] X. Zhang and M. Haenggi, "Delay-optimal power control policies," *IEEE Transactions on Wireless Communications*, vol. 11, no. 10, pp. 3518 –3527, 2012.

[93] P. H. J. Nardelli, P. Cardieri, and M. Latva-aho, "Efficiency of wireless networks under different hopping strategies," *IEEE Transactions on Wireless Communications*, vol. 11, no. 1, pp. 15–20, Jan. 2012.

[94] P. H. J. Nardelli, M. Kaynia, P. Cardieri, and M. Latva-aho, "Optimal transmission capacity of ad hoc networks with packet retransmissions," *IEEE Transactions on Wireless Communications*, vol. 11, no. 8, pp. 2760 –2766, Aug. 2012.

[95] P. H. J. Nardelli, M. Kountouris, P. Cardieri, and M. Latva-aho, "Throughput optimization in wireless networks under stability and packet loss constraints," *IEEE Transactions on Mobile Computing*, accepted.

[96] ——, "Stable transmission capacity in Poisson wireless networks with delay guarantees," in *Proceedings of 2012 IEEE Wireless Communications and Networking Conference*, Paris, France, April 2012.

[97] P. H. J. Nardelli, P. Cardieri, and M. Latva-aho, "Spatial capacity of Poisson wireless networks under different decoding rules," *IEEE Transactions on Mobile Computing*, submitted.

[98] ——, "Spatial capacity of ad hoc wireless networks with Poisson distributed nodes," in *Proceedings of 2012 IEEE Wireless Communications and Networking Conference*, Paris, France, April 2012.

[99] ——, "Maximising transmission capacity of ad hoc networks via transmission system design," *Electronics Letters*, vol. 47, no. 5, pp. 348–349, 2011.

[100] P. H. J. Nardelli, G. T. F. de Abreu, and P. Cardieri, "Multi-hop aggregate information efficiency in wireless ad hoc networks," in *Proceedings of 2009 IEEE International Conference on Communications*. Dresden, Germany, 2009.

[101] P. H. J. Nardelli and G. T. F. de Abreu, "Analysis of hopping strategies in multi-hop wireless networks," in *Proceedings of 2009 Workshop on Positioning, Navigation and Communication*. Hannover, Germany, 2009.

[102] G. Rahmatollahi, P. H. J. Nardelli, M. D. Perez Guirao, and G. T. F. de Abreu, "Aggregate information efficiency in IR-UWB ad-hoc single-hop WSNs," in *Proceedings of 2009 Workshop on Positioning, Navigation and Communication*. Hannover, Germany, 2009.

[103] P. H. J. Nardelli and G. T. F. de Abreu, "On hopping strategies for autonomous wireless networks," in *Proceedings of 2009 IEEE Global Telecommunications Conference*. Honolulu, USA, 2009.

[104] M. Kaynia, P. H. J. Nardelli, P. Cardieri, and M. Latva-aho, "On the optimal design of MAC protocols in multi-hop ad hoc networks," in *Proceedings of 2010 IEEE Modeling and Optimization in Mobile, Ad Hoc and Wireless Networks*. Avignon, France, 2010.

[105] P. H. J. Nardelli, M. Kaynia, and M. Latva-aho, "Efficiency of the ALOHA protocol in multi-hop networks," in *Proceedings of 2010 IEEE International Workshop on Signal Processing Advances in Wireless Communications*. Marrakech, Morocco, 2010.

[106] M. Kaynia, P. H. J. Nardelli, and M. Latva-aho, "Evaluating the information efficiency of multi-hop networks with carrier sensing capability," in *Proceedings of 2011 IEEE International Conference on Communications*. Kyoto, Japan, 2011.

[107] P. Cardieri and P. H. J. Nardelli, *A survey on the characterization of the capacity of ad hoc wireless networks*. InTech, 2011, ch. 20, pp. 453–472.

[108] ——, "Tutorial: Measuring capacity in wireless ad hoc networks," in *9th International Information and Telecommunication Technologies Symposium*. Rio de Janeiro, Brazil, 2010.

[109] R. Ahlswede, "The capacity region of a channel with two senders and two receivers," *The Annals of Probability*, vol. 2, no. 5, pp. pp. 805–814, 1974.

[110] M. Haenggi, "On distances in uniformly random networks," *IEEE Transactions on Information Theory*, vol. 51, no. 10, pp. 3584–3586, 2005.

[111] A. Baddeley, "Spatial point processes and their applications." Springer, 2007, pp. 1–75.

[112] C. Galarza, P. Piantanida, and M. Kountouris, "On the block error probability of finite-length codes in decentralized wireless networks," in *Proceedings of 2011 Allerton Conference on Communication, Control, and Computing*. Cambridge, USA, 2011.

[113] M. Yacoub, *Foundations of Mobile Radio Engineering*. CRC Press, 1993.

[114] H. Inaltekin, M. Chiang, H. Poor, and S. Wicker, "On unbounded path-loss models: Effects of singularity on wireless network performance," *IEEE Journal on Selected Areas in Communications*, vol. 27, no. 7, pp. 1078–1092, 2009.

[115] M. Haenggi, "Outage, local throughput, and capacity of random wireless networks," *IEEE Transactions on Wireless Communications*, vol. 8, no. 8, pp. 4350–4359, 2009.

[116] R. Ganti and M. Haenggi, "Interference and outage in clustered wireless ad hoc networks," *IEEE Transactions on Information Theory*, vol. 55, no. 9, pp. 4067–4086, 2009.

[117] ——, "Spatial and temporal correlation of the interference in aloha ad hoc networks," *IEEE Communications Letters*, vol. 13, no. 9, pp. 631–633, 2009.

[118] P. C. Pinto and M. Z. Win, "Communication in a Poisson field of interferers–Part I: Interference distribution and error probability," *IEEE Transactions on Wireless Communications*, vol. 9, no. 7, pp. 2176–2186, 2010.

[119] ——, "Communication in a Poisson field of interferers-Part II: Channel capacity and interference spectrum," *IEEE Transactions on Wireless Communications*, vol. 9, no. 7, pp. 2187–2195, 2010.

[120] P. Cardieri, "Modeling interference in wireless ad hoc networks," *IEEE Communications Surveys & Tutorials*, vol. 12, no. 4, pp. 551–572, 2010.

[121] M. Haenggi, "Mean interference in hard-core wireless networks," *IEEE Communications Letters*, vol. 15, no. 8, pp. 792–794, 2011.

[122] M. Kaynia, N. Jindal, and G. E. Oien, "Improving the performance of wireless ad hoc networks through MAC layer design," *IEEE Transactions on Wireless Communications*, vol. 10, no. 1, pp. 240–252, 2011.

[123] F. Baccelli and B. Baszczyszyn, "A new phase transitions for local delays in manets," in *Proceedings of 2010 IEEE International Conference on Computer Communications*, 2010.

[124] W. Szpankowski, "Stability conditions for some distributed systems: Buffered random access systems," *Buffered Random Access Systems, Advanced Applied Probability*, vol. 26, pp. 498–515, 1993.

[125] D. Gross and C. M. Harris, *Fundamentals of Queueing Theory*, 3rd ed. Wiley-Interscience, 1998.

[126] W. Luo and A. Ephremides, "Stability of N interacting queues in random-access systems," *IEEE Transactions on Information Theory*, vol. 45, no. 5, pp. 1579–1587, 1999.

[127] K. Leyton-Brown and Y. Shoham, *Essentials of Game Theory: A Concise, Multidisciplinary Introduction*, ser. Synthesis Lectures on Artificial Intelligence and Machine Learning. Morgan and Claypool Publishers, 2008, vol. 2, no. 1.

[128] G. Hardin, "The tragedy of the commons," *Science*, vol. 162, no. 3859, pp. 1243–1248, Dec. 1968.

[129] V. Mordachev and S. Loyka, "On node density - outage probability tradeoff in wireless networks," *IEEE Journal on Selected Areas in Communications*, vol. 27, no. 7, pp. 1120–1131, 2009.

[130] R. Vaze and R. Heath, "Transmission capacity of ad-hoc networks with multiple antennas using transmit stream adaptation and interference cancellation," *IEEE Transactions on Information Theory*, vol. 58, no. 2, pp. 780–792, 2012.

[131] K. Huang, J. Andrews, D. Guo, R. Heath, and R. Berry, "Spatial interference cancellation for multi-antenna mobile ad hoc networks," *IEEE Transactions on Information Theory*, vol. 58, no. 3, pp. 1660–1676, 2012.

[132] J. Blomer and N. Jindal, "Transmission capacity of wireless ad hoc networks: Successive interference cancellation vs. joint detection," in *Proceedings of 2009 IEEE International Conference on Communications*, 2009.

[133] M. Nowak, "Evolving cooperation," *Journal of Theoretical Biology*, vol. 299, pp. 1–8, Apr. 2012.

[134] E. Onur, Y. Durmus, and I. Niemegeers, "Cooperative density estimation in random wireless ad hoc networks," *IEEE Communications Letters*, vol. 16, no. 3, pp. 331–333, Mar. 2012.

[135] Z. Yang and Y. Liu, "Understanding node localizability of wireless ad hoc and sensor networks," *IEEE Transactions on Mobile Computing*, vol. 11, no. 8, pp. 1249–1260, Aug. 2012.

[136] M. Mitchell, *Complexity: A Guided Tour*. Oxford University Press, 2009.

[137] S. Haykin, "Cognitive radio: Brain-empowered wireless communications," *IEEE Journal on Selected Areas in Communications*, vol. 23, no. 2, pp. 201–220, 2005.